Cybersickness Analysis Using Symbolic Machine Learning Algorithms

Thesis · May 2021

DOI: 10.22409/PGC.2021.d.11875620761

3 authors:

Thiago Porcino
Universidade Federal Fluminense

Daniela G. Trevisan
Universidade Federal Fluminense

Esteban Clua
Universidade Federal Fluminense

UNIVERSIDADE FEDERAL FLUMINENSE

THIAGO MALHEIROS PORCINO

Cybersickness Analysis Using Symbolic Machine Learning Algorithms

NITERÓI

2021

UNIVERSIDADE FEDERAL FLUMINENSE

THIAGO MALHEIROS PORCINO

Cybersickness Analysis Using Symbolic Machine Learning Algorithms

Thesis presented to the Graduate School of Computer Science of Universidade Federal Fluminense as a partial requirement for obtaining the Doctor of Science degree in Computer Science. Field: Computer Science

Advisor:
Esteban Clua

Co-advisor:
Daniela Trevisan

NITERÓI

2021

Ficha catalográfica automática - SDC/BEE
Gerada com informações fornecidas pelo autor

P834c Porcino, Thiago
Cybersickness Analysis Using Symbolic Machine Learning Algorithms / Thiago Porcino ; Esteban Clua, orientador ; Daniela Trevisan, coorientadora. Niterói, 2021.
105 f. : il.

Tese (doutorado)-Universidade Federal Fluminense, Niterói, 2021.

DOI: http://dx.doi.org/10.22409/PGC.2021.d.11875620761

1. Realidade virtual. 2. Dispositivos HMD. 3. Desconforto na realidade virtual. 4. Aprendizado de máquina simbólico. 5. Produção intelectual. I. Clua, Esteban, orientador. II. Trevisan, Daniela, coorientadora. III. Universidade Federal Fluminense. Instituto de Computação. IV. Título.

CDD -

Bibliotecário responsável: Debora do Nascimento - CRB7/6368

THIAGO MALHEIROS PORCINO

Cybersickness Analysis Using Symbolic Machine Learning Algorithms

Thesis presented to the Graduate School of Computer Science of Universidade Federal Fluminense as a partial requirement for obtaining the Doctor of Science degree in Computer Science. Field: Computer Science

Aproved in April, 2021.

EXAMINERS

Prof. Dr. Esteban Clua - Advisor, UFF

Prof. Dr. Daniela Trevisan - Co-advisor, UFF

Prof. Dr. Flavia Bernardini, UFF

Prof. Dr. Anselmo Montenegro, UFF

Prof. Dr. Fátima Nunes, USP

Helmut Hlavacs

Prof. Dr. Helmut Hlavacs, Universität Wien

Prof. Dr. Lucile Sassatelli, Université Côte d'Azur

Niterói

2021

"Once we accept our limits, we go beyond them."

Albert Einstein

Acknowledgements

First of all, I want to thank God for everything, and then my family for all the support provided during all these years.

A special thanks for my advisors Dr. Prof. Esteban Clua and Dr. Prof. Daniela Trevisan, who taught me a different view of academic life and how to sail through those hard times.

I want to thank the examiners' board Dr. Prof. Flavia Bernardini, Dr. Prof. Fátima Nunes, Dr. Prof. Anselmo Montenegro, Dr. Prof. Helmut Hlavacs, and Dr. Prof. Lucile Sassatelli for their valuable suggestions and useful comments throughout this research work.

Another special thanks to my friend Dr. Prof. Érick O. Rodrigues, for their valuable suggestions, ideas, and tips.

I extend this acknowledgment to all of you who helped direct or indirect throughout these tough times. Thank you all.

Finally, I also thank the *Universidade Federal Fluminense* for providing support and conditions to develop this thesis. Lastly, I thank CAPES for providing financial support for this work.

Resumo

A realidade virtual (RV) e os *head-mounted displays* (HMD) estão constantemente ganhando popularidade em vários segmentos, tais como: educação, militar, entretenimento e saúde. Embora tais tecnologias possibilitem uma grande sensação de imersão, elas também podem desencadear sintomas de desconforto. Tal condição é chamada de *cybersickness* (CS) e é bastante popular em publicações recentes sobre realidade virtual. Propõe-se neste trabalho uma nova análise experimental usando aprendizado de máquina simbólico para classificar as causas potenciais de CS em jogos de RV. Primeiramente, as teorias de manifestações de desconforto geralmente atribuídas a ambientes de realidade virtual foram revisadas. Além disso, também foram revisadas as estratégias existentes com o objetivo de minimizar os problemas de CS. Foi discutido como a medição da CS pode ser realizada com base em dados subjetivos, biossinais (ou dados objetivos) e de perfil dos usuários. Em segundo lugar, uma nova abordagem foi proposta para prever as próximas manifestações da CS. O resultado foi uma solução capaz de sugerir se o usuário de RV está entrando em uma situação de CS, com 99.0% de acurácia no melhor caso. Foi adotado o classificador *random forest* após uma validação envolvendo 16 classificadores diferentes de aprendizado de máquina, listados no capítulo 5 deste trabalho. O conjunto de dados foi construído por meio de um questionário de perfil de CS e dois jogos de realidade virtual que também foram elaborados neste trabalho. Terceiro, são estimadas as causas da CS e são classificadas de acordo com seu impacto pelo algoritmo de aprendizado de máquina simbólico desenvolvido. Os experimentos foram realizados usando dois jogos de realidade virtual e 6 protocolos experimentais, juntamente com 37 amostras válidas de um total de 88 voluntários. Em resumo, os resultados mostram que a rotação e a aceleração desencadearam a CS com mais frequência em um jogo de voo em comparação a um jogo de corrida. Pode-se observar também que indivíduos menos experientes com RV são mais propensos a sentir o desconforto. Os resultados corroboram com a confirmação da hipótese de que a experiência prévia com RV desempenha um papel mais importante no jogo de corrida, pois este jogo oferece mais liberdade ao usuário em termos de controladores, mais alternativas de deslocamento e uma aceleração mais autocontrolada. Adicionalmente, diferentes causas que desencadeiam a CS surgem com base em exposições de RV de curto ou longo prazo. São sugeridas estratégias para mitigar a CS para esses dois cenários: experiências de exposição de curto e longo prazo.

Palavras-chave: Realidade virtual, dispositivos HMD, desconforto na realidade virtual, aprendizado de máquina simbólico, classificação.

Abstract

Virtual reality (VR) and head-mounted displays are continually gaining popularity in various fields such as education, military, entertainment, and health. Although such technologies provide a high sense of immersion, they can also trigger symptoms of discomfort. This condition is called cybersickness (CS) and is quite popular in recent virtual reality research. This work proposes a novel experimental analysis using symbolic machine learning to rank potential causes of CS in VR games. First, we reviewed the literature on theories of discomfort manifestations usually attributed to virtual reality environments. Additionally, we reviewed existing strategies aimed at minimizing CS problems and discussed how the CS measurement has been conducted based on subjective, bio-signal (or objective), and users profile data. Second, we propose a novel approach for predicting upcoming CS symptoms. As a result, with an accuracy of 99.0% (best case), our solution can suggest whether the user of VR is entering into an illness situation. We performed supervised classification using 16 Weka's decision tree classifiers (listed in chapter 5), which random forest presented the best results. We built our dataset through a CS profile questionnaire and two virtual reality games that we also propose in the present work for training purposes. Third, we estimate CS causes and rank them according to their impact on the classical machine learning classification task. Experiments are performed using two virtual reality games and six experimental protocols along with 37 valid samples from a total of 88 volunteers. In summary, our results show that rotation and acceleration triggered cybersickness more frequently in a flight game in contrast to a racing game. We could also observe that participants that are less experienced with VR are more prone to feel discomfort. Former experience plays a more critical role in the race game, as this game provides more liberty to the user in terms of controllers, more displacement alternatives, and a more self-controlled acceleration. Furthermore, different causes that trigger discomfort arise based on short or long-term VR exposures. We suggest strategies for mitigating CS for these two scenarios: short and long-term exposure experiences.

Keywords: Virtual reality, head-mounted displays, cybersickness, symbolic machine learning, classification.

List of Figures

List of Tables

List of Abbreviations and Symbols

α	:	alfa
β	:	beta
γ	:	gama
θ	:	teta
3D	:	3-dimensions
CAVE	:	Cave automatic virtual environment
CS	:	Cybersickness
DoF	:	Depth of field
DT	:	Decision tree
EDA	:	Electrodermal activity
EEG	:	Electroencephalogram
FoV	:	Field of View
FPS	:	Frames per second
GSR	:	Galvanic skin response
HMD	:	Head-mounted display
MS	:	Motion sickness
MSSQ	:	Motion sickness susceptibility questionnaire
RF	:	Random Forest
ROI	:	Region of interest
SS	:	Simulator sickness
SSQ	:	Simulator sickness questionnaire
VIMS	:	Visually induced motion sickness
VR	:	Virtual reality
VRSQ	:	Virtual reality sickness questionnaire

Contents

Chapter 1

Introduction

Activities such as virtual training environments, simulations and entertainment in immersive virtual formats are constantly becoming more popular with the continued development and public interest in VR technologies over the last years [19]. In 2019, the VR hardware market was valuated at 4.4 billion US dollars and is expected to reach 10 billion US dollars by 2022 [140].

Head-mounted displays (HMDs) is one of the means of achieving immersive virtual reality. These devices usually consist of electronic displays and lenses that are fixed over the head where the display and lenses face the eyes of the user. HMDs are used for various purposes in the industry such as in games that focus on entertainment [142], military [129], education [3], therapy [22] and simulators for numerous contexts [78].

Unfortunately, HMDs are strongly related to frequent manifestations of discomfort [74]. Among the possible manifestations, cybersickness (CS) deserves special attention as it is the most frequent and is usually associated to long exposures to HMDs. According to Ramsey et al. [119], approximately 80% of participants who have already experienced HMD-based VR reported discomfort sensations after just 10 minutes of exposure. Additionally, more than 60% of usability problems are strongly related to discomfort [74].

The most frequent symptoms caused by CS are general discomfort, headache, stomach awareness, nausea, vomiting, sweating, fatigue, drowsiness, disorientation, and apathy [139, 33]. These symptoms impact the user experience and affects the profit and coverage of the VR game industry. In addition, discomfort symptoms can vary across individuals, where some people are more susceptible than others.

Several works in the literature address the CS phenomenon and mitigation strategies for immersive VR applications using HMDs [96, 31, 124, 117]. While most previous works

[64, 70, 62] are mainly focused on detecting and predicting CS events, this work estimates and rank the attributes that contribute the most in terms of triggering cybersickness, enabling a selection of the most adequate strategy to mitigate CS. We propose an approach that enables cause estimation while the user is under the VR condition. However, the suggestion of strategies can be implemented afterwards by the game designer. In this direction, as symbolic machine learning is based on human-readable logic representations, is adequate to this approach, where understanbility is essential [90].

1.1 Objective

This work proposes a novel experimental analysis using symbolic machine learning to rank potential causes of CS in VR games.

Our central hypothesis is that symbolic machine learning models will understandably enable us to interpret the machine learning results in terms of predictability. The human-readable characteristic of symbolic machine learning models may help us to understand the discomfort manifestation reasons in our experimental games. Once we can identify causes of discomfort in a VR experience, we will suggest one or more strategies to overcome the cybersickness generated symptoms in specific games and users.

For this reason, we intend to highlight the main factors that contribute to the manifestation of CS symptoms. Consequently, we intend to create a relationship analysis between leading discomfort causes and strategies to minimize CS in virtual environments. Moreover, We intend to identify the causes of such discomfort using a symbolic machine learning solution to estimate CS causes in VR games. At last, we intend to suggest strategies for mitigating CS in short and long-term VR exposure experiences.

The complete methodology flow has five main stages: Literature review, Protocols and experiments, Pre-selection of classifiers using Weka, implementation of symbolic machine learning models to estimate CS causes, and analysis of ranked CS causes to suggest strategies (Figure 1.1).

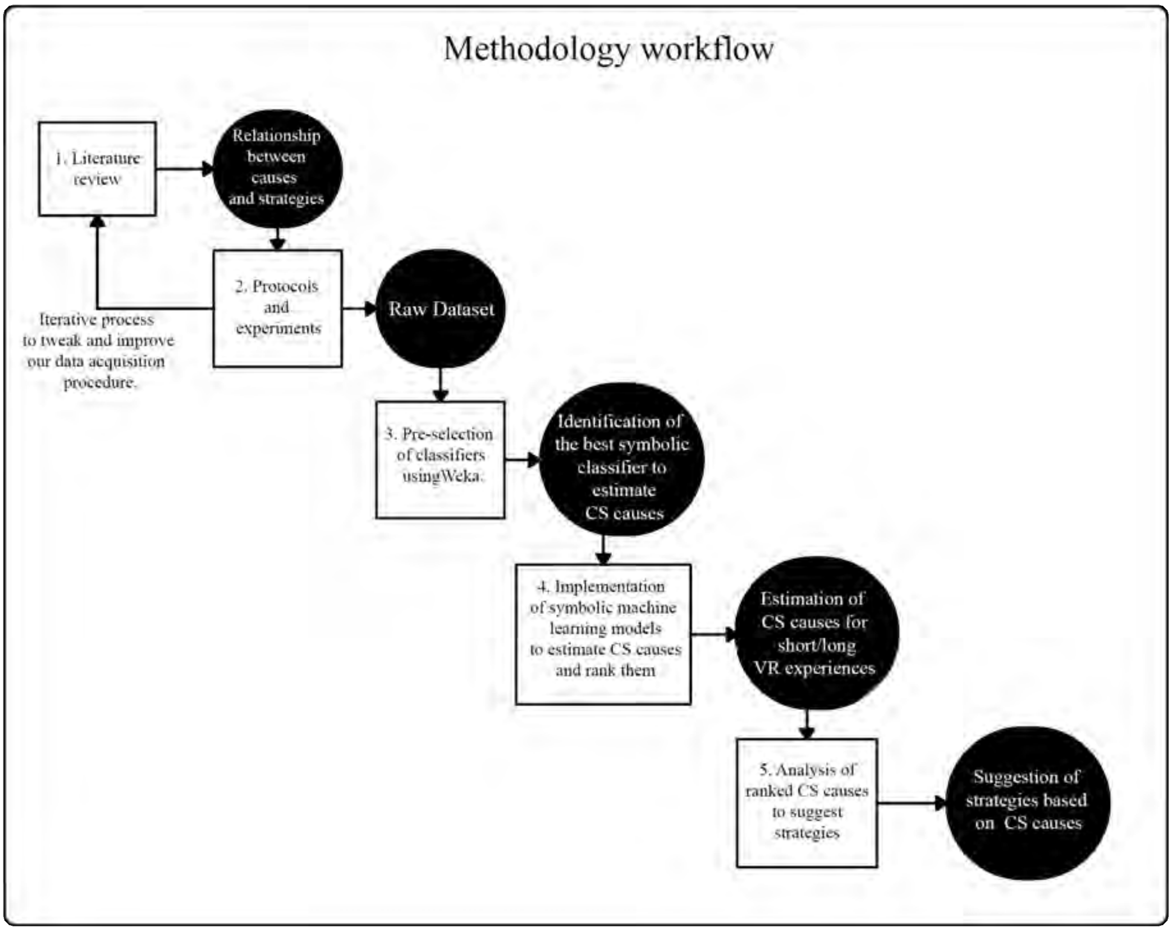

Figure 1.1: In (1), the literature review stage helps us to identified the leading causes of discomfort and strategies to overcome CS. In (2) protocols and experiments, we conduct user tests and six experimental protocols to create our raw dataset for further analysis. Moreover, in (3), we perform 16 machine learning classifications to find the best model in terms of understandability and predictability of CS causes, which random forest showed the most appropriated for our purposes. Furthermore, in (4), we implement random forest and decision tree models and estimate the CS causes using 37 valid samples from a total of 88 volunteers, which generated a rank of CS causes in terms of short and long exposures for our two VR developed games. In (5), analyzed results and suggest strategies for short and long VR experiences.

1.2 Publications

Through this research, we have been publishing and submitting studies to mitigate cybersickness problems in virtual reality environments:

1. Porcino, T.; Clua, E.; Vasconcelos, C.; Trevisan, D. Dynamic focus selection for first-person navigation with head mounted displays. *SBGames* (2016)

2. Porcino, T. M.; Clua, E.; Trevisan, D.; Vasconcelos, C. N.; Valente, L. Minimizing cyber sickness in head mounted display systems: design guidelines and applications. In *Serious Games and Applications for Health (SeGAH), 2017 IEEE 5th International Conference on* (2017), IEEE, pp. 1–6

3. Porcino, T.; Trevisan, D.; Clua, E. Minimizing cybersickness in head-mounted display systems: causes and strategies review. In *2020 22nd Symposium on Virtual and Augmented Reality (SVR)* (2020), IEEE, pp. 154–163

4. Porcino, T.; Rodrigues, E. O.; Silva, A.; Clua, E.; Trevisan, D. Using the gameplay and user data to predict and identify causes of cybersickness manifestation in virtual reality games. In *2020 IEEE 8th International Conference on Serious Games and Applications for Health (SeGAH)* (2020), IEEE, pp. 1–8

5. Porcino, T.; Rodrigues, E. O.; Bernardini, F.; Trevisan, D.; Clua, E. Can we identify user- and game-specific causes that lead to cybersickness? In *2020 IEEE Conference on Games (CoG)* (2021), IEEE [Submitted for evaluation]

6. Porcino, T.; Rodrigues, E. O.; Bernardini, F.; Trevisan, D.; Clua, E. Identifying cybersickness causes in virtual reality games using symbolic machine learning algorithms. *Entertainment Computing* (2021) [Submitted for evaluation]

1.3 Contributions

The main contributions of this thesis are:

1. **Providing a extensive cybersickness literature review**. We elaborate on known strategies aimed at minimizing cybersickness, splitting the causes into 10 categories: locomotion, acceleration, field of view (FoV), depth of field, rotational movements, exposure time, static rest frames, postural instability, latency lag, and degree of control. Our review facilitates researchers to identify the leading causes for most discomfort situations in virtual reality environments and associate the most recommended strategies to minimize such discomfort. Additionally, Kemeny et al. [65] cited part of this work in their book, entitled Getting rid of cybersickness in

virtual reality, augmented reality, and simulators. At the moment, 65 works cited part of this study previous published [118].

2. **Best Review Paper Award** Part of this work [117] was awarded in best review paper category at the symposium on virtual and augmented reality (SVR), the premier conference on VR/AR on Brazil.

3. **Proposing the cybersickness profile questionnaire - CSPQ**. We create the CSPQ based on our literature findings. The CSPQ contains 9 questions about use profile tied to cybersickness manifestations.

4. **Proposing symbolic machine learning models to identify causes of cybersickness in virtual reality environments**. Symbolic machine learning models have never been properly explored in terms of cybersickness minimization in games (see Chapter 3.4). We are the first to use symbolic classifiers (decision tree and random forest) to analyze and estimate CS causes during a gameplay experience. Additionally, we show how CS causes vary according to the moment of the gameplay and the type of game.

5. **Strategies suggestion based on user and gameplay data**. This work is the first to suggest strategies to overcome cybersickness based on user and gameplay data using symbolic machine learning models.

6. **Providing a public virtual reality users database**. The raw dataset of this work is published in a public domain for further reproduction and comparisons [112].

1.4 Organization

The content of this thesis is organized as follows. Chapter 2 describes the theoretical background, including the main theories about discomfort manifestations related to VR and types of sickness associated with VR. Chapter 3 describes the cybersickness literature review, including a revision of causes, strategies, CS measurements, and CS machine learning approaches focused CS classification. Chapter 4 describes our protocols and experiments, including our user data collection methodology and the identification of relevant CS prediction data. Chapter 5 describes the cybersickness prediction approach, classifiers, and preliminary results. Chapter 6 presents the causes identification approach, including the symbolic machine learning approach, a description of the evaluation method, comparing results for two symbolic machine learning models: decision tree and random forest, and the identified CS causes using our approach. Chapter 7 presents the strategies to overcome CS effects. At last, Chapter 8 describes the conclusion, limitations, and future work.

Chapter 2

Theoretical background

Recent works point out that the discomfort generated by virtual environments is still not fully explored and explained in the literature [85],[56]. However, this work gathers all the main theories about discomfort manifestations possibly related to VR, which are described below.

- **Evolution theory** - Also known as "poison theory" (due to its resemblance to poison ingestion by the human body). This theory defends the axiom that it is crucial for the human body to detect forms of incorrect movement (e.g., equilibrium of a stationary body). When this occurs, a psychological conflict effect is generated, involving the coordination of the body's sensory systems; such conflict causes the body to enter a defense mode, which produces toxic substances in the stomach. When it occurs, the immediate body's response is the emesis (vomiting) process to remove toxins [147].

- **Postural instability theory** - According to a study [127], all individuals are incited to devise tools with which to maintain a balanced and robust posture. Some virtual scenes may not ensure stable user posture control and may induce the maintenance of incorrect postures for long periods. Unstable and incorrect postures for extended durations can cause discomfort [141]. According to Farkhatdinov et al. [39], postural instability induces the disease of movement (motion sickness), which is also associated with an individual's behavioral profile.

- **Sensory conflict theory** - This study (the most accepted and cited theory) is based on the principle that discomfort in virtual reality environments originates from the conflict between the human visual system [145] and human vestibular system [53]. Such a conflict occurs when an individual expects a sensory control from a sensory system but receives unexpected information from another. For example, a conflict occurs when an individual's vision system (eyes) receives movement information that differs from that received by his vestibular system. According to Reason et al. [122], author of one of the most cited theories on the topic of movement disease, such a malaise is a phenomenon caused by inadequate adaption arising at either the beginning or end owing to discrepancies between sensory systems.

- **Rest frames theory** - this theory assumes that the human brain has a particular model of representation for stationary and moving objects. The brain perceives the remaining picture as part of a stationary scene to which it then assigns a movement relative to the previous picture [82]. In the real world, the background is generally considered the remaining picture. Take as an example a visual scene composed of a room and a ball. The human brain considers a ball movement in a room as being more natural than the reverse. To detect movement, the brain first chooses stationary objects (for example, the remaining frame). The movement of other objects is measured relatively against the stationary object (remaining frame). It is thus possible to assert that motion sickness is directly associated with the mental model's stability of representation of stationary or moving objects [20].

- **Eye movement theory** - This theory states that discomfort can be generated by unnatural eye movement, when the retina of the human eye attempts to stabilize a scene's image [151]. This conflict occurs when images move differently from the visual system's expectations (as in VR). In VR, eyes move in an unnatural way to try to stabilize the image produced in the retina, leading to discomfort symptoms [43]. According to Jerald et al. [63], fixing the visual attention at a stationary point helps to reduce induced eye movement, thereby minimizing the sense of self-movement.

2.1 Human Sensory System

Recent research has continued to address the causes of VR discomfort [46], [79]. The idea that the human sensory and nervous systems are linked to the manifestation of these causes is strongly consolidated. For this reason, it is necessary to study how the human sensory system behaves when interacting with VR content.

Other recent work shows that vision is the most dominant sense among all human senses [77]. Through it, neurons communicate and several body muscles are activated, executing a whole chain process in the human system. In the context of VR, this reaction is observed during ocular vergence-accommodation. During accommodation, ocular variation occurs, which enables a vision focus change to keep images clearly and distinctly visualized on the retina. When the eyes spot a region of interest in the real world, the brain commands eye muscles to change their focal position and decrease focused region blurs [150]. At vergence, through stimuli, both eye lenses are manipulated and directed toward the region of interest. This ensures that the projected image will be correctly positioned for visualization by eye lenses. Accommodation stimuli and vergence are connected, meaning that any vergence alteration stimulates accommodation alteration, or vice versa [32].

VR devices are considered unfavorable environments for the vergence-accommodation processes. First, images are displayed very close to the user's eyes, despite the fact that virtual images often simulate a greater distance compared with the actual distance from the lenses. For this reason, when a human eye looks around a simulated virtual scene, the focal distance of lenses does not vary, so neural commands signal a smaller depth than the simulated depth. Accommodation remains the same, but being connected to the vergence, it ends up inducing unnatural vergence in the human eye [65]. Such discrepancy and artificial manipulation of the depth of field causes sensory conflict, which contributes to motion sickness (MS), visually induced motion sickness (VIMS), and CS symptoms.

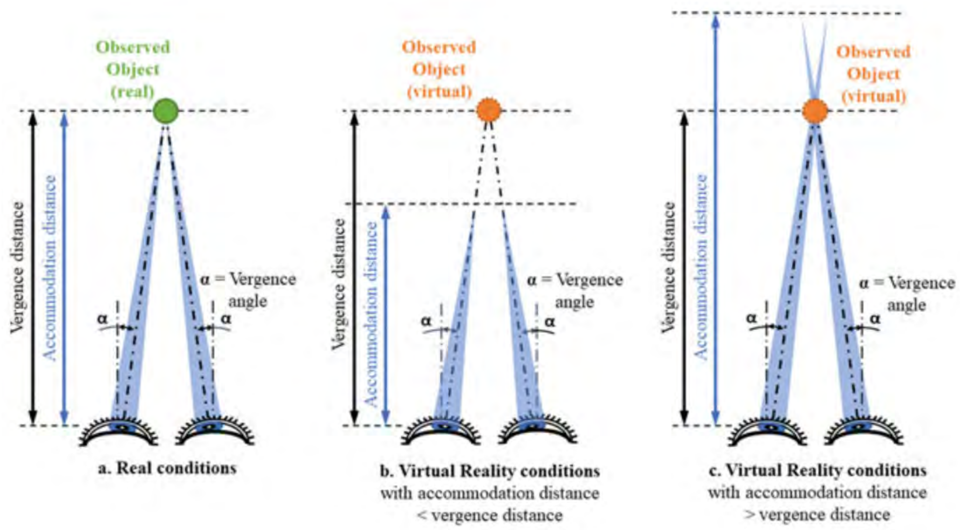

Figure 2.1: Kemeny's vergence-accommodation conflict example. In natural conditions (a), vergence distance and accommodation distance are the same. In VR (b and c), the vergence distance produced by HMD frequently differs from the accommodation distance [65].

2.2 Self-motion Perception and Cybersickness

This section presents a fundamental understanding of motion perception concerning motion sickness's primary distinctions and its subcategories. MS manifests itself because of the information divergence emitted by the human sensory system. This occurs when there are conflicts between the sensory organs that define an individual's orientation and spatial positioning. MS is defined as the discomfort felt during a forced visual movement (without body movement), for example, airplane trips, boats, or land vehicles [60],[84], [11]. Such discomfort is also experienced in virtual environments and is called VIMS.

This type of discomfort also occurs in virtual environments and is called visually induced motion sickness (VIMS). Merhi et al. [94] defined the event of VIMS during experiments with video games as a game disease (gaming sickness). Moreover, in VR, articles usually label VIMS that occurs in VR as CyberSickness (CS) [91]. In contrast, VIMS that occurs during flight or drive simulators is often called simulator sickness [16]. Overall, MS can be split into two subcategories [65]: transportation sickness, which is tied to the real world and simulator sickness, which is associated to the virtual world and includes cybersickness (CS), as shown in Figure 2.2.

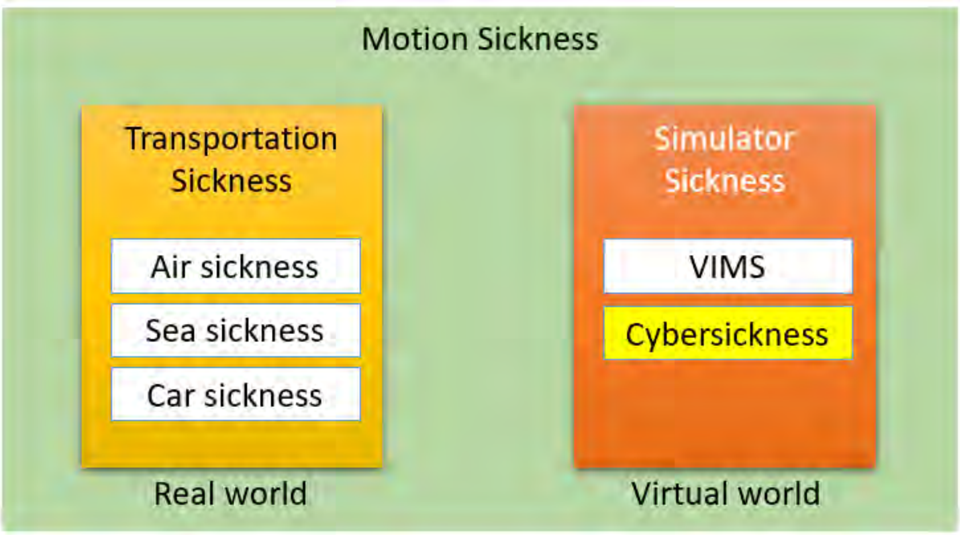

Figure 2.2: Motion sickness and its subcategories according to environments and trigger mechanisms.

Cybersickness symptoms, in turn, are comparable with MS symptoms occurring in the real world such as nausea, vertigo, dizziness, and upset stomach [57]. CS Symptoms occur mainly with the use of VR devices, known as HMDs (Oculus Rift, HTC lives, among others) [125]. Kolasinski [74] described more than 40 possible VIMS causes. These factors were grouped into three sets: simulator, task, and individual factors. Renkewitz et al. [126] expanded Kolasinski's work by tabling and dividing potential factors for CS manifestations into three groups: simulator (display system), individual, and task. However, in a recent work, Rebenitsh [126] stated that many factors and configurations related to discomfort are still unknown. For example, a virtual environment may allow the user to choose the view from a first-person view perspective or the simulation of a large screen. The same applies to monoscopic rendering (an image for both eyes) or stereoscopic (an image for each eye), or even movement by accessories of VR devices (mouse, keyboard, joystick, and tracking). These examples result in an exponential number of configurations.

This thesis focuses on the study and resolution of problems related exclusively to CS. In other words, symptoms are related exclusively to discomfort manifestation in VR environments with HMD devices.

Chapter 3

Cybersickness Literature Review

Some works in the literature [124], [31], [96] have discussed general aspects related to CS such as current measurements of incidence of CS, ergonomic aspects, varying effects due to display and rendering mode, and usability issues. However, none of them has focused on the relationship between causes and strategies to minimize CS effects.

We conduct this research following these bibliography databases: ACM Digital Library, IEEE, SpringerLink, Google Scholar, and applying the query string below:

- ("cybersickness") AND ("virtual reality") OR (“review”) OR ("strategies")
- ("cybersickness") AND ("motion sickness") OR (“review”) OR ("strategies")
- ("cybersickness") AND ("VIMS") OR (“review”) OR ("measures")

3.1 Causes

Several factors can cause pain and discomfort when using HMD [157]. Manifestations of CS can lead to more intense symptoms, such as nausea, eye fatigue, neuralgia, and dizziness [67]. According to the literature [137], [88], [35], [74], it is possible to highlight the main factors that contribute to the manifestation of CS symptoms.

1. **Locomotion** - According to Rebenitsch [125], locomotion can be correlated to CS. When the participant travels and has greater control of his movements and is close to natural movements, he will experience less CS. However, when the user experiences continuous visual movement stimulation while resting (also known as vection), it

can induce painful sensations. Moreover, this problem reduces the time limit of using virtual reality in a comfortable state.

2. **Acceleration** - Visual accelerations without generating any response in the corresponding vestibular organs cause uncomfortable sensations that result in CS symptoms. High accelerations during movements produce higher degrees of CS [82], [139]. An example of this report is considered by Laviola [82] using a virtual reality driving simulator as example. High-frequency acceleration movements contribute more to the CS. In contrast, the lower ones generate more comfortable experiences. This fact occurs because, during the acceleration increase, sensory conflicts can occur. Such conflicts make the body manifest discomfort information. However, the critical issue is the constant deceleration and acceleration. In other words, the duration of the acceleration change, not its magnitude, which makes people feel CS symptoms. An instantaneous acceleration from 0 to 100, instantaneous displacement, does not cause much discomfort than accelerations that frequently occur [1].

3. **Field of view** - In VR environments, a wide field of view generates a great sense of immersion. However, a wide field of view contributes to the CS manifestation. In contrast, a narrow field of view creates a more comfortable experience in VR but decrease the user's immersion [157], [35].

4. **Depth of field** - Inadequate simulation of focus on stereoscopic HMDs with flow tracking devices creates unbelievable images and, consequently, causes discomfort. In the human eye, focus forces blur effects naturally that depend on the depth of field (DoF) and distance range of objects in the observed area. Due to ocular convergence, objects outside this range, located behind or in front of the eyes, are blurred [118].

5. **Degree of control** - According to Stanney and Keneddy [139], interactions and movements that are not being controlled by the user may cause CS.

6. **Duration use time** - Many works have showed that time exposure to VR experiences might raise discomfort in a proportional way [91],[139], [113].

7. **Latency—lag**, has persisted for years as an obstacle in the previous generations of HMDs [101]. Latency is the delay between action and reaction latency is the time difference between the time of input given and the corresponding action to take place in a virtual scenario. High latency may drastically increase CS levels.

8. **Static rest frame** - The lack of a static frame of reference (static rest frame) can cause sensory conflicts and, ultimately, CS [20]. According to Cao et al. [20] most users are able to better tolerate virtual environments created by projectors such as cave automatic virtual environments (CAVEs) [29] compared to HMDs devices.

9. **Camera rotation** - Rotations in virtual environments with HMDs increase the chances of sensory conflicts. The feeling of vection is greater in rotations when two axes are used in comparison to just one axis [13].

10. **Postural instability** - Postural instability (Ataxia) is a postural imbalance or lack of coordination [141], [82], [4], caused when the body tries to maintain an incorrect posture due to the sensory conflict caused by the virtual environment. In other words, postural instability is the reactive response to information received by the vestibular and visual organs, which leads to CS.

3.2 Strategies Associated to Causes

In this section we describe strategies pointed out in the literature to overcome the diverse CS causes. In Table 3.1 is shown all strategies found in the literature with its related authors and in Table 3.2 is presented the association between causes and strategies identified in this study.

1. **Locomotion** Teleportation techniques help to solve the problem of locomotion in VR environments. Most VR applications use the teleportation strategy (teleporting). In teleportation, users can travel great distances by specifying the trip's destination point with the help of a marker [81]. This technique works as follows: using a controller, the user points to the destination location and squeezes a trigger button, which immediately transports the user to the new location, also called "pointing and teleport". Another technique called "trigger walk" uses the concept of natural walking to reach a destination. In this case, to move around, the user uses VR control triggers instead of legs. Each control is handled by each of the user's hands in a relaxed and comfortable position (with minimum energy consumption). The user moves a step closer to the direction indicated at each pull of the trigger [133].

2. **Acceleration** According to Berthoz et al.[8], it is possible to induce a sensation of movement using a visual response (haptic feedback). According to Pavard et al. [105], the human visual system can adapt to illusive motion but not acceleration.

Various applications of VR (e.g., games and training applications) require support for haptic perception. This is because haptic perceptions can induce the sensation of acceleration in its users. When correctly applied, artificial acceleration sensation can help avoid sensory conflict. In some virtual environments (racing game), it is possible to minimize CS problems using haptic responses. Haptics is a way of transmitting physical sensations to the user, which are compatible with those captured by the user's visual system. Bouyer et al. [14] used haptic feedback outside a VR environment while still managing to provide users an enhanced sense of reality. According to Plouzeau et al. [108], it is possible to measure CS acceleration using electro-dermal activity (EDA). Plouzeau et al., changed and adjusted the acceleration to visualize EDA changes. When EDA values increase, the acceleration decreases proportionately. According to research [146], the more predictable the camera movement and acceleration, the lesser the CS effects will be. The slow motion effects technique provides less sudden movements and a lower acceleration rate. This effect works best when combined with blur (image blurring), whose main goal is to return the user to a comfortable state.

3. **Field of view** The application of strategies that manipulate the FoV in commercial games is quite common. Vignette is a technique used to gradually shorten the FoV, thus reducing discomfort in VR environments [41]. A variation of this technique is the one applied in the works of Bolas et al.[12], where the size of the vignette and dynamic FoV are related to the camera acceleration values. Tunnel or Tunneling [144] is also used to solve locomotion problems. Such a strategy reduces the size of the user's FoV at the exact moment of the locomotion, thereby minimizing sensory conflict problems. Similar to the vignette, the tunnel significantly reduces the FoV. However, it is only applied during locomotion.

4. **Depth of field** Some studies include a DoF simulation agent with blur software to minimize the convergence and accommodation problems [21, 113]. The solution presented by Carnegie and Rhee [21] pointed to the decrease of discomfort in HMD applications. Specifically, they suggested a GPU-based solution for the simulation of DoF in these applications. Eventually, ray-tracing techniques can mitigate this problem in a simple way. In an initial work [113], a model of focus and region of interest (ROI) dynamics for visualization of objects in VR was developed. Unlike Carnegie, they use the term "dynamic" to suggest that the model moves the ROI in the 3D scene using the application. This prototype simulates a visual focus self-extraction tool, which limits the ROI in the visual field. The model uses ROI

to determine DoF effects in real time, minimizing discomfort when using HMD. Additionally, [118] designed a methodological guide for CS minimization on VR application. On the other hand, field depth simulation techniques can produce low frame rates, inducing high latency, thereby causing CS. Recently, in the work of [75] and [102], an approach was adopted to apply simulated DoF using an external interface, solving the problem of low frame rate. However, such a strategy is contingent on the application of specific hardware.

5. **Degree of control** Anticipating and preparing the user's visual motion experience can reduce the problem of lack of control by user and consequently the discomfort. According to Lin et al.[88]: *"Having an avatar that foreshadows impending camera movement can help users anticipate and prepare for the visual motion, potentially improving the comfort of the experience"*.

6. **Duration use time** The study by Melo et al. [92] relates the exposure time with discomfort manifestation and also suggests short-term or interval virtual experiences. This principle suggests that if paused periodically, VR applications could avoid CS symptoms. Consequently, the application should allow users to interrupt the experience to take a rest and then be able to return to the exactly point paused before.

7. **Latency-lag** The asynchronous time warp is a method for overcoming latency by improving a rendered (warped) image based on the latest head-tracking data [100]. According to [149] study, this method is based on augmented reality "CamWarp" (that is applied in see-through augmented reality devices) also reduces discomfort in VR environments.

8. **Static rest frame** According to studies [135, 71], people show longer tolerance to discomfort during experiences based on VR projections (example: CAVES). One of the biggest differences between VR and projection-based systems is rest frames. In projection-based systems, the screen edges and real-world visible elements beyond the screens act as rest frames. [10]. This raises the hypothesis that the simulation of rest frames in virtual environments can create comfortable experiences. However, adding elements to create a false rest frame that hides part of the screen may not be a good strategy for all types of VR games. It can work well for racing games, where the player is naturally inserted into a car. However, this approach may not work so well for games with first-person cameras, as they create unnatural circumstances for the player.

9. **Camera rotation** Several other works applied various techniques such as head movement amplification, whereby individual movements are amplified in VR [76], [108]. Another example is the blurring rotation, a technique implemented by Budhiraja et. al [18] that uniformly applies Gaussian blurs based on the magnitude of acceleration and rotation values. There are also experiments deploying more basic techniques that lock the users' head to avoid rotational movements. According to Kemeny et al. [66], such a strategy reduces the CS manifested during rotation by 30% compared with the use of controls to perform rotational movements. Nevertheless, the authors concluded that participants found the technique nonintuitive because it reduced the sensation of presence in the virtual environment. It is worth noting that both this technique and rotation blurring only apply to rotational movements.

10. **Postural instability** In this research, we did not find studies that reported strategies to overcome postural instability‘s CS cause. As with other forms of motion sickness, the feeling can intensify or decrease based on factors such as the length of time exposed to the instability and the magnitude of it. In the same way as our body adjusts to the postural instability on a boat, our body can also adjust to VR postural instability. As our body gradually learns how to control posture and balance in VR, symptoms of motion sickness will likely decrease [4].

3.3 CS Measurements

CS measuring is not trivial. The first problem is that the lack of a unique variable for discomfort level. VR users may experience multiple symptoms and some adverse effects that may not be described in the literature. Another difficulty is the considerable variation of CS susceptibility. Some users are more susceptible to CS symptoms than others. Meanwhile, research shows several ways to capture data for CS quantification. Such data can be classified as subjective, bio-signal and profile data (biological or behavioral profile).

3.3.1 Subjective Data

The best-known way to measure CS in VR is through subjective data captured from users by applying questionnaires. Such a methodology is simple and has been historically used.

Table 3.1: Strategies to overcome cybersickness

Authors	**Strategies**
Langbern (2018) [81]	Teleporting
Farmani (2018) [40]	Tunneling
Sapuri (2017) [133]	Trigger Walking
Berthoz (1975) [8] Pavard (1977) [105] Bouyer (2017) [14]	Haptic Feedback
Plouzeau (2018) [108]	Changes on acceleration
Kemeny (2017) [66]	Headlock
Skopp (2013) [136]	Holosphere
Cirio (2013) [25]	Trajectory Visualization
Budhiraja (2017) [18]	Rotational blur
Carnegie (2015) [21] Porcino (2016, 2017) [113, 118] Konrad (2017) [75] Padmanaban (2017) [102]	DoF Simulation
Waveren (2016) [149]	Async. Time Warping for Latency
Kim (2012) [71] Sharples (2016) [135]	"Cabin" Static Frame
Kim (2017)[68]	Slow-motion
Bolas (2017) [12]	Dynamic FoV
Norouzi (2018) [99]	Dynamic Vignetting
Hillaire (2008) [55] Plouzeau (2018) [108]	Amplified Movements
Hillaire (2008) [55]	Blur Effects
Melo (2018) [92]	Time Exposure Interval
Lin (2004) [88]	Preparing the user‘s visual motion

However, the results can be very subjective and dependent directly on the participants' responses.

The Kennedy Questionnaire (Simulator Sickness Questionnaire - SSQ) [67] is the most cited tool for measuring manifestations reflecting most VR disease problems. In the SSQ, 16 symptoms of discomfort were grouped into three categories: oculomotor, disorientation, and nausea. The oculomotor assembly includes eye fatigue, trouble concentrating, blurred vision, and headache. The disorientation group comprises dizziness and vertigo. The nausea set covers upset stomach, increased salivation, and vomiting urges. When taking the questionnaire, participants classified each of the 16 symptoms on the following scale of discomfort: none (none), mild (mild), moderate (moderate), or severe (severe). The results of the SSQ are calculated and presented on four score scales: total disease (overall) and three sub-punctuations, i.e., oculomotor, disorientation, and nausea. To date, SSQ is the most widely used tool to detect symptoms of CS-associated discomfort [21],[17].

Table 3.2: Strategies associated with causes (1 - Locomotion , 2 - Acceleration, 3 - Field of View, 4 - Depth Of Field, 5 - Degree of Control, 6 - Time Exposure, 7 - Latency, 8 - Static rest frame, 9- Camera's rotation, 10 - Postural Instability, 11 - Speed)

Strategies X Causes	1	2	3	4	5	6	7	8	9	10	11
Teleporting	x										
Tunneling	x								x		
Trigger Walking	x										
Haptic Feedback		x									
Changes on acceleration		x									
Headlock					x						
Holosphere	x										
Trajectory Visualization	x										
Rotational Blur	x								x		
DoF Simulation				x							
Async. Time Warping for Latency							x				
"Cabin" Static Frame								x			
Slow-motion		x							x		x
Dynamic FoV		x	x								
Dynamic Vignetting	x		x								
Amplified Movements									x		
Blur Effects	x	x	x	x					x		
Interval	x	x	x	x	x	x	x	x	x	x	x
Preparing the user`s visual motion					x						

Moreover, each individual has a different CS susceptibility level.The Motion Sickness Susceptibility Questionnaire (MSSQ) [122, 47] was not created for VR but it is sometimes used in VR studies [124]. The MSSQ can be used to determine the time taken by VR users to manifest MS symptoms in VR. This survey contains questions about the frequency with which individuals experience feelings of discomfort similar to those of MS. In MSSQ, the following scale is used: never, rarely, occasionally, and frequently. The issues are grouped into two phases of an individual's life: childhood and last "decade." This census made it possible to account for significant individual differences in MS levels.

Kim H. et al. [69] revised and modified the traditional SSQ, proposing the Virtual Reality Sickness Questionnaire (VRSQ). The New VRSQ has nine items split in two classes of symptoms called "oculomotor" and "disorientation." Some recent research [154] has adhered to VRSQ use. Sevinc et al. [134] state that SSQ is not suitable for VR applications, given the psychometric quality issues. It also states as a disadvantage the fact that tests were conducted on 32 individuals only, which is an insufficient sample of all VR users.

3.3.2 Bio-signal Data

Electrical activity of the brain is bio-signal data that often helps detect illness and behavioral body symptoms. Electroencephalography (EEG) is a monitoring methodology used to record the human brain's electrical activity. Many diseases and brain problems are diagnosed through the evaluation of such devices' data. In adults and healthy people, signs vary depending on different states, for example, awake, aware, or asleep. The characteristics of brain waves also vary according to an individual's age. Brain waves can be distinguished and separated into five different groups of frequency bands. These waves range from low to high frequencies. These are known as alpha, theta, beta, delta, and gamma waves [6, 132].

According to studies [95],[23], it is possible to capture (delta, theta, and alpha) from certain regions of the human brain. Such regions exhibit an Motion Sickness (MS) level. Lin et al. [87] found that 9–10 Hz values in the brain's parietal and motor regions are linked to MS levels. These values increased to 18–20 Hz in individuals exposed to MS. Other studies reported an increase in theta signal in situations similar to MS [59],[98].

An individual's exposure to VR environments can induce stomach reactions. Studies used electrogastrogram (EGG) information to evaluate MS. According to Hu et al. [58] and Xu et al. [153], gastric myoelectric activities are MS indicators. Wink movements are linked to MS emergence [34]. Blinking and eye movement were observed in the work of Kim et al. [72]. Eye-tracking systems can collect information in VR environments (eye movement, pupil diameter, winks quantity, etc.) [110]. Unnatural eye movements can contribute to CS emergence. Eye fixation can minimize the effect of discomfort [156].

Through the body's electrodermic activity, also known as galvanic skin response (GSR), it is possible to obtain information about actions within the autonomic parasympathetic nervous system, which indicate alterations associated with cognition, emotion, and attention levels. [109]. Nalivaiko et al. [97] experimented with rats that were exposed to MS triggering situations. According to the authors, thermoregulation (sweating) disturbance plays a role in the pathophysiology of nausea. Despite testing on rats, similarities with human symptoms are verifiable. The work of Nalivaiko et al. concludes that nausea is part of the body's natural defense against poisoning and so validating the poison theory presented earlier in this review. Body cooling after "toxin" detection possibly represents a beneficial evolutionary "defensive hypothermia." This type of defensive hypothermia occurs in both humans and animals. Therefore, it is possible to conclude that visual or vestibular disorders can trigger the same type of defensive action by the human body. Studies have pointed out that the cardiac rate can significantly increase during experiments that cause MS [72].According to Sugita et al. [143], cardiac frequency can be considered a strong indicator of MS or CS. In VR environments, Yang et al. [155] report that heart disease rates are even higher compared with other environments. Such cardiac elevation can induce visual discomfort [24].

Some studies reviewed during this thesis captured bio-signal data using external medical equipment (see in Chapter 3.4). The latter is not commonly used during RV content production. For this reason, in this thesis, we focus on data captured without the use of such specific accessories. Specifically, we recorded the gameplay data, more detailed in Chapter 5). Thus, this thesis evaluation consists only of data captured without equipment that could affect the user's experience. In other words, we have not used bio-signals in this work.

3.3.3 Profile Data

VR user profile data such as gender, age, health condition, experience, and visual fatigue are associated with manifestations of discomfort.

With respect to gender, women and men see in different ways [2]. According to Biocca et al. [9], women are more inclined to MS manifestations than men. According to

Kolasinski et al. [74], this is due to a gender difference in the peripheral view. Women usually have wider FoVs than men. A wide FoV increases the likelihood of discomfort. Age is another factor that can increase CS or MS sensitivity.

According to Reason [121], susceptibility is a product of an individual's experience as a whole and relates to MS. This theory states that older people have less susceptibility to MS than children, for example. However, several studies [38],[104], [16] showed that older participants were more susceptible to MS than younger ones. According to Arns et al. [5], assuming that CS follows the same pattern as MS may lead to erroneous conclusions.

Previous studies show, for example, that MS is more prevalent in younger groups. However, the study by Arns et al. demonstrated that the opposite happens in the case of CS. This difference may also be because although MS shares some similarities with CS, it does not occur in virtually simulated environments. The theory of Reason et al. [122] treats experience as a whole, that is, life experience (from an individual's birth to one's present). The younger the individual, the less chance one would have to be exposed to such a situation. At the time of those publications, 1975 and 1978, driving and navigating would be experiences children would not normally experience. Nowadays, however, children can be exposed to CS symptoms through VR environments.

Moreover, health conditions can contribute to increased susceptibility to MS or CS once individuals are exposed to favorable environments. According to Frank et al. [45] and Laviola et al. [82], any symptoms, such as stomach pain, flu, stress, hangover, headache, visual fatigue, lack of sleep, or respiratory illnesses, can lead to increased susceptibility to visual discomfort.

Furthermore, flicker is a phenomenon of visual physical discomfort. Such a phenomenon causes physical and psychic fatigue [128]. Flicker sensitivity varies from person to person. An environment with high fps rates will possibly contribute to the user not noticing the flicker [9].

Eye dominance is an important information and has been described as the inherent tendency of the human visual system to prefer scene perception from one eye over the other [111]. According to Meng et al. [93], the eye dominance information can be used as a guide to produce less complex VR scenes without user perception loss based on foveated rendering. An efficient render produces high fps rates. Consequently, a high fps average contributes to avoid virtual reality discomfort.

Previous exposure to MS experiences are key in terms of discomfort susceptibility

[121, 80]. Individuals that are more frequently exposed to MS activities (e.g., driving, playing electronics games, etc) are less susceptible to discomfort. This is most probably due to their ability to predict scenarios and situations in these environments [51].

In this work, we propose the Cybersickness Profile Questionnaire (CSPQ). The CSPQ considers user profile data previously described in this section. In Chapter 4, we provide a more detailed description of CSPQ.

3.4 Machine Learning Approaches

This chapter presents some approaches used to classify CS in distinct virtual reality experiences, such as VR games and immersive videos.

Several studies have been conducted using deep learning models, such as convolutional neural network (CNNs) and recurrent neural networks (RNNs). Kim, J. et al. [70], proposed a deep learning architecture to estimate the cognitive state using brain signals and how they are related to CS levels. Their approach is based on deep learning models, such as long short-term memory (LSTM) RNN and CNN [83, 49, 130, 61]). The models learn the individual characteristics of the participants that lead to the manifestation of CS symptoms when watching a VR video or playing a VR game.

Jin et al. [64] grouped CS causes as follows: hardware characteristics (VR device settings and features), software characteristics (content of the VR scenes), and individual user. The authors used classifiers to estimate the level of discomfort. A total of three machine learning algorithms (CNN, LSTM-RNN, and support vector regression [36]) were used. According to the results, the LSTM-RNN obtained the best results.

Jeong et al. [62] focused on 360° VR streaming content. They analyzed the scenarios where CS is associated with brain signals. Their work uses data from 24 individuals to discover the common characteristics of VR stream patterns associated to CS manifestation. They examined the VR content segments and observed the segments when several individuals felt discomfort at the equivalent time. However, they did not find specific and individual CS causes. Two deep learning models were used: Deep Neural Network and CNN.

Islam et al. [61] presented an automated framework to detect cybersickness levels during a VR immersion. The framework record participants' data at specific intervals using external sensors. They used a pre-trained neural network to predict CS and adjusted the environment using with two CS reduction techniques considering the predicted level of discomfort. Moreover, Islam et al. used a deep neural network comprised of an LSTM and three densely connected layers.

In contrast, some works [103, 46] have made use of symbolic machine learning models, such as bagged decision trees [120], support-vector machines [54], and k-nearest neighbors [27] to estimate and predict levels of discomfort. Padmanaban et al. [103] designed a VR sickness predictor. In this approach, a dataset is created with some questionnaires to evaluate the physiological causes of sickness and individual historical elements to get a more precise result from users. They used the combination of two sickness questionnaires: MSSQ and SSQ, to find a single sickness value. They collected SSQ scores data from 96 participants using a set of 109 one-minute streaming stereoscopic content. Moreover, the training was performed by bagged decision tree on hand-crafted features, such as speed, direction, and depth from each video content.

Garcia-Agundez et al. [46] aimed to classify the level of CS. The proposed model used a combination of bio-signal and game settings. User signals, such as respiratory and skin conductivity of 66 participants were collected. As a result, they mentioned a classification accuracy of 82% (SVM) for binary classification and 56% (KNN) for ternary.

Besides, Kim, J. et al. [70] and Jeong et al. [62] capture data using external medical equipment. This equipment is not mainstream in terms of VR content. We focused on data captured without specific accessories. Hence, we discard the use of any external medical equipment that could harm the user experience.

Further, the above-mentioned works do not classify the CS with actual data obtained during the gameplay. In Jin's work [64], the best result was achieved by recurrent neural networks. This is not a surprise, as the CS is linked to the amount of exposure time and also to a time series problem. Recurrent neural networks (RNNs) show good results for time series problems. Although Islam et al. [61] more closely matches the goals of our study, they used deep learning models and these models are problematic for humans' understanding and interpretation. On the other hand, Padmanaban et al. [103], and Garcia-Agundez et al. [46] used symbolic machine learning models. However, they didn't analyze the discomfort causes and didn't focus on interactive VR applications, such as VR games.

In summary, all these works were focused on predicting the CS manifestation but not the causes. Moreover, most of these works used deep learning models. Although recent approaches apply techniques to make deep learning models explainable [50, 131, 152], the literature is still not strongly affirmed. For this reason, we used symbolic classifiers to analyze the discomfort patterns that give more details about the neural network decisions and has a great support from literature [37, **?**].

Specifically, in this work we proposes the use of a machine learning-based approach to predict the discomfort and further analyze the decision paths along the decision tree to identify one or more causes of discomfort for each user. Moreover, our framework considers the entire VR experience: before, during, and after the participation. As we are interested in understanding the most relevant attributes, the use of symbolic classifiers is paramount for an appropriate analysis and understanding of the decision, as opposed to deep learning methods (more detailed in section 6.1). To perform this investigation, we conduct a data collection involving protocols and experiments.

Chapter 4

Protocols and Experiments

This chapter describes our protocols and experiments, including our data collection methodology and developed games.

As we are aiming to have better control of recorded data during the experiments with users, we used Unity 3D [28] to create two different VR games: (1) a race game and (2) a flight game as shown in Figure 4.2. In our protocol, we require the participants to fill in questionnaires (CSPQ [116] and pre and post VRSQ questionnaires, available in Appendix A and B, only in portuguese) before and after participating in a 5 or 20 minutes VR game session of our games.

Different from Kolasinski et al. [74], we adopted 5 minutes of exposure (instead of 10 minutes) in our first protocol to avoid high incidences of discomfort. 3 of 4 users from the first protocol felt discomfort. For this reason, we adopted 5 minutes as short experience exposure time. Moreover, we further adopted 20 minutes for prolonged exposure to produce high levels of discomfort in participants. More detailed, the long exposure needs more attention and care with participants after the lengthy and discomfort able exposition.

In the race game interaction, the acceleration varies according to the choice of the user (they push the acceleration according to their will). In contrast, the flight game simulates an almost-constant acceleration. The player experience with both games is detailed in Figure 4.1.

The data collection occurred in a few different places such as schools, universities, and technological events. We spent a total of tree months collecting data with two HMD devices (HTC Vive and Oculus Rift). All participants agreed with their anonymous participation in the study and signed consent forms (available in Appendix C, in portuguese).

Figure 4.1: The experience begins with the participants filling the Cybersickness Profile Questionnaire (CSPQ), followed by the VRSQ. Next, participants play the game for 5 (or 20) minutes. Finally, they fill a post-VRSQ questionnaire.

The participants were allowed to quit the experiment whenever they wanted.

4.1 Data Capture

An incrementally improving protocol of data collection was used to gather all the information. We were learning along with the experience and improving the data collection protocol accordingly. In other words, at each protocol, immediately when we noticed a problem in our approach, we stopped the tests to correct the obstacles and started a new protocol. Moreover, we constantly updated our features according to literature research. For this reason, we performed six protocols.

These steps and the knowledge acquired during this process are shown in the following five protocols of data collection (P1, P2, P3, P4, P5, and P6) shown in Table 4.1.

- P1: In protocol one, just the race game is used. In total, four participants (ages ranging from 18 to 60 years) participated, 1 female and 3 male. In this protocol, gameplay data was recorded at every second. The camera view was also captured along with the gameplay data.

- P2: Gameplay tests were conducted with four participants (1 woman and 3 men), where ages ranged from 18 to 36. At this stage, the gameplay screen was not longer captured in order to avoid drops and variations of frame rate. Next, the flight game was included in the data collection, where participants were able to freely select one of the two games for the VR experience. At this point, we also collected data using the SSQ form.

- P3: Six participants (1 woman and 5 men) participated in this protocol. A total of three participated in the flight game (1 woman and 2 men), and 3 men in the race game. User ages ranged between 18 and 36. In this step, we captured the user discomfort using voice recognition commands as they played.
- P4: Both games were brought to a public technology event called the Symposium on Virtual and Augmented Reality (SVR). A total of 37 participants (7 women and 30 men) participated, where 25 played the flight game and 12 the race game. We included the VRSQ questionnaire before and after the user participation.
- P5: Experiments were performed using two HMD devices: Oculus Rift CV1 and HTC Vive. A total of 35 individuals participated in the experiment (9 females and 26 males). Twenty experienced the flight game, whereas 15 participated in the race game. The ages of the 18 participants varied from 18 to 54 years old.
- P6: Long-exposure experiments were performed using Oculus Rift CV1. A total of 2 males participated, 42 and 44 years old. In this case, we conducted 20 minutes of VR exposure for each game experience. We warned participants that they could experience highly uncomfortable sensations. For safety reasons, after the complete exposure, we provided 5 minutes of adequate rest for each participant to self-recovery from CS symptoms.

No overlap of participants was recorded during the six protocols of data collection. In other words, all participants are different participants for each instance of user data. At the end of protocol 6, a total of 37 valid users (9 women, 28 men) with ages ranging between 18 and 60 answered all the questionnaires correctly and completed the whole game interaction.

Each participant was required to complete four (Figure 4.1) tasks in P5 (short-exposure) and P6 (long-exposure), as follows:

- fill in the profile questionnaire (CSPQ). This questionnaire considers gender, age, previous experience with virtual environments, flicker sensitivity, any pre-symptoms (such as stomach pain, flu, stress, hangover, headache, visual fatigue, lack of sleep or respiratory diseases), any vision impairments, presence of eyeglasses, posture (seated or standing) and eye dominance.
- fill in the VRSQ questionnaire [69];

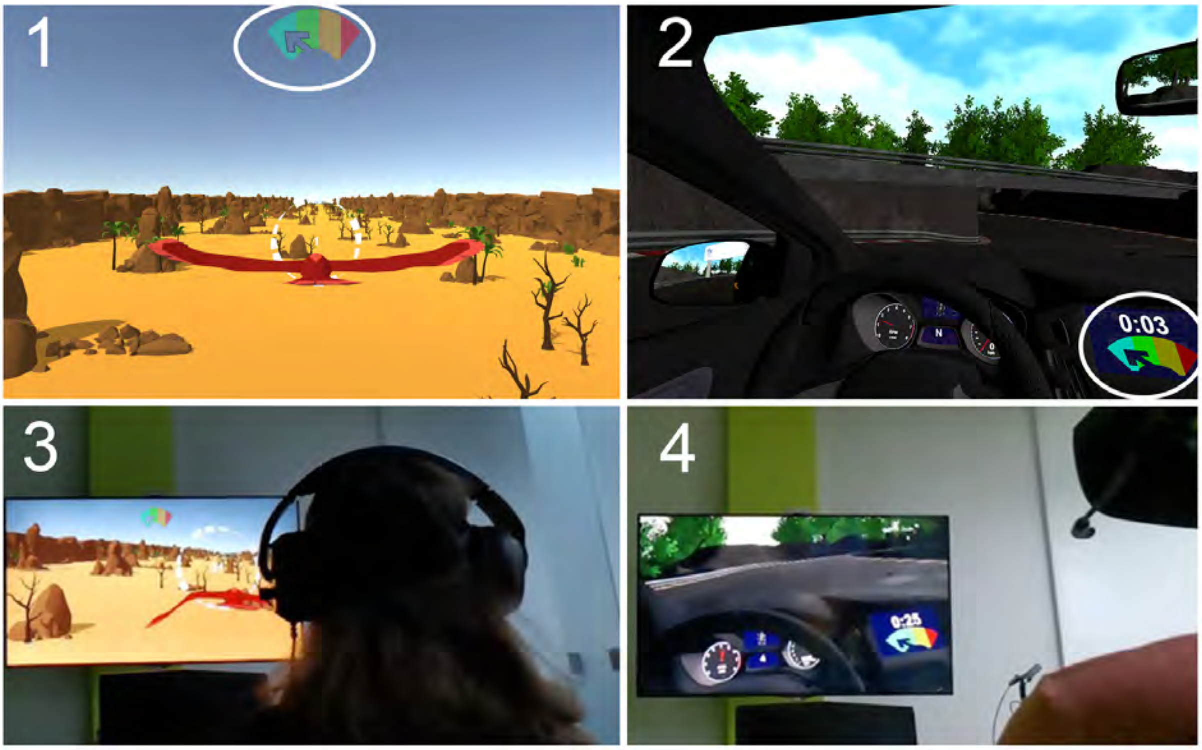

Figure 4.2: Participants playing the flight game at the left (1 and 3) and the race game at the right (2 and 4). In images 1 and 2, it is possible to see a visual feedback of their current discomfort level, marked with a circle.

- participate in one of the VR games for up to 5 minutes (in P5) and 20 minutes (in P6) while mentioning the numbers 0 (none), 1 (slight), 2 (moderate), or 3 (severe) for each time their level of discomfort changed during the gameplay experience;
- and, at last, fill in the VRSQ questionnaire after the experience.

The preliminary dataset, after applying these incremental and experimental protocols, our dataset contains 28 attributes obtained from the following sources: profile data, questionnaire data, and gameplay data. All the features were captured considering two dependent variables: type of hardware and type of game. The complete recorded parameters are found in Table 5.1. Moreover, the applied VRSQ questionnaires estimated the prevalence of cybersickness for participants in P5 and P6 protocols.

4.2 VRSQ Results

The scores in Figure 4.3 were obtained from the VRSQ output values [69]. Some P5 participants (8 from the race game and 12 from the flight game) were associated to zero discomfort according to the VRSQ. These cases were justified as follows:

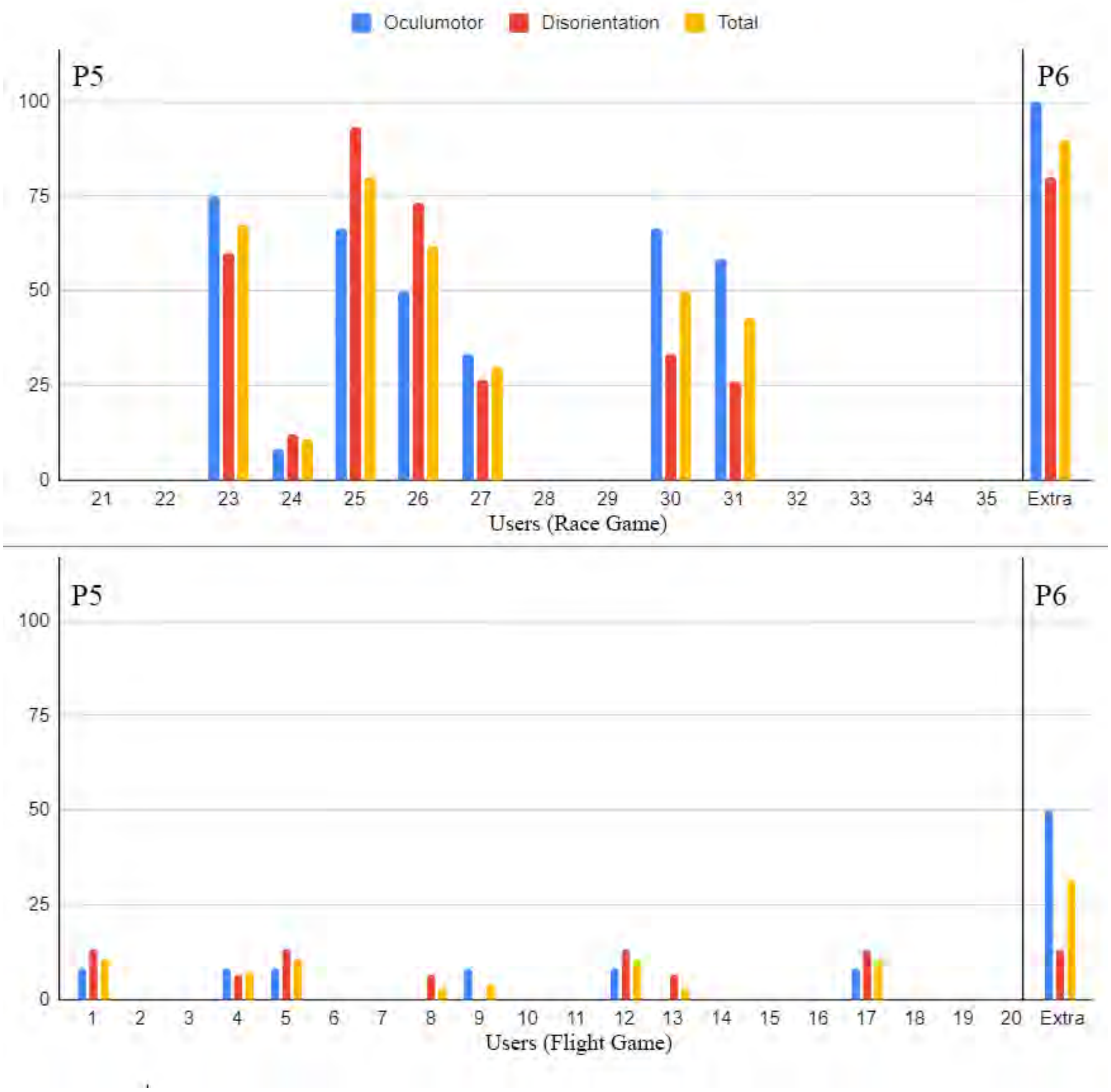

Figure 4.3: Obtained VRSQ scores in P5 and P6. Concerning both game scenarios, 15 users achieved positive scores from P5 and 2 from P6.

Table 4.1: Five experimental Protocols (P1, P2, P3, P4, P5, and P6) and the captured features in each of them.

Features	P1	P2	P3	P4	P5	P6
Number of participants						
Total	4	4	6	37	35	2
Gender identification						
Male	3	3	5	30	26	2
Female	1	1	1	7	9	0
Age range						
18 to 36	2	4	6	33	28	0
37 to 50	2	0	0	4	4	2
above 50	0	0	0	0	3	0
Used hardware						
Oculus Rift CV1	4	4	6	37	15	2
HTC Vive	0	0	0	0	20	0
Game						
Race	4	0	3	12	15	1
Flight	0	4	3	25	20	1
Exposure in minutes						
Race	5	5	5	5	5	20
Flight	5	5	5	5	5	20

- The participant immediately felt better when removing the HMD equipment, and for this reason, the participant replied as “feeling no discomfort”.
- The participant did not experience discomfort during the experiment.
- The participant marked the questionnaire with no care.

The scores in Table 4.2 were obtained from the VRSQ [69]. Twenty participants scored 0. In terms of VRSQ results, 8/16 users from the race game scored positive for CS. When it comes to the flight game, 9/21 users reported discomfort. These scores represent 50% and 42.8%, respectively. The following aspects justified the zero discomfort cases:

- The participant immediately felt better when removing the HMD equipment, and for this reason, the participant replied as “feeling no discomfort”.
- The participant did not experience discomfort during the experiment.
- The participant marked the questionnaire with no care.

For this reason, the further experimental analysis of this work (ranking of causes)

Table 4.2: A summary of valid recorded data in race and flight games. Concerning both scenarios, 11722 instances were captured, and 17 participants achieved positive scores for VRSQ (in highlight).

Race Game				**Flight Game**			
User	Instances	Exposure (minutes)	VRSQ (total)	User	Instances	Exposure (minutes)	VRSQ (total)
21♂	300	5	0	1♂	103	1.71	10.83
22♂	104	1.73	0	2♂	300	5	0
23♂	300	5	67.5	3♀	300	5	0
24♂	300	5	10.83	4♂	300	5	7.5
25♂	300	5	80	5♂	102	1.7	10.83
26♂	300	5	61.6	6♂	300	5	0
27♂	300	5	30	7♂	300	5	0
28♀	24	0.4	0	8♂	300	5	3.3
29♀	300	5	0	9♀	300	5	4.16
30♀	287	4.78	49.9	10♂	300	5	0
31♀	250	4.16	42.5	11♂	300	5	0
32♀	300	5	0	12♂	300	5	10.83
33♂	300	5	0	13♂	52	0.86	3.33
34♀	300	5	0	14♂	300	5	0
35♀	300	5	0	15♂	300	5	0
ExtraA♂	1200	20	90	16♂	300	5	0
				17♂	300	5	10.83
				18♂	300	5	0
				19♂	300	5	0
				20♂	300	5	0
				ExtraB♂	1200	20	31.6
Total	**5165**	**86.08**	**432.33**		**6557**	**109.28**	**93.21**

considers just the data from users whose VRSQ scores were positive. This translates to a total of 17 participants out of the 37 mentioned before (Figure 4.3 and Table 4.2).

Specifically, at each second of gameplay, we collect a new instance, and in total, we recorded 11722 instances with the same attribute set. In other words, the more precise way to look at this problem is to be second-oriented, as the instance (or each second) is the object of classification in terms of prediction of CS manifestation and further analysis.

4.3 Identification of Relevant CS Prediction Data

Following the observations obtained through the experimentation stage, we proposed a preliminary dataset composed of 28 (all) attributes obtained from the following sources: profile data, questionnaires data and gameplay data. All these features are captured taking into account two dependent variables: type of hardware and type of game. The complete profile and gameplay parameters recorded can be observed in Table 5.1.

The profile data was selected based on the literature and also on the experience acquired during pilot tests for this work. We gathered this data through our CS Profile Questionnaire (CSPQ). The CSPQ available in Appendix C (in portuguese) contains nine questions such as:

- **Gender** - The gender of the participant is noted [9], [74] and women are more likely to experience visual discomfort compared to men.
- **Age** - We recorded the age of participants in three who are divided into three groups (18-36, 37-50, and above 50). According with studies, older participants are more susceptible to CS compared to younger ones [73], [123].
- **Experience in VR** - Level experience of the user with virtual environments was divided into two categories (without experience, with experience). According to Reason [121] sickness susceptibility is a product of the individual's overall experience with MS.
- **Flicker sensitivity** - Users are asked whether they feel discomfort when they are near the digital screens in order to discover the user's flicker sensitivity. Flicker is a phenomenon of visual physiological discomfort and may cause physical and psychic fatigue in users in the vicinity of the disturbing load [128].

- **Pre-symptoms** - Health conditions can contribute to increased susceptibility to MS or CS when individuals are exposed to favorable environments. According to Frank et al. [45] and Laviola et al. [82], any symptoms, such as stomach pain, flu, stress, hangover, headache, visual fatigue, lack of sleep or respiratory diseases can lead to increased susceptibility to visual diseases.

- **Glasses Wearing** - According to Rebenitsch [123], vision correction can be correlated with CS and the correction of glasses for better view can create additional refraction of light and make a participant more able to feel CS symptoms.

- **Vision Impairments** - Although HMDs are compatible with the use of glasses or lenses by users with vision problems, we decided to ask if the user has one or more vision problems, such as myopia, hypermetropia or astigmatism.

- **Posture** - Postural instability is the reactive response to information incorrectly received by the vestibular and visual organs. According to Stroffegen et al. [141], the effects of postural instability precede CS symptoms, if they occur in VR environments. We also noted whether the user was seated or standing.

- **Dominant Eye** - According to Collins and Blackwell [26] most people have one dominant eye. In other words, the dominant eye sees more frequently and longer than the less dominant eye. HMDs show images to each eye simultaneously and separately. Because of this reason, we considered whether eye dominance has any connection to CS susceptibility and questioned the user for his dominant eye.

The questionnaire data contains information filled in by the user about discomfort symptoms before and after the experiment. The symptoms listed are from the VRSQ [69] (available in Appendix B in portuguese), which is a modified version of Kennedy's traditional SSQ to address specifically virtual reality environments with HMDs and the non-categorical (which are numerical or boolean) features considered are:

(1) The game data such as timestamp, speed, acceleration, player rotation axis, player position, the region of interest, size of the FOV, frame rate and discomfort level, class reported by the user at any time during the gameplay. (2) Boolean information such as existence of static resting frames, the existence of haptic response, level of user control over the camera, the existence of depth of field simulation (DoF) and whether the game primary camera moves automatically (without user intervention) or not.

For categorical features, all passed by a discretization process (Table 4.3).

Table 4.3: Categorical features after the discretization process

Categorical Features Values Mapping					
Gender		**Pre-Symptoms**		**Region of Interest**	
Female	0	No	0	Foreground	0
Male	1	Yes	1	Middleground	1
Age		**Vision Impairments**		Background	2
18-36	0	None	0	**Static frame**	
37-50	1	Myopia	1	No	0
above 50	2	Astigmatism	2	Yes	1
VR Experience		Astig. and Myopia	3	**Haptic feedback**	
Without	0	Hyperopia	4	No	0
With	1	Astig. and Hyper.	5	Yes	1
Flicker sensitivity		**Dominant Eye**		**Degree of Control**	
None	0	Left	0	None	0
Some	1	Right	1	Half	1
Glasses Wearing		**Posture**		Total	2
No	0	Sitted	0	**Dof Simulation**	
Yes	1	Standing	1	No	0
				Yes	1
		Automatic Camera		**Player Locomotion**	
		No	0	No	0
		Yes	1	Yes	1

Chapter 5

Prediction of CS Manifestation

The manifestation of CS symptoms can occur due to several factors and configurations. As presented in the Cybersikcness literature review chapter, some of them use biological signals to quantify CS. Such data are already used by modern medicine to early detect diseases and malfunctions (i.e: heart problems). However, the use of specific equipment for capturing biological signals is intrusive and not practical.

As mentioned before, CS problems traditionally are quantified through discomfort questionnaires (such as SSQ, VRSQ) and susceptibility (by using the MSSQ). Such questionnaires are widely used nowadays and most of them focus their strategy for collecting subjective data of the state of the participant. However, in our research we noticed that the SSQ is not specifically aimed at detecting the CS but rather for quantifying the simulator sickness. For this reason, the use of VRSQ was chosen. However, no susceptibility identification questionnaires were used to quantify CS.

Moreover, for problems involving CS, the classifiers based on deep learning is proved to be a most suitable one, as CS problems associated with the time of using HMD devices are known. On the other hand, deep network classifiers are complex to understand. In other words, even if they produce a goo final result, it is not trivial to discover the reasons for what reasons the neural network made such a decision. In contrast, decision trees and random forests are examples of symbolic machine learning that support human readability.

In this part of this thesis, we are interested in understand which are the most relevant attributes in observed CS situations and which are best classifiers in terms of human interpretability. After this, the methodology of this research will be based on the combination of both subjective data (from users) and gameplay information, collected during users' interaction with the VR environment. However, for a supervised machine-learning algorithm to learn, needs examples of outputs for a given set of attributes.

These output attributes are defined as classes. In the context of this work, the classes can be considered analogous to the four levels of SSQ discomfort (none, slight, moderate and severe). To capture data during the interaction and classify them in relation to the four levels of discomfort, we created interactive experiments where the user could interact and label in real time his level of discomfort. In addition to the data of the participants (subjective data), real time game data such as acceleration, head orientation, scene position among others, are also recorded. As far as we know, this combination of data is a totally novel approach in the context of data collection and machine-learning usage.

Table 5.1: Raw feature set captured in Protocols 5 and 6, which contains numerical (N) and categorial (C) features.

Preliminary Feature set			
Gameplay data		Users data	
Feature	Type	Feature	Type
Time Stamp	N	Gender	C
Speed	N	Age	C
Acceleration	N	VR Experience	C
Rotation (x, y and z)	N	Flicker sensitivity	C
Position (x, y and z)	N	Pre-symptoms	C
Region Of Interest	C	Glasses wearing	C
Size of FOV	N	Vision Impairments	C
Frame Rate	N	Posture	C
Static Frame	C	Dominant Eye	C
Haptic Feedback	C	Discomfort Level	N
Degree of Control	C		
DoF Simulation	C		
Player Locomotion	C		
Automatic Camera	C		

5.1 Weka's Classifiers Evaluation

In machine-learning, it is a common practice to validate the data and ensure that its format is valid before starting the training process. To ensure that, the collected and recorded raw data are converted into categorical values in a discretized pattern. Redundant attributes and objects in each data set are removed.

Our proposal is based on symbolic classifiers based on decision trees, such as random forest (RF). RFs or random decision classification, regression and other tasks that operate by constructing a multitude of decision trees at training time and outputting the class that is the mode of the classes or mean prediction of the individual trees. Using RF the input of each tree is tested from the original dataset. Moreover, a subset of features is randomly picked from these arbitrary features to improve the tree per node. Typically, random forest facilitates a wide number of inadequate classifiers to form a strong classifier [89].

We also evaluated other decision tree-based symbolic classifiers, such as BF Tree, CDT, Decision Strump, ForestPA, FT, Hoeffding, J48, J48 Graft, JCHAID Star, LAD Tree, Logistic model trees (LMT), Nb Tree, Random Tree, Rep Tree, and Simple Cart.

For validating the predictive model we use of k-fold cross-validation for all evaluated symbolic classifiers. Tripathi and Taneja [148] define k-fold cross-validation as a statistical method to estimate the machine-learning potential associated with a predictive model. This method is generally used for comparing and selecting a model for a given predictive modeling problem.

5.1.1 Classification Procedure

Once the data is collected, machine learning algorithms were trained to classify the CS in Weka [52]. Each of the inputs stored by the experiment contains a rating given by users related to discomfort (from 0 to 3, where 0 is none and 3 is severe) during the gameplay.

To further analyze the collected data, we categorize the experiments into three main scenarios: A, B and C. These scenarios are:

- Scenario A classification consisting of data from the Racing game in P5 protocol (3993 samples).
- Scenario B classification consisting of data from the Flight game in P5 protocol (5397 samples).
- Scenario C classification using data from both scenarios together A and B in P5 protocol (9390 samples).

Experiments were run using a 10-fold cross-validation in all scenarios. We also separated scenarios A, B, and C into two new groups. The first group is a binary classification (0-none or 1-discomfort, which includes from slight to severe classes). The second group is a quarterly classification containing all four classes (none, slight, moderate and severe).

The distribution of classes can be seen in Figure 5.1. Although the quarterly classification prevailed unbalanced, we still stored it because other researchers can explore, conduct further analysis, and obtain new results.

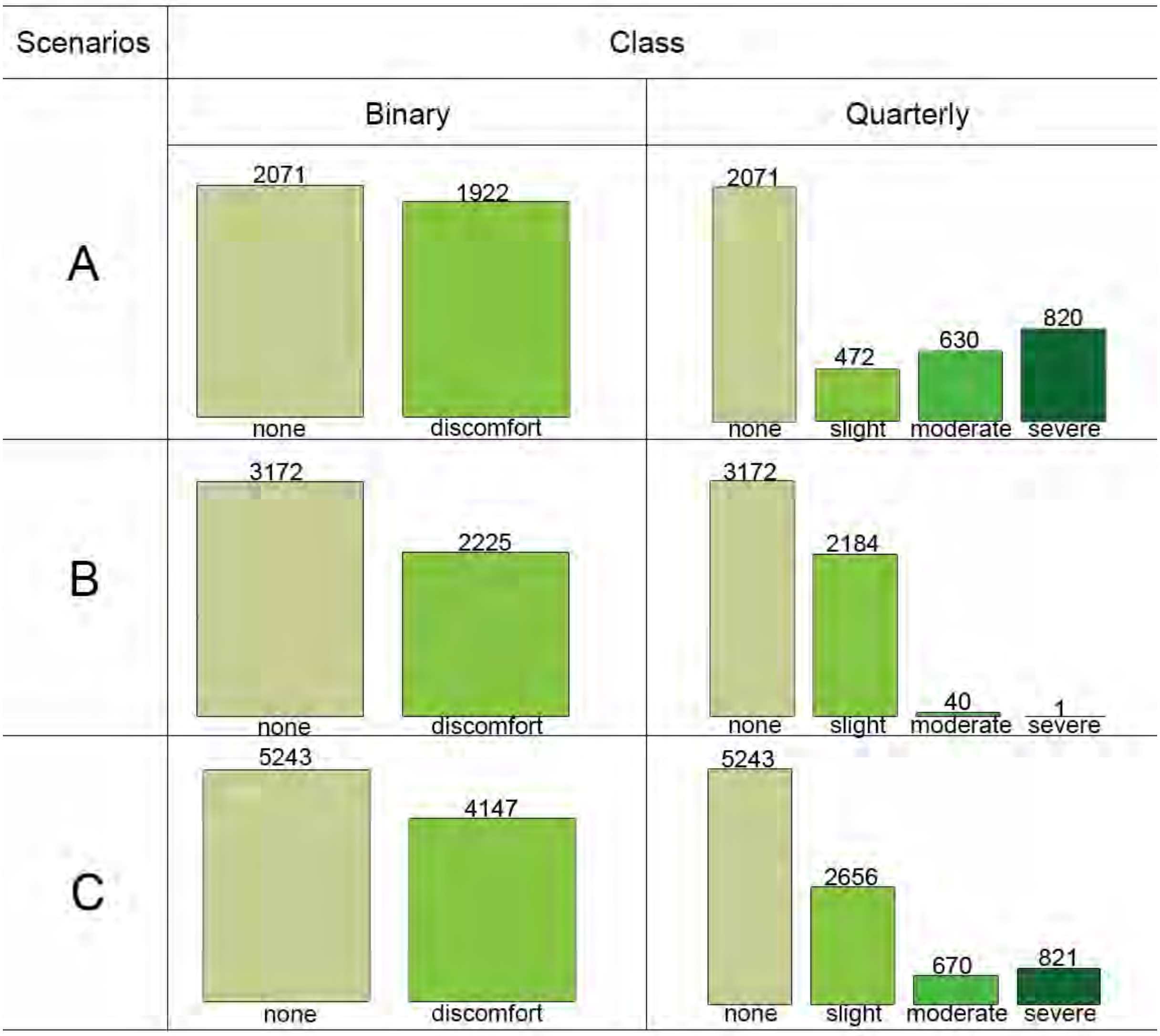

Figure 5.1: Binary and quarterly class samples distribution in scenarios A (Racing game), B (Flight game) and, C (both games).

Tables 5.2 and 5.3 show the accuracy and Kappa index for binary and quarterly classifications over scenarios A, B, and C.

5.2 Preliminary Results

This section presents the obtained results with the analysis of the captured data in the P5 protocol and usage of the developed immersive environments.

5.2.1 Gender Differences Analysis

To perform the first analysis of the recorded data, we build a data visualization application using Unity 3D (Figure 5.2). This application read our recorded dataset in CSV format and create graphical visualizations using position and discomfort attributes from data acquired in our protocols.

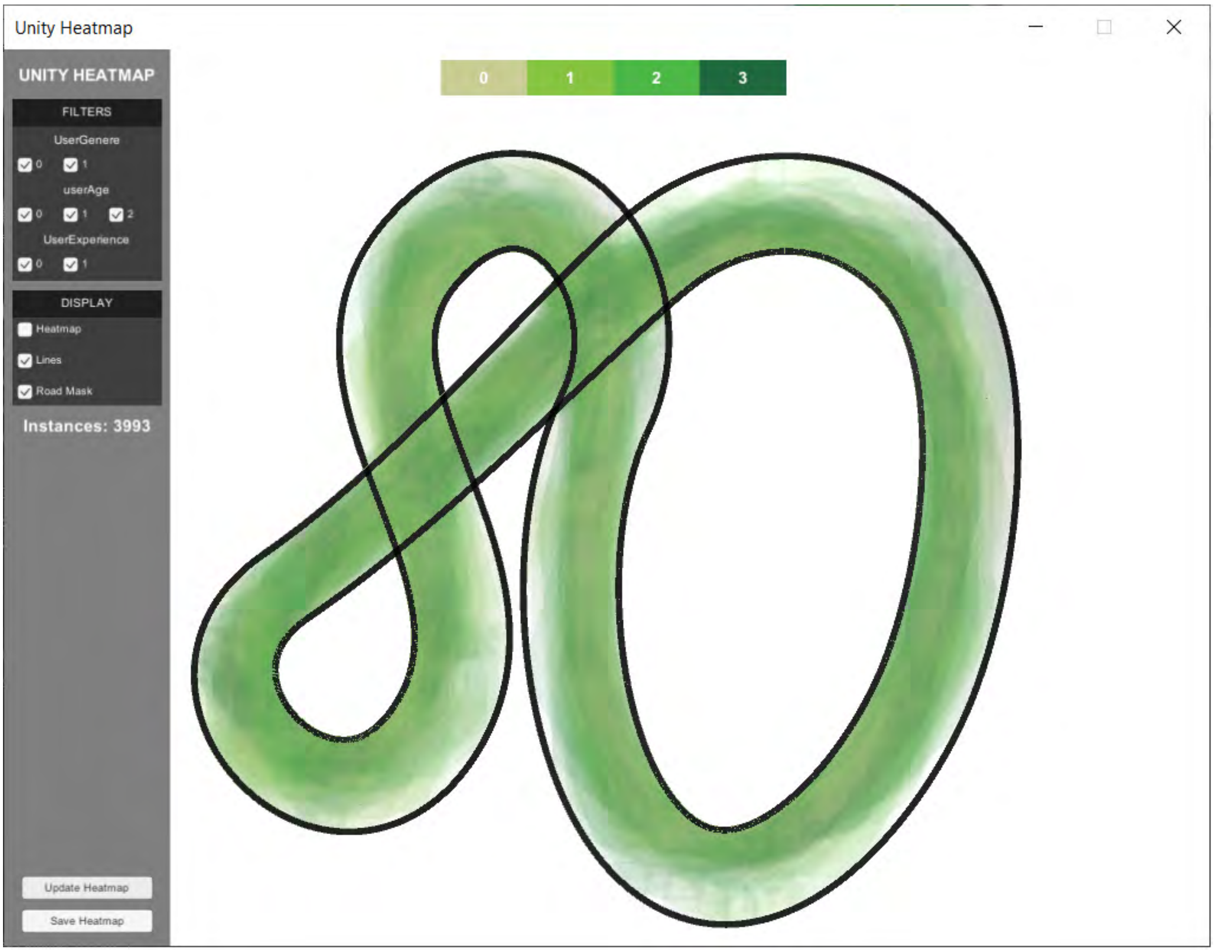

Figure 5.2: Race game data visualizer application was developed in this work to perform the first analysis without machine learning support

In this analysis, we used 3993 samples from P5' race game recorded data. We observed that the occurrence of the discomfort reported by individuals occurs throughout the track (Figure 5.3) using position and discomfort level data presented in Table 5.1. However, the discomfort levels in specifics regions of track have a more significant accumulation.

In a comparative sample of reports of discomfort between individuals of the female gender (7 females with 1772 samples) and male (8 males with 2221 samples), We observed that in an accumulated result, the male participants reported discomfort values greater than zero more often than individuals of the female gender (illustrated in Figure 5.4).

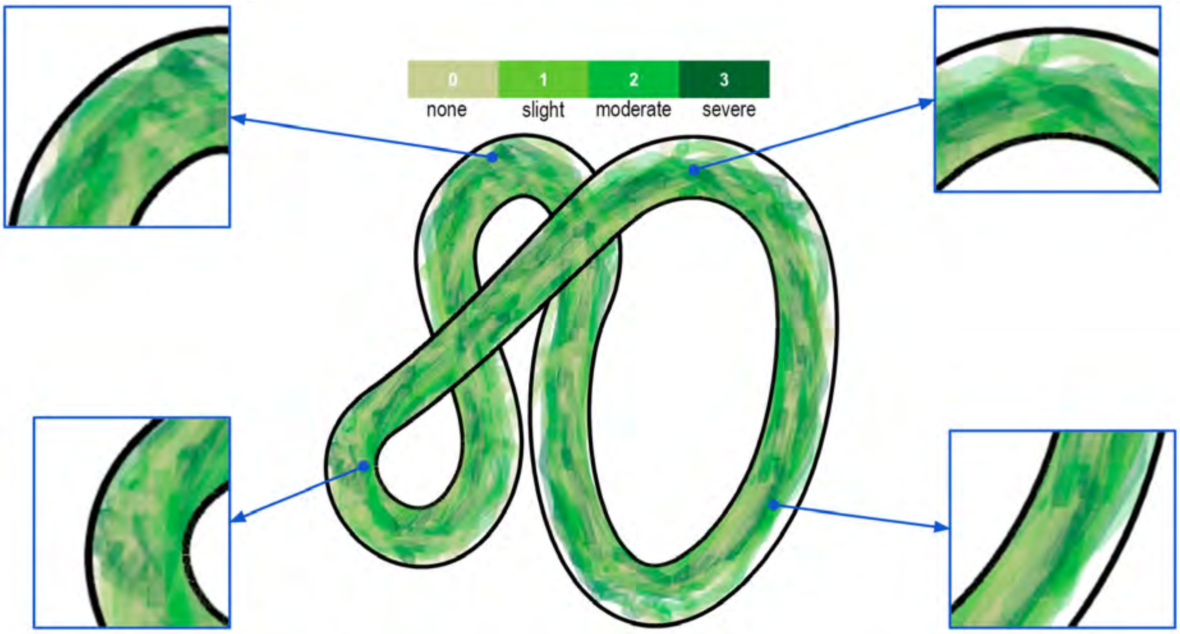

Figure 5.3: Visualization of all moments where the participants of the elapsed game reported some of the levels of discomfort during the experiment. In the image, the intensity of discomfort reported by users varies from 0 (none) to 3 (severe) represented by the legend colors

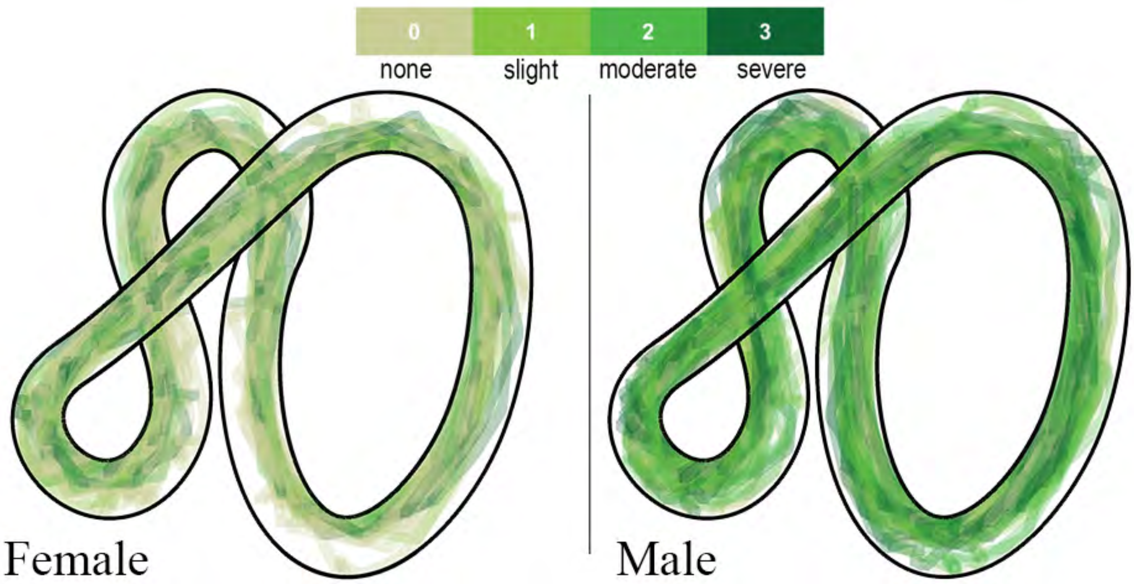

Figure 5.4: comparative of the discomfort reported by female and male participants. In the image, the intensities of discomfort reported by users vary from 0 (none) to 3 (severe) represented by the legend colors.

Biocca [9] and Kolasinski [74], who report those female individuals are more susceptible to symptoms of MS. Despite being similar diseases, they have different environments and manifestations. Because of this, for this case, there is no way to say if there is a difference between genders for the manifestation of CS-based only on Biocca [9] and Kolasinski [74] works cited in this thesis. However, in this specific testing stage, the race track analysis results showed that the female audience reported less discomfort than the male audience.

Furthermore, we checked men participants performed the race game more competitively than women during the experiment, alternating acceleration shift frequency, and even crashing into track's corners. On the other hand, women played with near-constant acceleration shift frequencies avoiding collisions.

Additionally, Curry et al. [30] conducted a similar experiment. They examined (with SSQ) the influence of gender susceptibility and vehicle control on discomfort in two different VR experience tasks, where participants played (as vehicle driver) or viewed (as vehicle passenger) the game for up to 15 minutes. They also verified who had discontinued early in these experiences. Concerning MS incidences, the authors found no MS discrepancies among the participant's gender or groups (drivers and passengers). On the other hand, according to the authors, females participants discontinued early because of discomfort. In other words, the VR exposure time for female participants was significantly less than for male participants. Moreover, the authors were limited to 2 tasks and not deeply explored other virtual reality tasks associated with virtual reality discomfort.

According to recent studies [86, 48, 30], female individuals experienced better performance or magnified cognitive skills, localization, and picture tasks in VR than males. These results corroborate and suggest that gender differences in cybersickness may change besides different tasks in virtual reality environments.

Considering the gender attribute analysis we observed from the P5' captured data of the race game (3993 samples, from 15 participants where seven are females and eight are males) that female individuals reported lower incidents of discomfort compared to male participants, as shown in Figure 5.5. This finding disagrees with literature in which Biocca [9] and Kolasinski [74] report that female individuals are more susceptible to symptoms of MS. However, such behavior was only observed in MS scenario and not in CS scenario. Anyways these findings need to be further investigated taking into account more samples and also with other games. Besides that, we were able to observe this effect only in the race game because in the flight game the gender data was not well distributed.

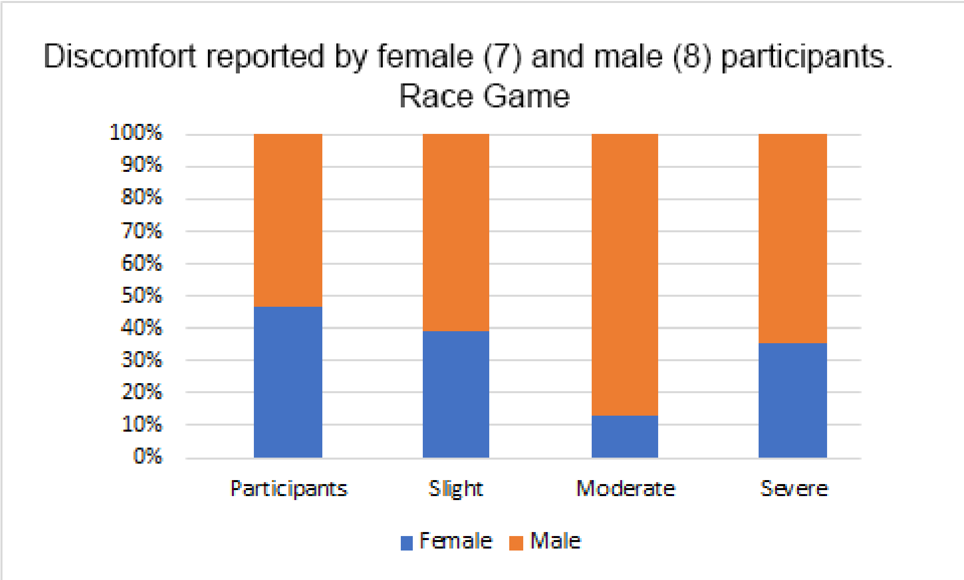

Figure 5.5: Comparison of the discomfort levels reported by female and male participants in the race game.

5.2.2 Binary Classification

As previously mentioned, we also merged the discomfort level into a single class in order to perform binary classifications, which are usually stronger than non-binary ones. Discomfort values that were previously represented as slight, moderate, and severe are represented as discomfort.

For all scenarios, that is, Scenario A, B, and C, the RF classifier is proved to be the best with an accuracy of 94.0%, 99.0%, and 96.6% for the binary case.

5.2.3 Quarterly Classification

For the quarterly classification, the dataset was not changed. This set of experiments were conducted based on four classes: none, slight, moderate and severe. In Scenario A, the classifier LMT achieved the best result, with accuracy of 92.4%. In the Scenario B, the best result was obtained with RF (98.9%). For Scenario C, RF also obtained the best classification accuracy (95.4%).

Tables 5.2 and 5.3 shows the Accuracy (ACC) and Kappa (KPP) index for binary and quarterly classifications over scenarios A, B and C. More detailed, the Kappa index is a metric that correlates an observed accuracy with predictable accuracy resulting in a K value. We used the kappa index to evaluate multiple classifiers amongst themselves. More detailed, K=1 indicates chance of agreement. A value greater than 0 means the

Table 5.2: Weka's binary classification

Binary Classification						
Scenarios	A		B		C	
Classificator	ACC	KPP	ACC	KPP	ACC	KPP
BFTree	91.8%	0.8364	96.8%	0.9353	93.0%	0.8584
CDT	89.7%	0.794	96.8%	0.9346	92.3%	0.8457
DecisionStrump	62.0%	0.2574	71.9%	0.4299	61.6%	0.2713
ForestPA	91.5%	0.8297	97.8%	0.9563	95.5%	0.909
FT	87.0%	0.7395	94.2%	0.881	90.9%	0.8154
Hoeffding	69.9%	0.393	78.1%	0.5363	71.9%	0.4251
J48	92.4%	0.8495	97.9%	0.9576	95.2%	0.9036
J48Graft	92.6%	0.853	97.9%	0.9575	95.2%	0.9036
JCHAIDStar	89.8%	0.7968	92.8%	0.894	91.6%	0.8582
LADTree	78.9%	0.5812	88.9%	0.7722	74.1%	0.4829
LMT	93.0%	0.86	98.1%	0.961	95.5%	0.9088
NbTree	88.1%	0.7624	98.6%	0.9728	95.0%	0.8993
RandomForest	**94.0%**	**0.8805**	**99.0%**	**0.9801**	**96.6%**	**0.9323**
RandomTree	89.2%	0.7838	96.6%	0.93	92.2%	0.8421
RepTree	90.7%	0.8147	96.9%	0.9368	93.0%	0.8595
SimpleCart	92.2%	0.8455	97.2%	0.9441	93.4%	0.8672

classifier is doing better. In other words, the higher the kappa index value betters the results of the classifiers [138].

5.2.4 Attribute Evaluation

As we are interested in better understanding of the causes involved in the discomfort event, we have to evaluate the attributes involved in the CS prediction decision.

We ranked the features in terms of importance using the Weka [52] classifier attribute evaluator, using the full training set and the "leave one attribute out" option. This strategy generated a ranking of all attributes using the best classifier of the previous experiments (Tables 5.2 and 5.3).

Specifically, this algorithm removes attributes from the dataset and evaluates how its removal influences on the performance of the classification, using this importance to create the final ranking. This result is shown from top to bottom in order of importance in Table 5.4 and Table 5.5.

For binary classifications and Scenario A (racing game), the most relevant attributes considered were (Table 5.4) : timestamp (time exposure amount), age, gender, rotation on

Table 5.3: Weka's quarterly classification

Quarterly Classification						
Scenarios	A		B		C	
Classificator	ACC	KPP	ACC	KPP	ACC	KPP
BFTree	88.8%	0.827	97.1%	0.9417	93.0%	0.8821
CDT	86.3%	0.7854	96.5%	0.93	92.3%	0.8698
DecisionStrump	51.0%	0	71.6%	0.4294	55.8%	0
ForestPA	87.6%	0.8017	97.4%	0.947	94.2%	0.9015
FT	83.1%	0.7375	93.7%	0.8731	89.4%	0.8227
Hoeffding	52.5%	0.0401	73.8%	0.4882	55.8%	0
J48	90.7%	0.8566	97.8%	0.9569	94.8%	0.9139
J48Graft	90.9%	0.8598	97.7%	0.9547	95.0%	0.9162
JCHAIDStar	77.7%	0.6513	92.3%	0.8793	86.0%	0.7824
LADTree	68.5%	0.4996	87.0%	0.7333	72.1%	0.4694
LMT	92.4%	0.8832	97.8%	0.9566	95.5%	0.9249
NbTree	88.7%	0.8246	98.7%	0.9747	94.4%	0.9052
RandomForest	**92.2%**	**0.8782**	**98.9%**	**0.9792**	**95.4%**	**0.9221**
RandomTree	85.1%	0.7709	96.8%	0.9355	89.5%	0.8243
RepTree	87.0%	0.7962	96.7%	0.9328	92.6%	0.8755
SimpleCart	88.9%	0.8288	97.3%	0.9464	93.0%	0.8821

the z-axis, and player speed. For Scenario B (flight game), attributes are as follows: age, VR experience, vision impairment, rotation on the z-axis, and timestamp. For Scenario C (both games), timestamp, age, gender, and player speed.

These ranking of positions of attributes for the different scenarios are also validated by the literature [82], [13], [122], [9]. For two out of three test scenarios, the timestamp was considered the most important for the classification of discomfort. Player speed, rotation on z-axis as well as gender and age were also essential attributes [9].

In quarterly attribute evaluation (Table 5.5), we obtained very similar results. For Scenario A: timestamp, age, gender, VR experience, and player speed were the top five. In Scenario B, the most relevant attributes were: age, VR experience, and vision impairments. In Scenario C: timestamp, age, gender, rotation on the z-axis and VR experience are important attributes [9].

Table 5.4: Weka's binary classification attribute evaluation

Binary Attribute Ranking (Leave One Attribute Out)			
Rank	Scenario A	Scenario B	Scenario C
1 (best)	Timestamp	Age	Timestamp
2	Age	Position Z	Age
3	Gender	VR Experience	Gender
4	Rotation Z	Vision Imp.	Player Speed
5	Player Speed	Rotation Z	Position Z
6	VR Experience	Timestamp	VR Experience
7	Rotation X	Rotation X	Vision Imp.
8	Rotation Y	Speed	Rotation Z
9	Eye Dominance	Eye Dominance	Rotation X
10	Region of Interest	Position Y	Auto Camera

Table 5.5: Weka's quarterly classification attribute evaluation

Quarterly Attribute Ranking (Leave One Attribute Out)			
Rank	Scenario A	Scenario B	Scenario C
1 (best)	Timestamp	Age	Timestamp
2	Age	Position Z	Age
3	Gender	VR Experience	Gender
4	VR Experience	Vision Imp.	Rotation Z
5	Speed	Timestamp	VR Experience
6	Rotation Z	Rotation X	Player Speed
7	Eye Dominance	Rotation Z	Position Z
8	Rotation Y	Speed	Vision Imp.
9	Rotation X	Gender	Rotation X
10	Position X	Eye Dominance	Position Y

Chapter 6

Identification of Causes

For our experimental approach, we merged the top six features for each one of the scenarios A and B (race and flight games) shown in Table 5.4. In addition, we discarded the position attribute. The position attribute is specific to each game and can produce overfitting or even end up producing low accuracy rates when used with games other than the ones used during the training protocol.

In specific, the acceleration and frame rate attributes did not appear in the binary attribute ranking created by the Weka algorithm. However, we still include these attributes on the following experiments considering their importance to specific developed games.

Conversely, the timestamp is indirectly associated to nearly all the other features. For this reason, we considered two evaluation methods, the first one using the feature set presented in Table 6.1, and the the second evaluation, we include the timestamp as an additional feature (Table 6.2). Later, extracted features were used as training data to construct the decision tree and random forest models.

Table 6.1: Feature set (without timestamp)

Gameplay data	Profile data
Speed	Gender
Acceleration	Age
Rotation Z	VR Experience
Frame Rate	Discomfort Level

Later, the data were sent to classifiers to construct the decision tree and random forest models. In what follows, we shift the attention toward the reasoning over the individual analysis of causes by analyzing the decision tree path.

Table 6.2: Feature set (with timestamp)

Gameplay data	Profile data
TimeStamp	Gender
Speed	Age
Acceleration	VR Experience
Rotation Z	
Frame Rate	Discomfort Level

6.1 Symbolic Machine Learning Approach

Although some of previous work suggest that deep learning classifiers are the most suitable approach for CS prediction [62, 70], deep neural networks are black boxes that are very difficult to grasp. For this reason, this research limited the analysis to symbolic machine learning algorithms that enable a straight understanding of the decision path.

In *symbolic classifiers*, the language description can be represented by a set of N_R unordered or disjoint rules, *i.e.* $\mathbf{h} = \{R_1, R_2..., R_{N_R}\}$. Symbolic classifiers are not new, as they have been used in many scenarios where explanation is needed [7]. The term unordered means that a rule can be individually used and analyzed, without the need to consider other rules in the set. It is worth noticing that most classification rule learning algorithms belong to the family of top down induction of decision trees (at left in Figure 6.1), which adopt divide-and-conquer strategies. These algorithms construct a global classifier using a top-down strategy to recursively refine a partial prediction theory. A decision tree can be written as a set of disjoint unordered rules [44, 42].

A *rule* R assumes the form **if** B **then** H or symbolically $B \rightarrow H$, where H stands for the head, or rule *conclusion*, and B for the body, or rule *condition*. The body consists of a disjunction of conjunctions of feature tests in the form of X_i *op Value*, where X_i is a feature name, *op* is an operator in the set $\{=, \neq, <, \leq, >, \geq\}$ and *Value* is a valid X_i feature value. In a *classification rule*, the head H assumes the form $class = C_i$, where $C_i \in \{C_1, ..., C_{N_{Cl}}\}$. Given a rule $R = B \rightarrow H$ and a set of examples T, let $\mathcal{B} \subset T$ be the set of examples that satisfy B and $\mathcal{H} \subset T$ be the set of examples that satisfy H [42].

Given a training *dataset* $\mathbb{X} = \{x_1, ..., x_n\}$ containing instances such that $\mathbb{X} \in \mathbb{R}^p, p$ being the number of attributes of the instances with corresponding labels $c(x) \in \{1, ..., L\}$, the classification problem consists of assigning a label $l \in \{1, ..., L\}$ to unlabelled instances y, given that $\mathbb{X}$ can assist the process.

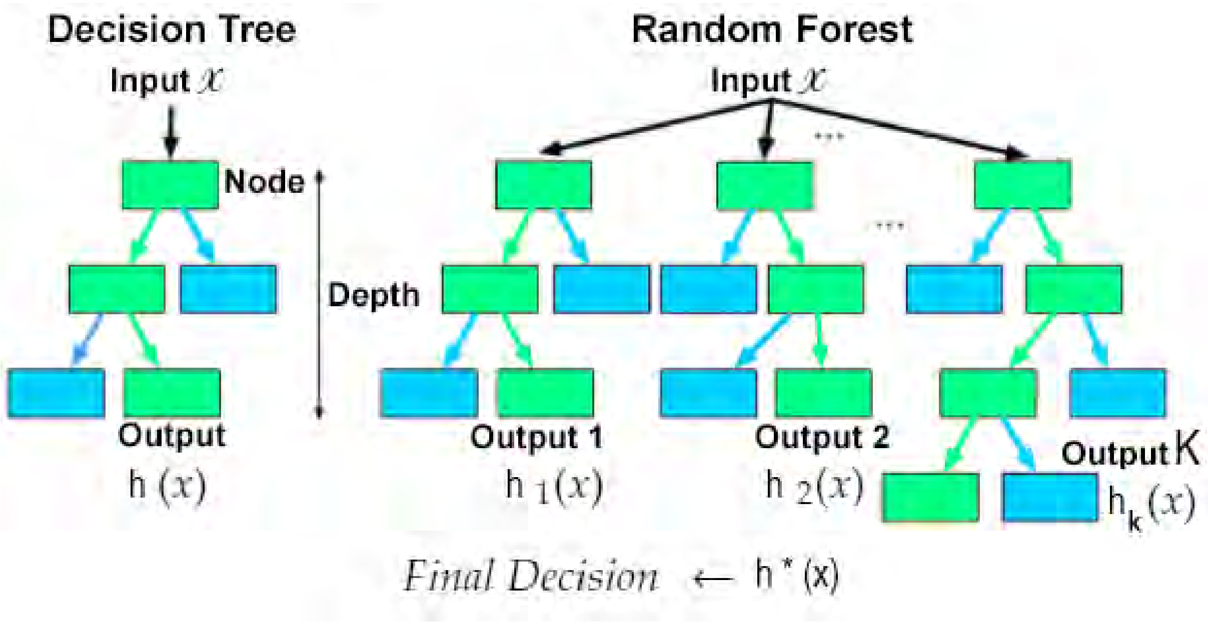

Figure 6.1: Decision tree and random forest. The green paths represent the outcome for this particular case.

When a decision tree is built, the set of instances in a decision tree leaf node is the one covered by the rule formed by the path starting in the root node up to the leaf node. A decision tree is illustrated in the left side of Figure 6.1. Moreover, a random forest, illustrated on the right side of Figure 6.1, is a classifier composed by a collection of K decision tree classifiers $\mathbf{h}_k(\mathbf{x}), k = 1, ..., K$. Each $\mathbf{h}_k(\mathbf{x})$ is constructed using a sample of features, randomly selected from X where the k are autonomous identically distributed by random vectors, and given an instance $\mathbf{x}$ to be classified by the forest $\mathbf{h} * (\mathbf{x})$, each component or decision tree votes for a class. The most prevalent class is the $\mathbf{h} * (\mathbf{x})$ final decision [15].

The logical prediction path of the decision trees inherits a personal fingerprint associated to attribute weights. Usually, attributes that are closer to the tree root are more important, as they often reduce the chaos in data more than the rest (information gain, less entropy). As a general rule, the frequency in which attributes appear in the decision path is also an important piece of information. We combine these two aspects to estimate the importance of the attribute (i.e., the most important causes of discomfort).

Let us suppose a decision tree described by 9 decision nodes, as shown in Figure 6.2, which contains in their conditions the features G (gender), R (rotation Z), A (acceleration) and S (speed). Furthermore, let us consider a path for an instance that was predicted as discomfort, highlighted in green in the same figure.

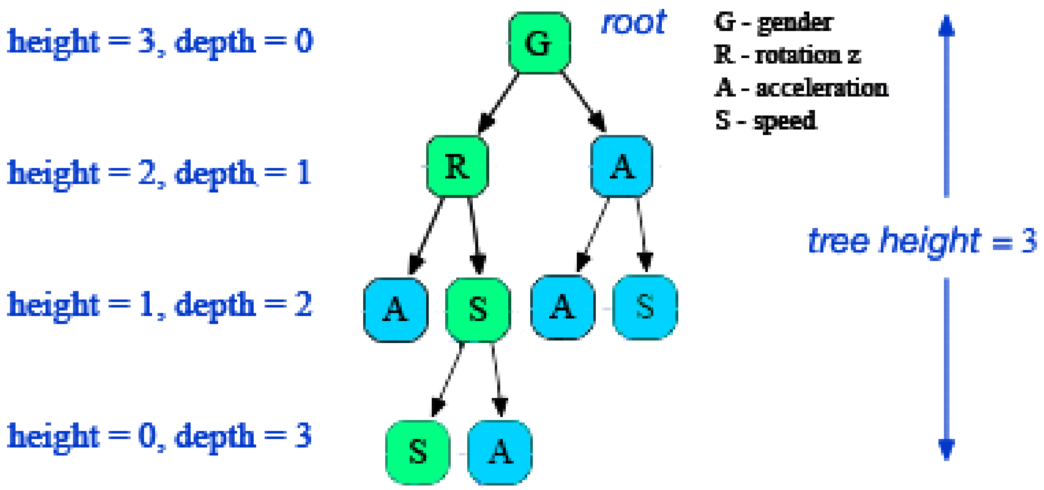

Figure 6.2: A decision tree model. The green path illustrates the decision path that uses the attributes G, R, S, and S. Each attribute is associated to height values 3, 2, 1, and 0, respectively.

We compute a potential-cause score (PCS) by summing up the heights of these features in the green path. In this case, G appeared once and has height 3, rotation R has height 2 and speed S has heights 1 and 0. Next, the output is divided by the sum of all depths of the tree, as follows: G=3/6 or 0.5, R=2/6 or approximately 0.33 and S=1/6 or approximately 0.17. In this case, we estimate gender as the most relevant cause for CS (Equation 6.1).

$$PCS(F) = \frac{\sum_{h=0}^{max\ height} \begin{cases} h, & if\ F\ belongs\ to\ the\ height \\ 0, & otherwise \end{cases}}{\sum_{h=0}^{max\ height} h} \tag{6.1}$$

The equation 6.1 h varies from 0 to the maximal tree height, and F is the feature being evaluated. PCS is computed considering just the decision path (e.g., the one hilighted in green)

Furthermore, the random forest model can be considered a set of decision trees. We sum the PCS results from each tree t if this tree's final decision is equal to the RF final decision. Otherwise, we sum 0 in this iteration. In Equation 6.2, we sum the PCS results from each tree t if the classification result of t is equal to the final RF classification result, where votes from several trees are scored together and a single class, e.g., the mode, is chosen as the classification result. Otherwise, we sum 0 at this iteration.

$$PCS_{RF}(F) = \sum_{t \; \epsilon \; T} \begin{cases} PCS(F), \; if \; the \; tree \; t \; decision \; is \; equal \; to \; RF \; final \; decision \\ 0, \; otherwise \end{cases} \tag{6.2}$$

Figure 6.3 shows the pipeline of the proposed approach. When a model is outputted in Figure 6.3(a), it is used as the "Trained Model" in Figure 6.3(a) on the input dataset S_u, composed by the profile data and gameplay data of a user u. It is worth noticing that S_u is composed by N_u instances (which is captured in each second of an entire gameplay experience) related to the collected X features. If all instances in S_u are classified as 0 (no discomfort), the flow goes to the output classification "No Discomfort". In case a subset of instances is classified as 1, the classification for this user is "Discomfort" and in this case we compute a potential-cause score (PCS).

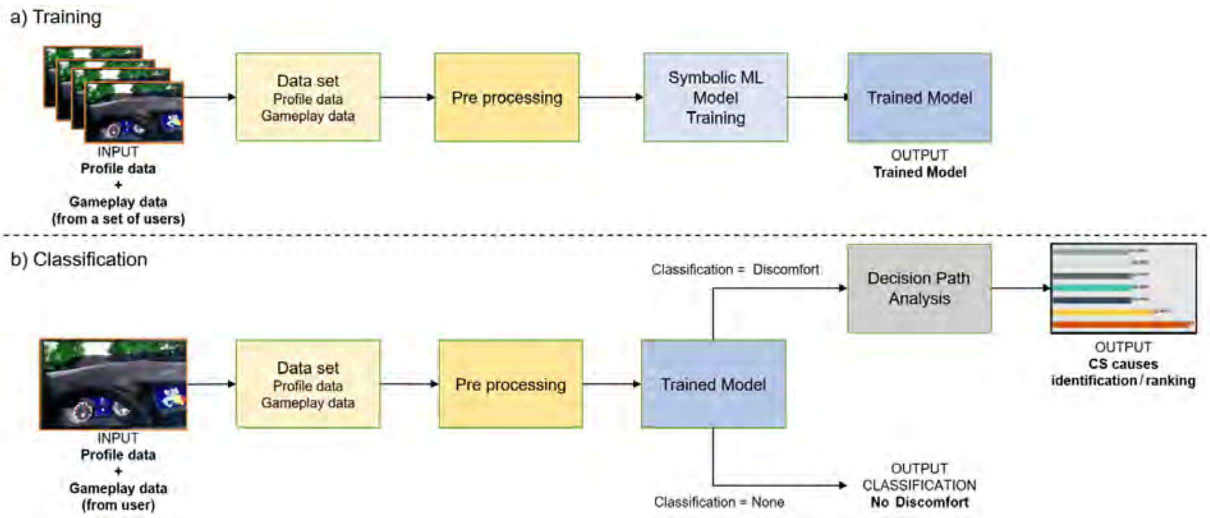

Figure 6.3: The pipeline of the proposed approach.

As a complementary remark, we use the random forest and decision tree algorithms from scikit-learn [107] python library (Python version: 3.7.5 , sci-kit learn version: 0.22.1). Next section shows the performed experiments.

6.2 Evaluation Method

Leave-one-out (leaving one participant out) was chosen as evaluation method, which is a particular case of the cross-validation technique where the number of folds matches the number of instances in the dataset. In other words, one participant was left out while the

Table 6.3: User-specific AUC scores in the race game without timestamp (tree depth 7).

User	Decision Tree		Random Forest	
	Train	Test	Train	Test
21	0.86	0.49	0.87	0.58
22	0.86	0.98	0.88	1.00
23	0.86	0.62	0.88	0.65
24	0.88	0.51	0.89	0.72
25	0.88	0.56	0.89	0.57
26	0.86	0.53	0.87	0.56
27	0.84	0.83	0.86	0.87
28	0.86	0.48	0.88	0.39
29	0.86	0.39	0.88	0.69
30	0.90	0.66	0.90	0.79
31	0.88	0.58	0.89	0.54
32	0.84	0.11	0.86	0.12
33	0.87	0.50	0.89	0.58
34	0.88	0.48	0.88	0.50
35	0.87	0.43	0.88	0.38
Average	**0.86**	**0.51**	**0.88**	**0.58**

algorithm was trained with n-1 participants and the model was tested with the left out participant. This process is repeated n times switching the left out participant.

We also perform an efficiency analysis in terms of the depth of the generated decision trees. For the race game the optimal tree depth was 7 and for the flight game it was 9. We focused on minimizing the minimum tree coverage, maximizing AUC scores, and minimizing the tree depth for better efficiency. No significant improvements on the AUC (area under the ROC curve) scores were observed with large depths. It is important to highlight that large trees also consume greater processing time, both in the case of training and classification, and also greater memory consumption.

6.2.1 Model Selection

The comparative results show that, concerning the AUC scores (Tables 6.3 and 6.4), the models obtain very similar performance values without timestamp in feature set (Table 6.1).

In contrast, when it comes to the comparative results, concerning the AUC scores and the timestamp inclusion in feature set (Table 6.2). The timestamp feature increases the AUC scores metrics results in terms of predictability (Tables 6.5 and 6.6). Moreover, the random forest classifier obtained the best results (Figure 6.4).

Table 6.4: User-specific AUC scores in the flight game without timestamp (tree depth 9).

User	Decision Tree		Random Forest	
	Train	Test	Train	Test
1	0.90	0.49	0.85	0.63
2	0.88	0.84	0.85	1.00
3	0.86	0.50	0.84	0.47
4	0.87	0.57	0.85	0.70
5	0.88	0.77	0.85	0.76
6	0.88	0.60	0.86	0.71
7	0.89	0.54	0.86	0.77
8	0.89	0.74	0.86	0.87
9	0.88	0.04	0.84	0.01
10	0.88	0.64	0.86	0.77
11	0.90	0.78	0.85	0.83
12	0.89	0.66	0.86	0.57
13	0.88	0.98	0.85	1.00
14	0.90	0.52	0.87	0.53
15	0.89	0.54	0.87	0.62
16	0.89	0.59	0.86	0.60
17	0.88	0.47	0.86	0.89
18	0.88	0.64	0.85	0.12
19	0.90	0.64	0.87	0.72
20	0.88	0.67	0.85	0.99
Average	**0.88**	**0.62**	**0.86**	**0.72**

Table 6.5: User-specific AUC scores in the race game with timestamp (tree depth 7).

User	Decision Tree		Random Forest	
	Train	Test	Train	Test
21	0.94	0.28	0.95	0.76
22	0.94	0.72	0.95	1.00
23	0.94	0.96	0.95	1.00
24	0.95	0.58	0.95	0.73
25	0.96	0.39	0.97	0.51
26	0.93	0.37	0.95	0.97
27	0.92	0.85	0.93	0.95
28	0.94	0.50	0.95	0.24
29	0.94	0.93	0.95	0.97
30	0.96	0.72	0.96	0.77
31	0.95	0.65	0.96	0.78
32	0.92	0.05	0.94	0.19
33	0.93	0.74	0.94	0.96
34	0.95	0.58	0.95	0.61
35	0.94	0.54	0.95	0.75
Average	**0.94**	**0.58**	**0.95**	**0.77**

However, random forest is an ensemble algorithm, and hence it is naturally more complex and slower in terms of run time when compared to a single decision tree. Despite of this fact and due to its great generalization capabilities, we adopted the random forest as the classifier for the further analyses of this manuscript.

We focus on minimizing the minimum tree coverage, maximizing AUC scores and minimizing the tree depth for better efficiency. This reasoning was used to choose the ideal tree depth. The ideal depths were 7 and 9 for the race and flight game, respectively.

Moreover, in sci-kit learn, the Random forest classifier also takes 'n$_{e}stimators'asaparameter.This$

Figures 6.5 illustrate the minimum coverage as the depth of the tree is increased, respectively.

Table 6.6: User-specific AUC scores in the flight game with timestamp (tree depth 9)

User	Decision Tree		Random Forest	
	Train	Test	Train	Test
1	0.98	0.62	0.97	0.54
2	0.98	0.99	0.96	1.00
3	0.98	0.50	0.96	0.80
4	0.99	0.77	0.97	0.83
5	0.99	1.00	0.97	1.00
6	0.98	0.95	0.97	0.99
7	0.99	0.93	0.97	0.99
8	0.99	0.81	0.97	0.95
9	0.98	0.33	0.97	0.09
10	0.98	0.82	0.97	0.95
11	0.99	0.83	0.98	0.94
12	0.99	0.49	0.98	0.26
13	0.98	1.00	0.97	1.00
14	0.99	0.77	0.97	0.93
15	0.99	0.92	0.97	1.00
16	0.99	0.75	0.97	0.82
17	0.98	0.53	0.97	0.90
18	0.98	0.48	0.97	0.46
19	0.99	0.92	0.98	0.97
20	0.98	0.55	0.97	0.98
Average	**0.99**	**0.79**	**0.97**	**0.95**

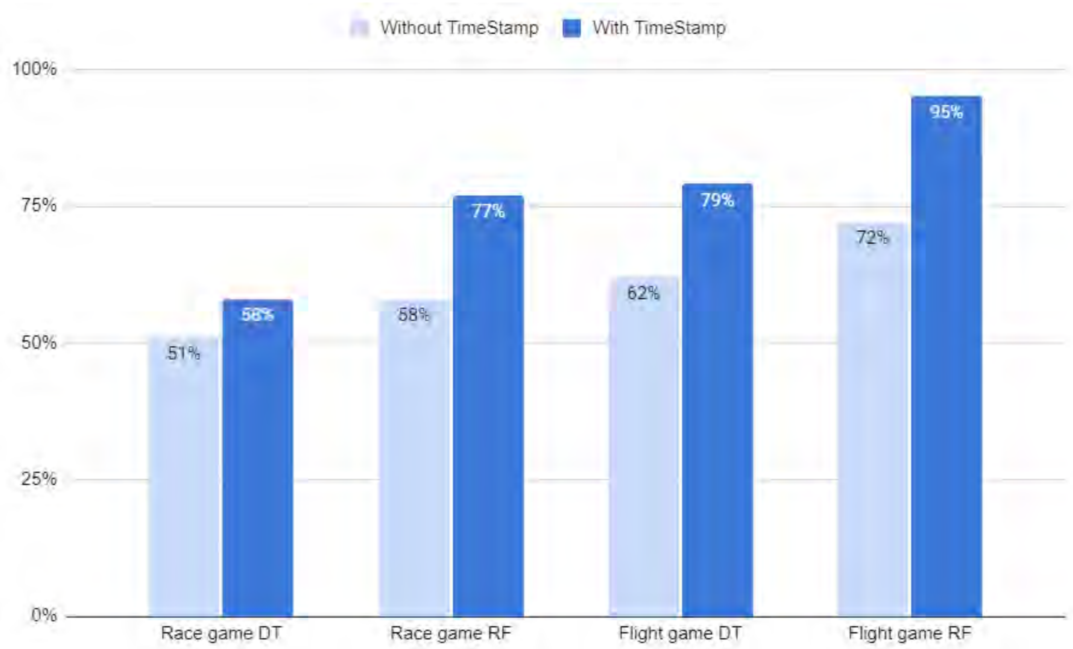

Figure 6.4: Comparison of decision tree (DT) and random forest (RF) AUC scores average for racing game and flight game with and without timestamp in feature set. Moreover, the race game provides more liberty to the user in terms of controllers, more displacement alternatives, and a more self-controlled acceleration. Consequently, the race game achieved low AUC scores compared to the flight game, a more static environment (less liberty to the user in terms of controllers). In other words, environments with fewer alternatives in terms of controllers are less complex for machine learning in terms of predictability.

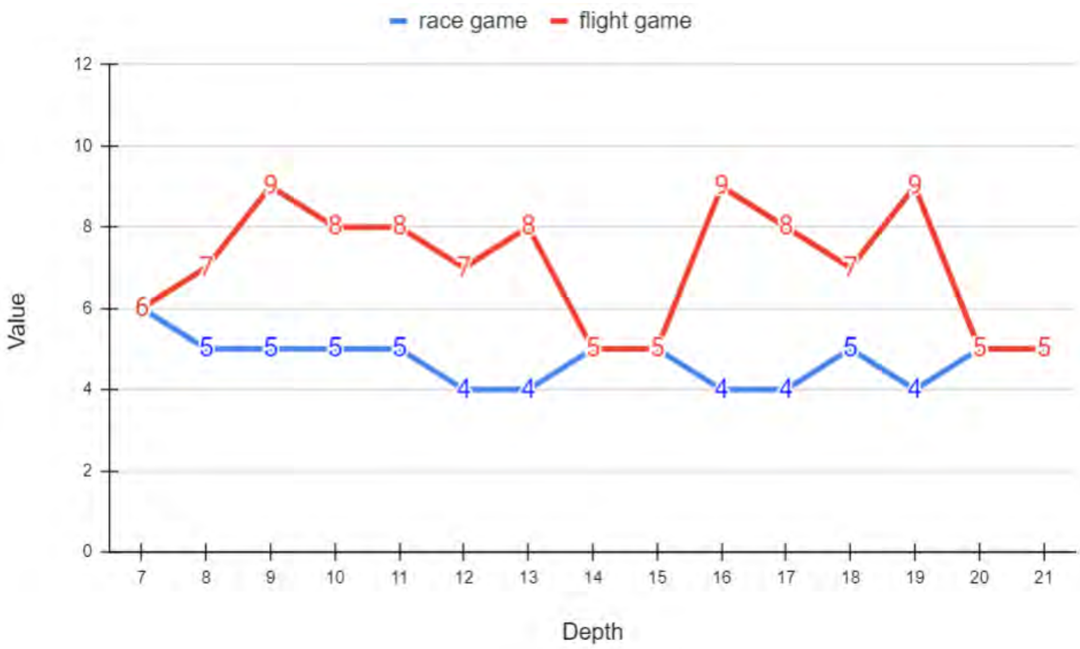

Figure 6.5: Minimum coverage in leaf nodes for race game and flight game.

6.3 Causes Identification Results

Predicting the cause of CS is not trivial. Every user has a specific susceptibility to discomfort. Furthermore, several attributes are related to the hardware and ergonomic aspects of the devices. We are still far from tracing very precise causes for all specific cases. However, so far, factors such as rotation, speed, gender, and previous VR experience, appeared as dominant factors that can trigger CS.

Our approach works with up to eight factors attributed to CS (Table 6.2). Previous works in the literature already proposed strategies for four of these attributes (time exposure, acceleration, speed, frame rate, and camera rotation on the z-axis) [92, 14, 18, 149]. The remaining causes (gender, VR experience, and age) are causes associated to the user profile and are still not associated to a clear strategy. In addition, we observed different patterns of causes for users in the race game when compared to the flight game.

Time exposure (timestamp) was the most frequent cause for discomfort. Overall, the race game contributed more to CS manifestation (39.4) when compared to the flight game (35.9). A possible suggestion is to reduce the time of exposure in the case of the race games. CS triggered by acceleration shifts controlled by users in the race game was less frequent (5.6) when compared to the case of the flight game, where acceleration was not controlled by the user (11.80).

Another feature that influences on the discomfort in both scenarios is the former VR experience. PCS was greater in the race game in contrast to the flight game, 8.25 and 4.76, respectively. In addition, rotation was marked as cause more frequently in the flight (18.70) when compared to the race game (13.83).

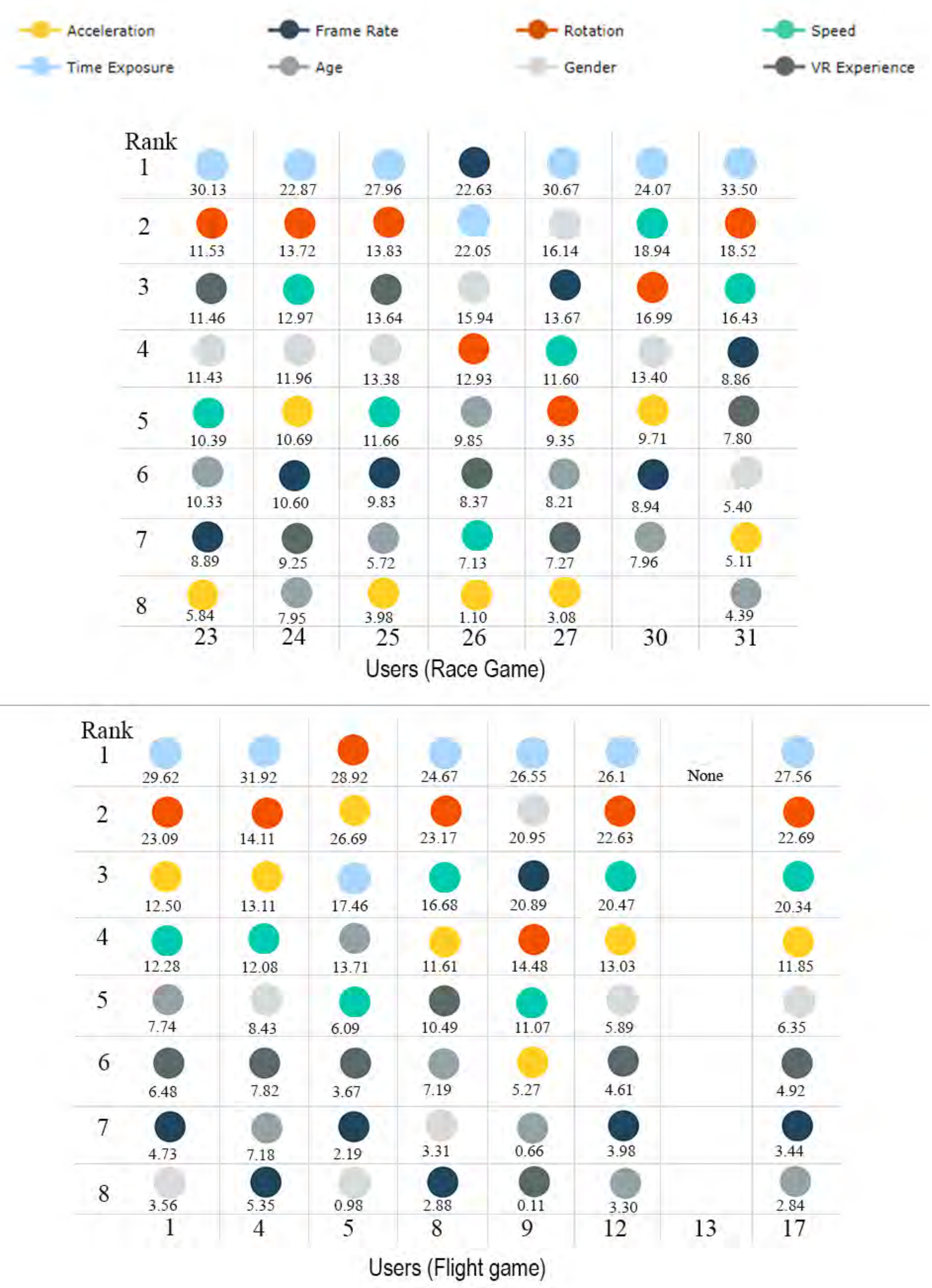

Figure 6.6: Random Forest feature ranking (identification of cybersickness causes) for the race (A) and flight game (B) for P5 participants.

Chapter 7

Suggestion of Strategies Based on User and Gameplay Data

We observed that most of PCS, when it comes to short-exposure cases, were tied to rotation and acceleration (Figure 6.6). This rank of causes enabled us to associate CS minimization strategies that conform to the literature. Moreover, these strategies can be used to minimize CS problems during short or long exposures. In what follows, we analyze different periods of a 20 minutes long gameplay experience (obtained in P6 protocol), in regards to the race and flight game.

We used our approach based on random forest to predict CS along a temporal line for the race and flight game (Appendix D and E, respectively). The resulting suggestion of strategies, as well as each rank of CS causes can be observed in Table 7.1 and Table 7.2. These strategies were chosen based on their obtained PCS and according to the usual strategies known to the literature and their application is simulated in the race game (Figure 7.2).

7.1 Race Game Strategies Suggestion Results

When it comes to the race game, the top rank cause of CS (Figure 7.1) was time exposure, where the PCS average was equal to 32.65. This rate lead us to suggest strategies to reduce the exposure such as introducing intervals within the VR experience (more details in Table 7.1).

When we analyse the 20 minutes of gameplay of participants from P6, the first 5 minutes indicate that velocity plays a very important role in the triggering of CS, achieving up to 28.97 of PCS, while later decreasing the PCS rate and ultimately achieving 8.59 at

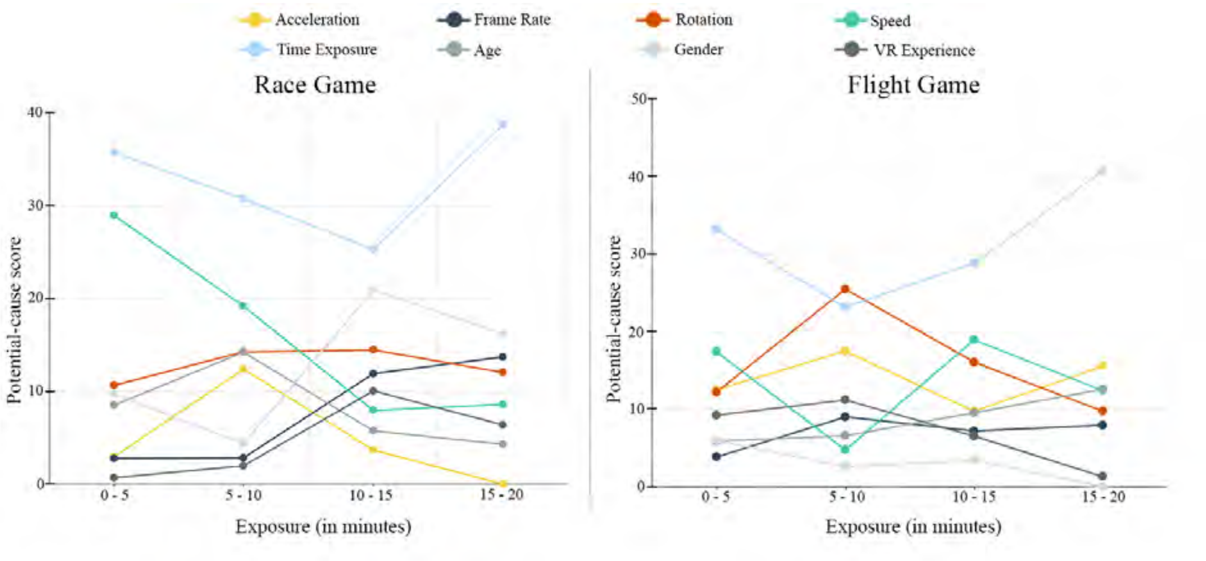

Figure 7.1: Race and flight game potential-cause score ranking along with different exposure moments for the P6 participants.

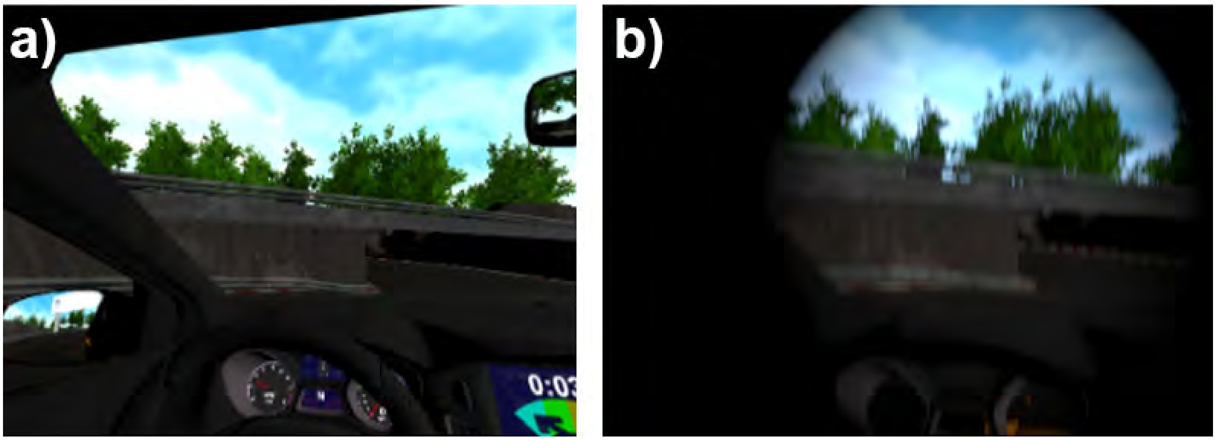

Figure 7.2: (a) The race gameplay on a curved track with no appliance of strategies. (b) The race gameplay using rotational blurring and tunneling, activated during the gameplay.

the end of the exposure. Strategies such as slow-motion [68] can be applied to minimize discomfort when velocity is the most important variable leading to the symptom.

We separated the 20 minutes long gameplay into four short sections to analyse how the rotation variable behaves in terms of triggering CS. In this case, the PCS were fairly similar, 10.65, 14.26, 14.47, and 12.04, respectively, for the entire experience (Table 7.1).

Overall, rotation was ranked 3rd in most gameplay experiences. This finding suggest the usage of strategies to cover rotational problems in a general basis. Rotational blurring [18] and tunneling [40] can be applied specially when high velocity curves are at stake.

Table 7.1: Strategies for the race game (P6 participants).

0 to 5 minutes				**10 to 15 minutes**			
Rank	Causes	PCS	Strategies	Rank	Causes	PCS	Strategies
1	Time Exposure	35.78	Interval	1	Time Exposure	25.32	Interval
2	Speed	28.97	Slow-motion	2	Gender	20.92	None
3	Rotation	10.65	Rotational blurring, Tunneling, Slow-motion	3	Rotation	14.47	Rotational blurring, Tunneling, Slow-motion
4	Gender	9.69	None	4	Frame rate	11.91	None
5	Age	8.5	None	5	VR Experience	10.05	None
6	Acceleration	2.95	Acceleration adjustment, Haptic feedback	6	Speed	7.93	Slow-motion
7	Frame rate	2.78	None	7	Age	5.73	None
8	VR Experience	0.68	None	8	Acceleration	3.66	Acceleration adjustment, Haptic feedback
5 to 10 minutes				**15 to 20 minutes**			
Rank	Causes	PCS	Strategies	Rank	Causes	PCS	Strategies
1	Time Exposure	30.76	Interval	1	Time Exposure	38.74	Interval
2	Speed	19.19	Slow-motion	2	Gender	16.23	None
3	Rotation	14.26	Rotational blurring, Tunneling, Slow-motion	3	Frame rate	13.7	None
4	Age	14.23	None	4	Rotation	12.04	Rotational blurring, Tunneling, Slow-motion
5	Acceleration	12.39	Acceleration adjustment, Haptic feedback	5	Speed	8.59	Slow-motion
6	Gender	4.37	None	6	VR Experience	6.39	None
7	Frame rate	2.83	None	7	Age	4.3	None
8	VR Experience	1.97	None	8	Acceleration	0	Acceleration adjustment, Haptic feedback

7.2 Flight Game Strategies Suggestion Results

As with the race game, the flight game also displays a high PCS for the time exposure variable (31.43), which is prevalent for the entire 20 minutes of game experience (Figure 7.1). The same strategy, the introduction of intervals, should also be considered in this case (more details in Table 7.2).

Rotation was the ranked first from minute 5 to minute 10 (PCS: 25.45). For this reason, rotational blur [18] combined to tunneling [40] are appropriate choices for this game.

Acceleration achieved high PCSs from minute 5 to minute 10 (PCS: 17.47), and also from minute 15 to minute 20 (PCS: 15.52). Real time adjustments of the acceleration are a good fit for this case [108].

Overall, causes were ranked differently over the gameplay exposure. CS can be triggered by different factors and combinations of them, where eventually a single variable will influence more than the remaining.

Table 7.2: Strategies for the flight game (P6 participants).

0 to 5 minutes				**10 to 15 minutes**			
Rank	Causes	PCS	Strategies	Rank	Causes	PCS	Strategies
1	Time Exposure	33.13	Interval	1	Time Exposure	28.80	Interval
2	Speed	17.37	Slow-motion	2	Speed	18.90	Slow-motion
3	Acceleration	12.48	Acceleration adjustment, Haptic feedback	3	Rotation	16.04	Rotational blurring, Tunneling, Slow-motion
4	Rotation	12.19	Rotational blurring, Tunneling, Slow-motion	4	Acceleration	9.70	Acceleration adjustment, Haptic feedback
5	VR Experience	9.21	None	5	Age	9.51	None
6	Gender	5.96	None	6	Frame rate	7.15	None
7	Age	5.85	None	7	VR Experience	6.51	None
8	Frame rate	3.82	None	8	Gender	3.39	None
5 to 10 minutes				**15 to 20 minutes**			
Rank	Causes	PCS	Strategies	Rank	Causes	PCS	Strategies
1	Rotation	25.45	Rotational blurring, Tunneling, Slow-motion	1	Time Exposure	40.67	Interval
2	Time Exposure	23.13	Interval	2	Acceleration	15.52	Acceleration adjustment, Haptic feedback
3	Acceleration	17.47	None	3	Age	12.54	None
4	VR Experience	11.15	None	4	Gender	12.54	None
5	Frame rate	8.97	None	5	Speed	12.38	Slow-motion
6	Age	6.55	None	6	Rotation	9.71	Rotational blurring, Tunneling, Slow-motion
7	Speed	4.71	Slow-motion	7	Frame rate	7.91	None
8	Gender	2.57	Acceleration adjustment, Haptic feedback	8	VR Experience	1.27	None

Chapter 8

Conclusion

In this work, we propose an approach to predict and identify causes of cybersickness in different virtual reality games using head-mounted displays. To the best of our knowledge, this is the first work that uses symbolic classifiers to analyze causes of cybersickness during the gameplay experience. Once the cause is identified, game designers are able to select the most adequate strategy to mitigate the impacts of CS, according to the literature.

On the literature side, this research contributes as a bibliographic collection, describing the main causes of discomfort in VR systems while outlining strategies to minimize discomfort caused by HMDs. Thus far, we produce an cause and strategies association that summarizes this study (Table 3.2).

Moreover, we built two virtual reality games (race game and flight game) and conducted 6 experimental protocols along with 37 valid samples from a total of 88 volunteers, translating in 11722 instances.

Additionally, we built a data visualization application and performed a first analysis of the collected data. It is possible to observe that in 3993 samples of the racing game captured in P5' protocol , most occurrences of discomfort reported by the participants occurred near or during curves of the virtual track, which reinforces the association of CS to rotations. We also made an analysis between genders which showed that female individuals reported lower incidents of discomfort compared to male participants in our data.

Subsequently, the first analysis in terms of machine learning consisted of three scenarios: Scenario A (data from the racing game), Scenario B (data from the flying game), and Scenario C (data from both games). We performed supervised binary and quarterly classifications using 16 Weka's decision tree classifiers. The best accuracy was 99.0% and was obtained with the random forest classifier for Scenario B (flight game) in the binary classification.

An attribute selection was also performed in order to identify the most relevant attributes. For all scenarios it was observed that the most relevant attributes were the same, and they were exposure time, z-axis rotation and profile attributes of the individual (gender, age, and VR experience). These results corroborate the importance of attributes related to the individuals in the prediction of CS. This assessment reinforces the theories and hypothesis present in the literature known so far [113], [82], [2], [73].

Furthermore, we proposed the use of two symbolic machine learning algorithms (decision tree and random forest), along with an analysis to identify the optimal tree depth for the generated models. Next, we performed a feature ranking to identify the most relevant causes of CS, which vary along with the gameplay experience and is related to the user. Causes were ranked differently over the games and user profiles.

The human-readable characteristic of decision tree and random forest helped us to understand the discomfort manifestation reasons in two different games. This fact, show that symbolic machine learning models are a good way to identify CS causes, where understability is essential to highlight causes and suggest strategies.

Conclusively, CS can be triggered as a result of different factors. Eventually, a single variable influences more in terms of triggering CS than the remaining. For this reason, different combinations of strategies can be applied according to the user and to the current section of the game. Designers can benefit from our approach by enabling the selection of the best strategy for a specific context.

As a final remark, the raw dataset of this work along with developed games are available in the following public domain: for further reproduction and comparison [112].

8.1 Limitations and Future Work

COVID-19 pandemic affected our experiments and protocols in terms of dataset construction. For this reason, some features were also not well represented, such as gender (for women), age (for older adults), and experience (for people with former VR experience). Moreover, the number of developed games not covered locomotion movements, which is specific for games where the user can walk virtually.

Future work involves including posture, vision impairments, locomotion, and others to our framework. Other possibilities to explore this approach's results are introducing more experiments considering the underrepresented user-profiles [106] such as women and older adults, and also to taken into account new games with other contexts.

Another straightforward way is to explore the gender differences tied to games and virtual reality tasks. Our results and other works [86, 48, 30] pointed out that specific tasks can produce different results of discomfort for different user profiles and groups, regarding and not limited to: gender, age, or health issues. Our symbolic machine learning approach can also help to further analysis.

Moreover, it is necessary to understand better the correlation of profile features with gameplay features, and also how results obtained from profile features (gender, age, VR experience) can be used to labeling VR experiences according to different group of users.

Besides, considering we are limited to two VR games (race game and flight game), meticulous research for different VR applications (simulators, VR movies) is necessary. Each specific VR application has some particularities and particular features that can be explored more using our approach.

Another challenge is to create a virtual reality experience that explores specific tasks individually tied to specific CS causes with a long exposure. The evaluation of individual tasks associated with CS causes may produce a more profound study isolating any other VR possible influences on CS results.

Moreover, it is necessary to perform a detailed research focused on strategies, acknowledging how strategies can vary in different VR applications. An example of applying this idea is an automatic recommendation software to suggest strategies to mitigate cybersickness problems in various VR applications. A complete recommendation software might be a crucial tool for VR game designers and the VR content production industry. This tool may optimize the VR production line, reducing the production time and the decision-making process from the game designer's team.

Finally, this thesis can be a start point to elaborate more accurate game design techniques for VR games and applications.

References

[1] Oculus Founder Palmer Luckey on What It Will Take to Make Virtual Reality Really Big. `https://www.technologyreview.com/2016/03/17/161530/`. Accessed: 2020-12-10.

[2] Abramov, I.; Gordon, J.; Feldman, O.; Chavarga, A. Sex and vision ii: color appearance of monochromatic lights. *Biology of sex differences 3*, 1 (2012), 21.

[3] Ahir, K.; Govani, K.; Gajera, R.; Shah, M. Application on virtual reality for enhanced education learning, military training and sports. *Augmented Human Research 5*, 1 (2020), 7.

[4] Arcioni, B.; Palmisano, S.; Apthorp, D.; Kim, J. Postural stability predicts the likelihood of cybersickness in active hmd-based virtual reality. *Displays 58* (2019), 3–11.

[5] Arns, L. L.; Cerney, M. M. The relationship between age and incidence of cybersickness among immersive environment users. In *IEEE Proceedings. VR 2005. Virtual Reality, 2005.* (2005), IEEE, pp. 267–268.

[6] Berger, H. Über das elektrenkephalogramm des menschen. *European archives of psychiatry and clinical neuroscience 87*, 1 (1929), 527–570.

[7] Bernardini, F.; Monard, M. C.; Prati, R. Constructing ensembles of symbolic classifiers. *International Journal of Hybrid Intelligent Systems 3*, 3 (2006), 159–167.

[8] Berthoz, A.; Pavard, B.; Young, L. Perception of linear horizontal self-motion induced by peripheral vision (linearvection) basic characteristics and visual-vestibular interactions. *Experimental brain research 23*, 5 (1975), 471–489.

[9] Biocca, F. Will simulation sickness slow down the diffusion of virtual environment technology? *Presence: Teleoperators & Virtual Environments 1*, 3 (1992), 334–343.

[10] Bles, W. Coriolis effects and motion sickness modelling. *Brain research bulletin 47*, 5 (1998), 543–549.

[11] Bles, W.; Bos, J. E.; De Graaf, B.; Groen, E.; Wertheim, A. H. Motion sickness: only one provocative conflict? *Brain research bulletin 47*, 5 (1998), 481–487.

[12] Bolas, M.; Jones, J. A.; McDowall, I.; Suma, E. Dynamic field of view throttling as a means of improving user experience in head mounted virtual environments, May 9 2017. US Patent 9,645,395.

[13] Bonato, F.; Bubka, A.; Palmisano, S. Combined pitch and roll and cybersickness in a virtual environment. *Aviation, space, and environmental medicine 80*, 11 (2009), 941–945.

[14] Bouyer, G.; Chellali, A.; Lécuyer, A. Inducing self-motion sensations in driving simulators using force-feedback and haptic motion. In *Virtual Reality (VR), 2017 IEEE* (2017), IEEE, pp. 84–90.

[15] Breiman, L. Random forests. *Machine learning 45*, 1 (2001), 5–32.

[16] Brooks, J. O.; Goodenough, R. R.; Crisler, M. C.; Klein, N. D.; Alley, R. L.; Koon, B. L.; Logan Jr, W. C.; Ogle, J. H.; Tyrrell, R. A.; Wills, R. F. Simulator sickness during driving simulation studies. *Accident Analysis & Prevention 42*, 3 (2010), 788–796.

[17] Bruck, S.; Watters, P. A., et al. Cybersickness and anxiety during simulated motion: Implications for vret. *Annual Review of Cybertherapy and Telemedicine 144* (2009), 169–173.

[18] Budhiraja, P.; Miller, M. R.; Modi, A. K.; Forsyth, D. Rotation blurring: Use of artificial blurring to reduce cybersickness in virtual reality first person shooters. *arXiv preprint arXiv:1710.02599* (2017).

[19] Calvelo, M.; Piñeiro, Á.; Garcia-Fandino, R. An immersive journey to the molecular structure of sars-cov-2: Virtual reality in covid-19. *Computational and Structural Biotechnology Journal* (2020).

[20] Cao, Z.; Jerald, J.; Kopper, R. Visually-induced motion sickness reduction via static and dynamic rest frames. In *2018 IEEE Conference on Virtual Reality and 3D User Interfaces (VR)* (2018), IEEE, pp. 105–112.

[21] Carnegie, K.; Rhee, T. Reducing visual discomfort with hmds using dynamic depth of field. *IEEE computer graphics and applications 35*, 5 (2015), 34–41.

[22] Carrión, M.; Santorum, M.; Benavides, J.; Aguilar, J.; Ortiz, Y. Developing a virtual reality serious game to recreational therapy using iplus methodology. In *2019 International Conference on Virtual Reality and Visualization (ICVRV)* (2019), IEEE, pp. 133–137.

[23] Chelen, W.; Kabrisky, M.; Rogers, S. Spectral analysis of the electroencephalographic response to motion sickness. *Aviation, space, and environmental medicine 64*, 1 (1993), 24–29.

[24] Cheung, B.; Hofer, K.; Heskin, R.; Smith, A. Physiological and behavioral responses to an exposure of pitch illusion in the simulator. *Aviation, space, and environmental medicine 75*, 8 (2004), 657–665.

[25] Cirio, G.; Olivier, A.-H.; Marchal, M.; Pettre, J. Kinematic evaluation of virtual walking trajectories. *IEEE transactions on visualization and computer graphics 19*, 4 (2013), 671–680.

[26] Collins, J. F.; Blackwell, L. K. Effects of eye dominance and retinal distance on binocular rivalry. *Perceptual and motor skills 39*, 2 (1974), 747–754.

[27] Cost, S.; Salzberg, S. A weighted nearest neighbor algorithm for learning with symbolic features. *Machine learning 10*, 1 (1993), 57–78.

[28] Creighton, R. H. *Unity 3D game development by example: A Seat-of-your-pants manual for building fun, groovy little games quickly.* Packt Publishing Ltd, 2010.

[29] Cruz-Neira, C.; Sandin, D. J.; DeFanti, T. A.; Kenyon, R. V.; Hart, J. C. The cave: audio visual experience automatic virtual environment. *Communications of the ACM 35*, 6 (1992), 64–73.

[30] Curry, C.; Li, R.; Peterson, N.; Stoffregen, T. A. Cybersickness in virtual reality head-mounted displays: Examining the influence of sex differences and vehicle control. *International Journal of Human–Computer Interaction* (2020), 1–7.

[31] Davis, S.; Nesbitt, K.; Nalivaiko, E. A systematic review of cybersickness. In *Proceedings of the 2014 Conference on Interactive Entertainment* (2014), ACM, pp. 1–9.

[32] Denieul, P. Effects of stimulus vergence on mean accommodation response, microfluctuations of accommodation and optical quality of the human eye. *Vision research 22*, 5 (1982), 561–569.

[33] Dennison, M. S.; D'Zmura, M. Cybersickness without the wobble: experimental results speak against postural instability theory. *Applied ergonomics 58* (2017), 215–223.

[34] Dennison, M. S.; Wisti, A. Z.; D'Zmura, M. Use of physiological signals to predict cybersickness. *Displays 44* (2016), 42–52.

[35] Draper, M. H.; Viirre, E. S.; Furness, T. A.; Gawron, V. J. Effects of image scale and system time delay on simulator sickness within head-coupled virtual environments. *Human Factors: The Journal of the Human Factors and Ergonomics Society 43*, 1 (2001), 129–146.

[36] Drucker, H.; Burges, C. J.; Kaufman, L.; Smola, A. J.; Vapnik, V. Support vector regression machines. In *Advances in neural information processing systems* (1997), pp. 155–161.

[37] Džeroski, S. Applications of symbolic machine learning to ecological modelling. *Ecological Modelling 146*, 1-3 (2001), 263–273.

[38] Edwards, C.; Creaser, J.; Caird, J.; Lamsdale, A.; Chisholm, S. Older and younger driver performance at complex intersections: Implications for using perception-response time and driving simulation.

[39] Farkhatdinov, I.; Ouarti, N.; Hayward, V. Vibrotactile inputs to the feet can modulate vection. In *World Haptics Conference (WHC), 2013* (2013), IEEE, pp. 677–681.

[40] Farmani, Y. *Discrete Viewpoint Control to Reduce Cybersickness in Virtual Environments.* Tese de Doutorado, Carleton University, 2018.

[41] Fernandes, A. S.; Feiner, S. K. Combating vr sickness through subtle dynamic field-of-view modification. In *2016 IEEE Symposium on 3D User Interfaces (3DUI)* (2016), IEEE, pp. 201–210.

[42] Flach, P. *Machine Learning: The Art and Science of Algorithms That Make Sense of Data*. Cambridge, 2012.

[43] Flanagan, M. B.; May, J. G.; Dobie, T. G. The role of vection, eye movements and postural instability in the etiology of motion sickness. *Journal of Vestibular Research 14*, 4 (2004), 335–346.

[44] Frank, E.; Hall, M. A.; Witten, I. H. *Data Mining: Practical Machine Learning Tools and Techniques*, 4th ed. ed. Morgan Kaufmann, 2016.

[45] Frank, L. H.; Kennedy, R. S.; McCauley, M.; Root, R.; Kellogg, R. Simulator sickness: Sensorimotor disturbances induced in flight simulators. Tech. rep., NAVAL TRAINING EQUIPMENT CENTER ORLANDO FL, 1984.

[46] Garcia-Agundez, A.; Reuter, C.; Becker, H.; Konrad, R.; Caserman, P.; Miede, A.; Göbel, S. Development of a classifier to determine factors causing cybersickness in virtual reality environments. *Games for health journal 8*, 6 (2019), 439–444.

[47] Golding, J. F. Motion sickness susceptibility questionnaire revised and its relationship to other forms of sickness. *Brain research bulletin 47*, 5 (1998), 507–516.

[48] Grassini, S.; Laumann, K. Are modern head-mounted displays sexist? a systematic review on gender differences in hmd-mediated virtual reality. *Frontiers in Psychology 11* (2020).

[49] Graves, A.; Mohamed, A.-r.; Hinton, G. Speech recognition with deep recurrent neural networks. In *2013 IEEE international conference on acoustics, speech and signal processing* (2013), IEEE, pp. 6645–6649.

[50] Gunning, D. Explainable artificial intelligence (xai). *Defense Advanced Research Projects Agency (DARPA), nd Web 2*, 2 (2017).

[51] Guo, C.; Tsoi, C. W.; Wong, Y. L.; Yu, K. C.; So, R. Visually induced motion sickness during computer game playing. In *Contemporary Ergonomics and Human Factors 2013*, vol. 51. ROUTLEDGE in association with GSE Research, 2013, pp. 51–58.

[52] Hall, M.; Frank, E.; Holmes, G.; Pfahringer, B.; Reutemann, P.; Witten, I. H. The weka data mining software: an update. *ACM SIGKDD explorations newsletter 11*, 1 (2009), 10–18.

[53] Hassan, B.; Berssenbrügge, J.; Al Qaisi, I.; Stöcklein, J. Reconfigurable driving simulator for testing and training of advanced driver assistance systems. In *Assembly and Manufacturing (ISAM), 2013 IEEE International Symposium on* (2013), IEEE, pp. 337–339.

[54] Hearst, M. A.; Dumais, S. T.; Osuna, E.; Platt, J.; Scholkopf, B. Support vector machines. *IEEE Intelligent Systems and their applications 13*, 4 (1998), 18–28.

[55] Hillaire, S.; Lécuyer, A.; Cozot, R.; Casiez, G. Depth-of-field blur effects for first-person navigation in virtual environments. *IEEE computer graphics and applications 28*, 6 (2008), 47–55.

[56] Hillenius, D. Augmented reality aided learn-ing of human embryo anatomy: A study on motivation and us-ability. *Science* (2018).

[57] Howarth, P.; Costello, P. The occurrence of virtual simulation sickness symptoms when an hmd was used as a personal viewing system. *Displays 18*, 2 (1997), 107–116.

[58] Hu, S.; McChesney, K. A.; Player, K. A.; Bahl, A. M.; Buchanan, J. B.; Scozzafava, J. E. Systematic investigation of physiological correlates of motion sickness induced by viewing an optokinetic rotating drum. *Aviation, space, and environmental medicine* (1999).

[59] Hu, S.; Stern, R. M.; Vasey, M. W.; Koch, K. L. Motion sickness and gastric myoelectric activity as a function of speed of rotation of a circular vection drum. *Aviation, space, and environmental medicine* (1989).

[60] Irwin, J. The pathology of sea-sickness. *The Lancet 118*, 3039 (1881), 907–909.

[61] Islam, R.; Ang, S.; Quarles, J. Cybersense: A closed-loop framework to detect cybersickness severity and adaptively apply reduction techniques.

[62] Jeong, D.; Yoo, S.; Yun, J. Cybersickness analysis with EEG using deep learning algorithms. In *2019 IEEE Conference on Virtual Reality and 3D User Interfaces (VR)* (2019), IEEE, pp. 827–835.

[63] Jerald, J. *The VR book: Human-centered design for virtual reality.* Morgan & Claypool, 2015.

[64] Jin, W.; Fan, J.; Gromala, D.; Pasquier, P. Automatic prediction of cybersickness for virtual reality games. In *2018 IEEE Games, Entertainment, Media Conference (GEM)* (2018), IEEE, pp. 1–9.

[65] Kemeny, A.; Chardonnet, J.-R.; Colombet, F. *Getting Rid of Cybersickness: In Virtual Reality, Augmented Reality, and Simulators.* Springer Nature, 2020.

[66] Kemeny, A.; George, P.; Mérienne, F.; Colombet, F. New vr navigation techniques to reduce cybersickness. *Electronic Imaging 2017*, 3 (2017), 48–53.

[67] Kennedy, R. S.; Lane, N. E.; Berbaum, K. S.; Lilienthal, M. G. Simulator sickness questionnaire: An enhanced method for quantifying simulator sickness. *The international journal of aviation psychology 3*, 3 (1993), 203–220.

[68] Kim, H. G.; Baddar, W. J.; Lim, H.-t.; Jeong, H.; Ro, Y. M. Measurement of exceptional motion in vr video contents for vr sickness assessment using deep convolutional autoencoder. In *Proceedings of the 23rd ACM Symposium on Virtual Reality Software and Technology* (2017), ACM, p. 36.

[69] Kim, H. K.; Park, J.; Choi, Y.; Choe, M. Virtual reality sickness questionnaire (vrsq): Motion sickness measurement index in a virtual reality environment. *Applied ergonomics 69* (2018), 66–73.

[70] Kim, J.; Kim, W.; Oh, H.; Lee, S.; Lee, S. A deep cybersickness predictor based on brain signal analysis for virtual reality contents. In *Proceedings of the IEEE International Conference on Computer Vision* (2019), pp. 10580–10589.

[71] Kim, K.; Rosenthal, M. Z.; Zielinski, D.; Brady, R. Comparison of desktop, head mounted display, and six wall fully immersive systems using a stressful task. In *2012 IEEE Virtual Reality Workshops (VRW)* (2012), IEEE, pp. 143–144.

[72] Kim, Y. Y.; Kim, H. J.; Kim, E. N.; Ko, H. D.; Kim, H. T. Characteristic changes in the physiological components of cybersickness. *Psychophysiology 42*, 5 (2005), 616–625.

[73] Knight, M. M.; Arns, L. L. The relationship among age and other factors on incidence of cybersickness in immersive environment users. In *ACM Siggraph 2006 Research Posters* (2006), ACM, p. 196.

[74] Kolasinski, E. M. Simulator sickness in virtual environments. Tech. rep., DTIC Document, 1995.

[75] Konrad, R.; Padmanaban, N.; Molner, K.; Cooper, E. A.; Wetzstein, G. Accommodation-invariant computational near-eye displays. *ACM Transactions on Graphics (TOG) 36*, 4 (2017), 88.

[76] Kopper, R.; Stinson, C.; Bowman, D. Towards an understanding of the effects of amplified head rotations. In *The 3rd IEEE VR Workshop on Perceptual Illusions in Virtual Environments* (2011), vol. 2.

[77] Kucuker, A.; Kilic, D. K. Different way of seeing. In *IOP Conference Series: Materials Science and Engineering* (2019), vol. 471, IOP Publishing, p. 072008.

[78] Kühnapfel, U.; Cakmak, H. K.; Maass, H. Endoscopic surgery training using virtual reality and deformable tissue simulation. *Computers & graphics 24*, 5 (2000), 671–682.

[79] Kuosmanen, T. The effect of visual detail on cybersickness: Predicting symptom severity using spatial velocity.

[80] Lackner, J. Human orientation, adaptation, and movement control. *Motion sickness, visual displays, and armored vehicle design* (1990), 28–50.

[81] Langbehn, E.; Lubos, P.; Steinicke, F. Evaluation of locomotion techniques for room-scale vr: Joystick, teleportation, and redirected walking. In *Proceedings of the Virtual Reality International Conference-Laval Virtual* (2018), ACM, p. 4.

[82] LaViola Jr, J. J. A discussion of cybersickness in virtual environments. *ACM SIGCHI Bulletin 32*, 1 (2000), 47–56.

[83] Lawrence, S.; Giles, C. L.; Tsoi, A. C.; Back, A. D. Face recognition: A convolutional neural-network approach. *IEEE transactions on neural networks 8*, 1 (1997), 98–113.

[84] Lawther, A.; Griffin, M. A survey of the occurrence of motion sickness amongst passengers at sea. *Aviation, space, and environmental medicine 59*, 5 (1988), 399–406.

[85] Lee, S.; Koo, A.; Jhung, J. Moskit: Motion sickness analysis platform for vr games. In *Consumer Electronics (ICCE), 2017 IEEE International Conference on* (2017), IEEE, pp. 17–18.

[86] Liang, H.-N.; Lu, F.; Shi, Y.; Nanjappan, V.; Papangelis, K. Evaluating the effects of collaboration and competition in navigation tasks and spatial knowledge acquisition within virtual reality environments. *Future Generation Computer Systems 95* (2019), 855–866.

[87] Lin, C.-T.; Chuang, S.-W.; Chen, Y.-C.; Ko, L.-W.; Liang, S.-F.; Jung, T.-P. Eeg effects of motion sickness induced in a dynamic virtual reality environment. In *2007 29th Annual International Conference of the IEEE Engineering in Medicine and Biology Society* (2007), IEEE, pp. 3872–3875.

[88] Lin, J. J.; Abi-Rached, H.; Lahav, M. Virtual guiding avatar: An effective procedure to reduce simulator sickness in virtual environments. In *Proceedings of the SIGCHI Conference on Human Factors in Computing Systems* (2004), ACM, pp. 719–726.

[89] Mao, W.; Wang, F. Cultural modeling for behavior analysis and prediction. In *New Advances in Intelligence and Security Informatics*. Academic Press, 2012, pp. 91–102.

[90] Maree, C.; Omlin, C. W. Towards responsible ai for financial transactions. In *2020 IEEE Symposium Series on Computational Intelligence (SSCI)* (2020), IEEE, pp. 16–21.

[91] McCauley, M. E.; Sharkey, T. J. Cybersickness: Perception of self-motion in virtual environments. *Presence: Teleoperators & Virtual Environments 1*, 3 (1992), 311–318.

[92] Melo, M.; Vasconcelos-Raposo, J.; Bessa, M. Presence and cybersickness in immersive content: effects of content type, exposure time and gender. *Computers & Graphics 71* (2018), 159–165.

[93] Meng, X.; Du, R.; Varshney, A. Eye-dominance-guided foveated rendering. *IEEE transactions on visualization and computer graphics 26*, 5 (2020), 1972–1980.

[94] Merhi, O.; Faugloire, E.; Flanagan, M.; Stoffregen, T. A. Motion sickness, console video games, and head-mounted displays. *Human factors 49*, 5 (2007), 920–934.

[95] Morales, R.; Chelen, W.; Kabrisky, M. Electroencephalographic theta band changes during motion sickness. *Aviation, Space, and Environmental Medicine 61* (1990), 507.

[96] Mousavi, M.; Jen, Y. H.; Musa, S. N. B. A review on cybersickness and usability in virtual environments. In *Advanced Engineering Forum* (2013), vol. 10, Trans Tech Publ, pp. 34–39.

[97] Nalivaiko, E.; Rudd, J. A.; So, R. H. Motion sickness, nausea and thermoregulation: the "toxic" hypothesis. *Temperature 1*, 3 (2014), 164–171.

[98] Naqvi, S. A. A.; Badruddin, N.; Jatoi, M. A.; Malik, A. S.; Hazabbah, W.; Abdullah, B. Eeg based time and frequency dynamics analysis of visually induced motion sickness (vims). *Australasian physical & engineering sciences in medicine 38*, 4 (2015), 721–729.

[99] Norouzi, N.; Bruder, G.; Welch, G. Assessing vignetting as a means to reduce vr sickness during amplified head rotations. In *Proceedings of the 15th ACM Symposium on Applied Perception* (2018), ACM, p. 19.

[100] Nvidia. VRWorks - Context Priority. `https://developer.nvidia.com/vrworks/headset/`. Accessed: 2020-07-01.

[101] Olano, M.; Cohen, J.; Mine, M.; Bishop, G. Combatting rendering latency. In *Proceedings of the 1995 symposium on Interactive 3D graphics* (1995), ACM, pp. 19–ff.

[102] Padmanaban, N.; Konrad, R.; Stramer, T.; Cooper, E. A.; Wetzstein, G. Optimizing virtual reality for all users through gaze-contingent and adaptive focus displays. *Proceedings of the National Academy of Sciences* (2017), 201617251.

[103] Padmanaban, N.; Ruban, T.; Sitzmann, V.; Norcia, A. M.; Wetzstein, G. Towards a machine-learning approach for sickness prediction in 360° stereoscopic videos. *IEEE Transactions on Visualization & Computer Graphics*, 1 (2018), 1–1.

[104] Park, G.; Rosenthal, T. J.; Allen, R. W.; Cook, M. L.; Fiorentino, D.; Viirre, E. Simulator sickness results obtainted during a novice driver training study. In *Proceedings of the Human Factors and Ergonomics Society Annual Meeting* (2004), vol. 48, SAGE Publications Sage CA: Los Angeles, CA, pp. 2652–2655.

[105] Pavard, B.; Berthoz, A. Linear acceleration modifies the perceived velocity of a moving visual scene. *Perception 6*, 5 (1977), 529–540.

[106] Peck, T. C.; Sockol, L. E.; Hancock, S. M. Mind the gap: The underrepresentation of female participants and authors in virtual reality research. *IEEE Transactions on Visualization and Computer Graphics 26*, 5 (2020), 1945–1954.

[107] Pedregosa, F.; Varoquaux, G.; Gramfort, A.; Michel, V.; Thirion, B.; Grisel, O.; Blondel, M.; Prettenhofer, P.; Weiss, R.; Dubourg, V., et al. Scikit-learn: Machine learning in python. *Journal of Machine Learning Research 12* (2011), 2825–2830.

[108] Plouzeau, J.; Chardonnet, J.-R.; Merienne, F. Using cybersickness indicators to adapt navigation in virtual reality: A pre-study. In *2018 IEEE Conference on Virtual Reality and 3D User Interfaces (VR)* (2018), IEEE, pp. 661–662.

[109] Poh, M.-Z.; Swenson, N. C.; Picard, R. W. A wearable sensor for unobtrusive, long-term assessment of electrodermal activity. *IEEE transactions on Biomedical engineering 57*, 5 (2010), 1243–1252.

[110] Poole, A.; Ball, L. J. Eye tracking in hci and usability research. In *Encyclopedia of human computer interaction*. IGI Global, 2006, pp. 211–219.

[111] Porac, C.; Coren, S. The dominant eye. *Psychological bulletin 83*, 5 (1976), 880.

[112] Porcino, T. Cybersickness Dataset. `https://github.com/tmp1986/UFFCSData`. Accessed: 2021-04-03.

[113] Porcino, T.; Clua, E.; Vasconcelos, C.; Trevisan, D. Dynamic focus selection for first-person navigation with head mounted displays. *SBGames* (2016).

[114] Porcino, T.; Rodrigues, E. O.; Bernardini, F.; Trevisan, D.; Clua, E. Can we identify user- and game-specific causes that lead to cybersickness? In *2020 IEEE Conference on Games (CoG)* (2021), IEEE.

[115] Porcino, T.; Rodrigues, E. O.; Bernardini, F.; Trevisan, D.; Clua, E. Identifying cybersickness causes in virtual reality games using symbolic machine learning algorithms. *Entertainment Computing* (2021).

[116] Porcino, T.; Rodrigues, E. O.; Silva, A.; Clua, E.; Trevisan, D. Using the gameplay and user data to predict and identify causes of cybersickness manifestation in virtual reality games. In *2020 IEEE 8th International Conference on Serious Games and Applications for Health (SeGAH)* (2020), IEEE, pp. 1–8.

[117] Porcino, T.; Trevisan, D.; Clua, E. Minimizing cybersickness in head-mounted display systems: causes and strategies review. In *2020 22nd Symposium on Virtual and Augmented Reality (SVR)* (2020), IEEE, pp. 154–163.

[118] Porcino, T. M.; Clua, E.; Trevisan, D.; Vasconcelos, C. N.; Valente, L. Minimizing cyber sickness in head mounted display systems: design guidelines and applications. In *Serious Games and Applications for Health (SeGAH), 2017 IEEE 5th International Conference on* (2017), IEEE, pp. 1–6.

[119] Ramsey, A.; Nichols, S.; Cobb, S. Virtual reality induced symptoms and effects (vrise) in four different virtual reality display conditions. In *Proceedings of HCI International (the 8th International Conference on Human-Computer Interaction) on Human-Computer Interaction: Ergonomics and User Interfaces-Volume I-Volume I* (1999), L. Erlbaum Associates Inc., pp. 142–146.

[120] Rao, J. S.; Potts, W. J. Visualizing bagged decision trees. In *KDD* (1997), pp. 243–246.

[121] Reason, J. T. Motion sickness adaptation: a neural mismatch model. *Journal of the Royal Society of Medicine 71*, 11 (1978), 819–829.

[122] Reason, J. T.; Brand, J. J. *Motion sickness.* Academic press, 1975.

[123] Rebenitsch, L.; Owen, C. Individual variation in susceptibility to cybersickness. In *Proceedings of the 27th annual ACM symposium on User interface software and technology* (2014), ACM, pp. 309–317.

[124] Rebenitsch, L.; Owen, C. Review on cybersickness in applications and visual displays. *Virtual Reality 20*, 2 (2016), 101–125.

[125] Rebenitsch, L. R. *Cybersickness prioritization and modeling.* Michigan State University, 2015.

[126] Renkewitz, H.; Alexander, T. Perceptual issues of augmented and virtual environments. Tech. rep., FGAN-FKIE WACHTBERG (GERMANY), 2007.

[127] Riccio, G. E.; Stoffregen, T. A. An ecological theory of motion sickness and postural instability. *Ecological psychology 3*, 3 (1991), 195–240.

[128] Riva, G. *Virtual reality in neuro-psycho-physiology: Cognitive, clinical and methodological issues in assessment and rehabilitation*, vol. 44. IOS press, 1997.

[129] Rizzo, A.; Parsons, T. D.; Lange, B.; Kenny, P.; Buckwalter, J. G.; Rothbaum, B.; Difede, J.; Frazier, J.; Newman, B.; Williams, J., et al. Virtual reality goes to war: A brief review of the future of military behavioral healthcare. *Journal of clinical psychology in medical settings 18*, 2 (2011), 176–187.

[130] Sak, H.; Senior, A. W.; Beaufays, F. Long short-term memory recurrent neural network architectures for large scale acoustic modeling.

[131] Samek, W.; Montavon, G.; Vedaldi, A.; Hansen, L. K.; Müller, K.-R. *Explainable AI: interpreting, explaining and visualizing deep learning*, vol. 11700. Springer Nature, 2019.

[132] Sanei, S.; Chambers, J. A. Eeg signal processing.

[133] Sarupuri, B.; Chipana, M. L.; Lindeman, R. W. Trigger walking: A low-fatigue travel technique for immersive virtual reality. In *2017 IEEE Symposium on 3D User Interfaces (3DUI)* (2017), IEEE, pp. 227–228.

[134] Sevinc, V.; Berkman, M. I. Psychometric evaluation of simulator sickness questionnaire and its variants as a measure of cybersickness in consumer virtual environments. *Applied Ergonomics 82* (2020), 102958.

[135] Sharples, S.; Cobb, S.; Moody, A.; Wilson, J. R. Virtual reality induced symptoms and effects (vrise): Comparison of head mounted display (hmd), desktop and projection display systems. *Displays 29*, 2 (2008), 58–69.

[136] Skopp, N. A.; Smolenski, D. J.; Metzger-Abamukong, M. J.; Rizzo, A. A.; Reger, G. M. A pilot study of the virtusphere as a virtual reality enhancement. *International Journal of Human-Computer Interaction 30*, 1 (2014), 24–31.

[137] So, R. H.; Lo, W.; Ho, A. T. Effects of navigation speed on motion sickness caused by an immersive virtual environment. *Human Factors: The Journal of the Human Factors and Ergonomics Society 43*, 3 (2001), 452–461.

[138] Srivastava, S. Weka: a tool for data preprocessing, classification, ensemble, clustering and association rule mining. *International Journal of Computer Applications 88*, 10 (2014).

[139] Stanney, K. M.; Kennedy, R. S.; Drexler, J. M. Cybersickness is not simulator sickness. In *Proceedings of the Human Factors and Ergonomics Society annual meeting* (1997), vol. 41, SAGE Publications Sage CA: Los Angeles, CA, pp. 1138–1142.

[140] Statista, A. The statistics portal. *Web site: https://www.statista.com/statistics/591181/global-augmented-virtual-reality-market-size/* (2020).

[141] Stoffregen, T. A.; Smart Jr, L. J. Postural instability precedes motion sickness. *Brain research bulletin 47*, 5 (1998), 437–448.

[142] Studios, B. G. *The elder scrolls v: Skyrim.* Bethesda Game Studios, 2015.

[143] Sugita, N.; Yoshizawa, M.; Tanaka, A.; Abe, K.; Chiba, S.; Yambe, T.; Nitta, S.-i. Quantitative evaluation of effects of visually-induced motion sickness based on causal coherence functions between blood pressure and heart rate. *Displays 29*, 2 (2008), 167–175.

[144] Teather, R. J. Viewpoint snapping to reduce cybersickness in virtual reality.

[145] Tovée, M. J., et al. *An introduction to the visual system.* Cambridge University Press, 1996.

[146] Tran, H. T.; Ngoc, N. P.; Pham, C. T.; Jung, Y. J.; Thang, T. C. A subjective study on qoe of 360 video for vr communication. In *2017 IEEE 19th International Workshop on Multimedia Signal Processing (MMSP)* (2017), IEEE, pp. 1–6.

[147] Treisman, M. Motion sickness: an evolutionary hypothesis. *Science 197*, 4302 (1977), 493–495.

[148] Tripathi, M.; Taneja, A. K-fold cross-validation machine learning approach on data imbalance for wireless sensor network.

[149] Van Waveren, J. The asynchronous time warp for virtual reality on consumer hardware. In *Proc. 22nd ACM Conference on Virtual Reality Software and Technology* (2016), pp. 37–46.

[150] Wallach, H.; Norris, C. M. Accommodation as a distance-cue. *The American journal of psychology 76*, 4 (1963), 659–664.

[151] Webb, N. A.; Griffin, M. J. Optokinetic stimuli: motion sickness, visual acuity, and eye movements. *Aviation, space, and environmental medicine 73*, 4 (2002), 351–358.

[152] Xie, N.; Ras, G.; van Gerven, M.; Doran, D. Explainable deep learning: A field guide for the uninitiated. *arXiv preprint arXiv:2004.14545* (2020).

[153] Xu, L.; Koch, K. L.; Summy-Long, J.; Stern, R. M.; Seaton, J. F.; Harrison, T. S.; Demers, L. M.; Bingaman, S. Hypothalamic and gastric myoelectrical responses during vection-induced nausea in healthy chinese subjects. *American Journal of Physiology-Endocrinology And Metabolism 265*, 4 (1993), E578–E584.

[154] Yan, Y.; Chen, K.; Xie, Y.; Song, Y.; Liu, Y. The effects of weight on comfort of virtual reality devices. In *International Conference on Applied Human Factors and Ergonomics* (2018), Springer, pp. 239–248.

[155] Yang, J.; Guo, C.; So, R.; Cheung, R. Effects of eye fixation on visually induced motion sickness: are they caused by changes in retinal slip velocity? In *Proceedings of the Human Factors and Ergonomics Society Annual Meeting* (2011), vol. 55, SAGE Publications Sage CA: Los Angeles, CA, pp. 1220–1224.

[156] Yang X, Wang D, H. H.; K, Y. P-31: Visual fatigue assessment and modeling based on ecg and eog caused by 2d and 3d displays. *SID Symposium Digest of Technical Papers 47*, 1 (2016), 1237–1240.

[157] Yao, R.; Heath, T.; Davies, A.; Forsyth, T.; Mitchell, N.; Hoberman, P. Oculus vr best practices guide.

APPENDIX A – CSPQ - Cybersickness Profile Questionnaire

1.	Gênero	Feminino		Masculino
2.	Idade	18 a 36	37 a 50	+50
3.	Experiência	Nenhum	Alguma	Muita
4.	Pré-Sintomas	Nenhum		Algum
5.	Sensibilidade a cintilação	Nenhum		Alguma
6.	Uso de óculos de grau	Não		Sim
7.	Postura de jogo	Sentado		Em pé
8.	Olho dominante	Esquerdo		Direito

Table A.1: Portuguese version of Cybersickness profile questionnaire (CSPQ).

APPENDIX B – VRSQ - Virtual Reality Sickness Questionnaire

1.	Desconforto geral	Nenhum	Leve	Moderado	Severo
2.	Fadiga (cansaço)	Nenhum	Leve	Moderado	Severo
3.	Fadiga (ocular)	Nenhum	Leve	Moderado	Severo
4.	Dificuldade de concentração	Nenhum	Leve	Moderado	Severo
5.	Dor de cabeça	Nenhum	Leve	Moderado	Severo
6.	"Cabeça Pesada"	Não	Sim (Leve	Moderado	Severo)
7.	Visão embaçada	Não	Sim (Leve	Moderado	Severo)
8.	Tontura	Não	Sim (Leve	Moderado	Severo)
9.	Vertigem	Não	Sim (Leve	Moderado	Severo)

Table B.1: Portuguese version of Virtual Reality Sickness Questionnaire (VRSQ) [69].

APPENDIX C – Termo de Consentimento Livre e Esclarecido

O(A) Sr.(ª) está sendo convidado(a) a participar do projeto de pesquisa Utilização dados de jogo e de jogadores para recomendação automática de estratégias de minimização de desconforto em ambientes de realidade virtual, de responsabilidade do pesquisador THIAGO MALHEIROS PORCINO. A sua participação é voluntária e que este consentimento poderá ser retirado a qualquer tempo, sem prejuízos à continuidade do tratamento (se for o caso) ou qualquer outra penalização.

A sessão consistirá no uso de uma câmera de vídeo no intuito de gravar a sua interação com o aplicativo e assim observar possíveis pontos positivos e negativos da aplicação projetada para o mesmo. Todos os dados de gravação de áudio e vídeo são confidenciais e não serão divulgados. Segundo estudos algumas pessoas podem sentir desconforto durante experiências com realidade virtual, como enjoo, dor nos olhos e tontura. Ao realizar este experimento você declara que é maior de 18 anos e de estar ciente que poderá sentir um ou mais sintomas de desconforto causados pelo uso de equipamentos de realidade virtual. Este estudo visa entender as causas destes sintomas de desconforto em ambientes de realidade virtual. Este procedimento não apresenta riscos à vida uma vez que nenhum tipo de intervenção será necessário. Sempre haverá um pesquisador próximo a você para qualquer manifestação de desconforto que deseje relatar. Não será realizada nenhum tipo de entrevista, e você poderá se retirar da sessão a qualquer momento. A equipe envolvida no estudo é composta por um estudante de doutorado(Thiago Malheiros), e os professores responsáveis (Dra. Daniela G. Trevisan e Dr. Esteban W. Clua). Agradecemos vossa participação e colaboração.

Os Comitês de Ética em Pesquisa (CEPs) são compostos por pessoas que trabalham para que todos os projetos de pesquisa envolvendo seres humanos sejam aprovados de acordo com as normas éticas elaboradas pelo Ministério da Saúde. A avaliação dos CEPs leva em consideração os benefícios e riscos, procurando minimizá-los e busca garantir que os participantes tenham acesso a todos os direitos assegurados pelas agências regulatórias. Assim, os CEPs procuram defender a dignidade e os interesses dos participantes, incentivando sua autonomia e participação voluntária. Procure saber se este projeto foi aprovado pelo CEP desta instituição. Em caso de dúvidas, ou querendo outras informações, entre em contato com o Comitê de Ética da Faculdade de Medicina da Universidade Federal Fluminense (CEP FM/UFF), por e.mail ou telefone, de segunda à sexta, das 08:00 às 17:00 horas: e-mail: etica@vm.uff.br Tel/fax: (21) 26299189

Eu, ______________________________________, declaro ter sido informado e concordo em ser participante, do projeto de pesquisa acima descrito.

Rio de Janeiro, ______________________________________

E-mail: ____

____

(nome e assinatura do participante ou responsável legal)

APPENDIX D – Race Game Timeline CS Prediction for P6 Subjects

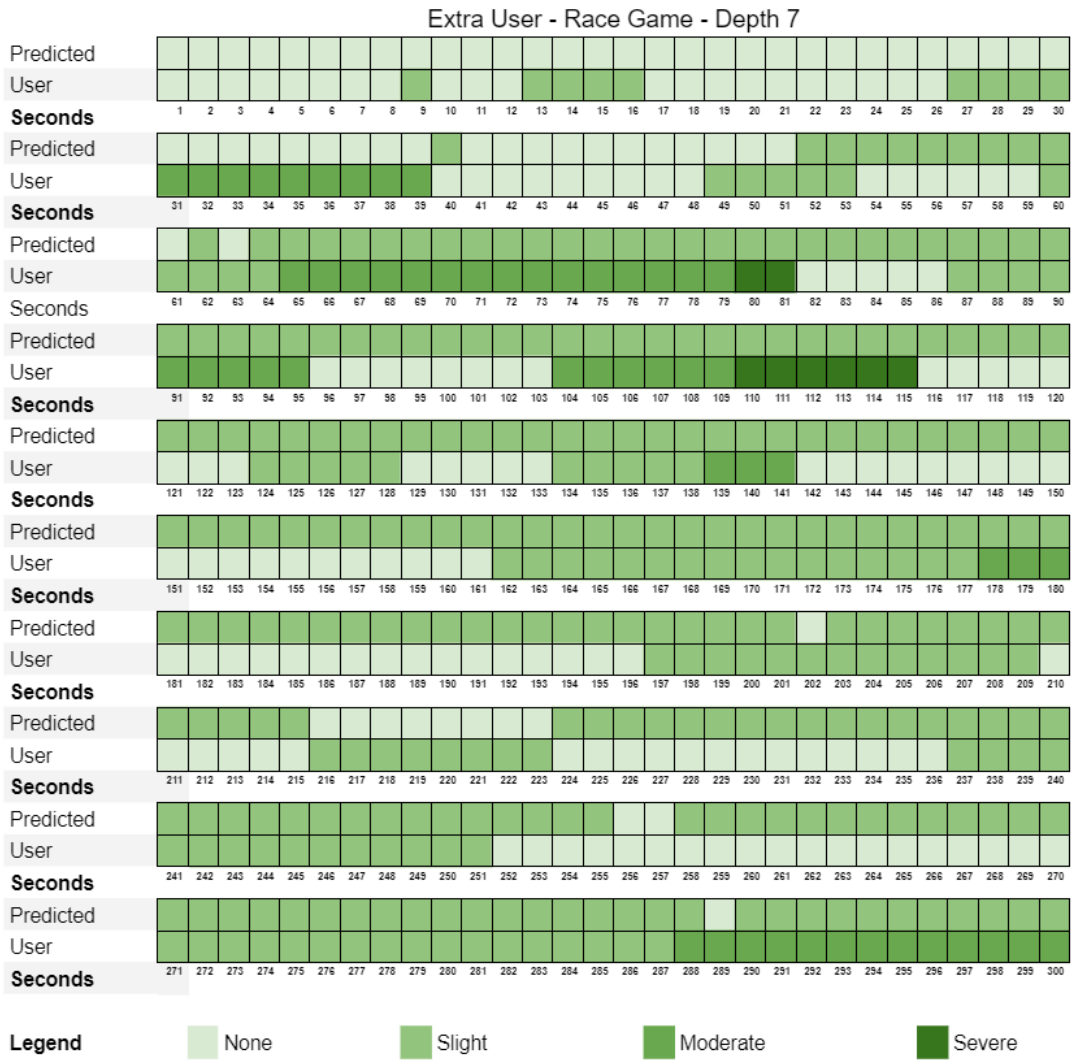

Figure D.1: CS prediction and CS-user discomfort level from 0 to 5 minutes in the race game.

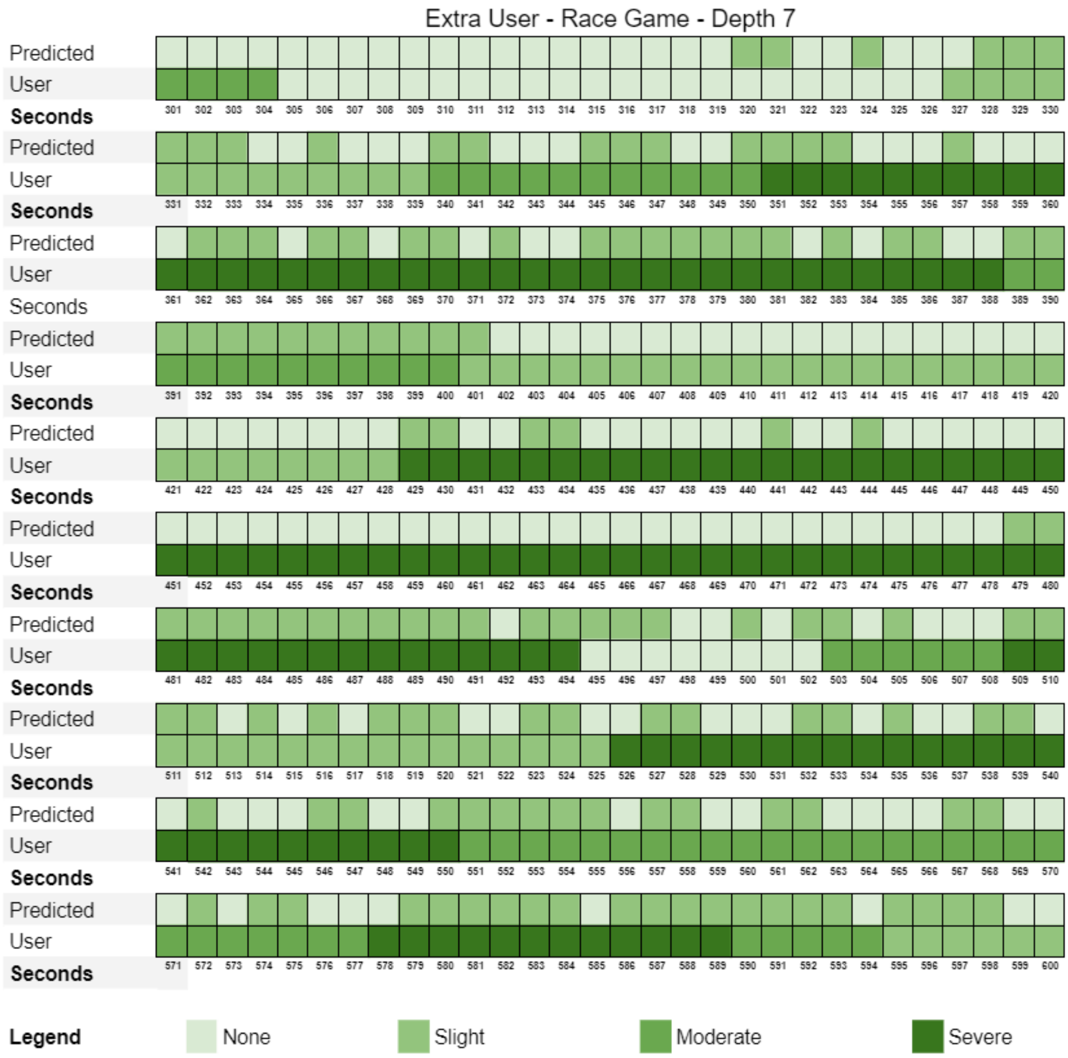

Figure D.2: CS prediction and CS-user discomfort level from 5 to 10 minutes in the race game.

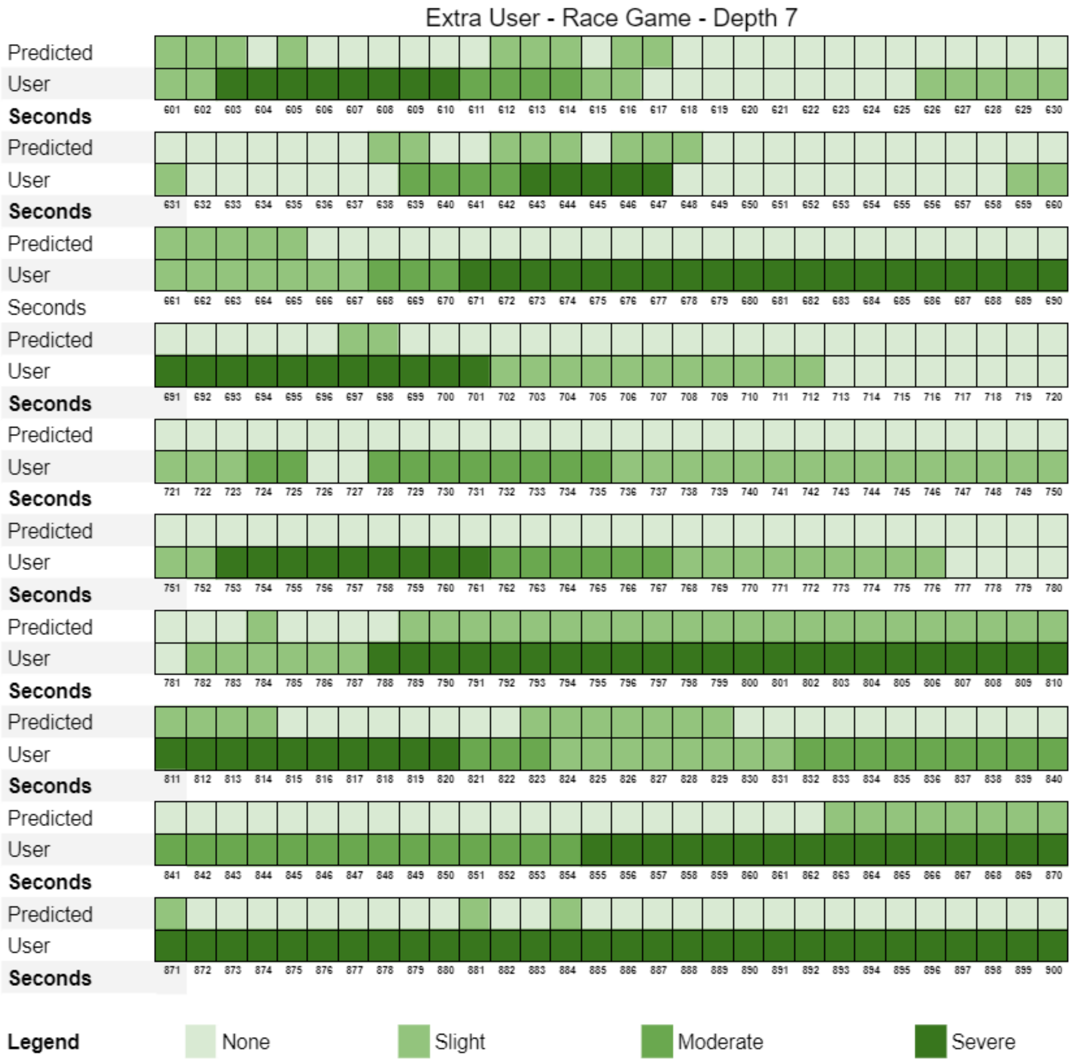

Figure D.3: CS prediction and CS-user discomfort level from 10 to 15 minutes in the race game.

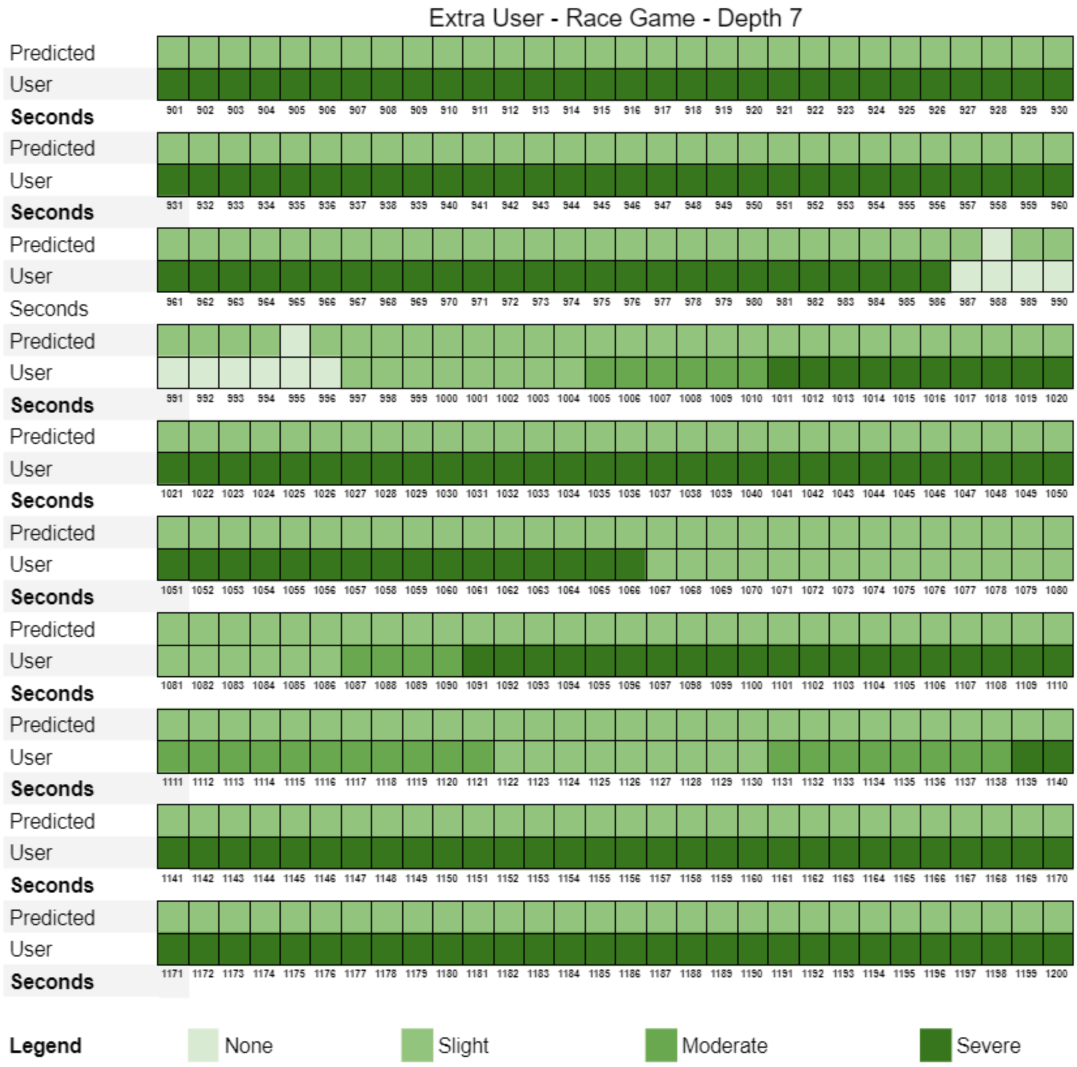

Figure D.4: CS prediction and CS-user discomfort level from 15 to 20 minutes in the race game.

APPENDIX E – Flight Game Timeline CS Prediction for P6 Subjects

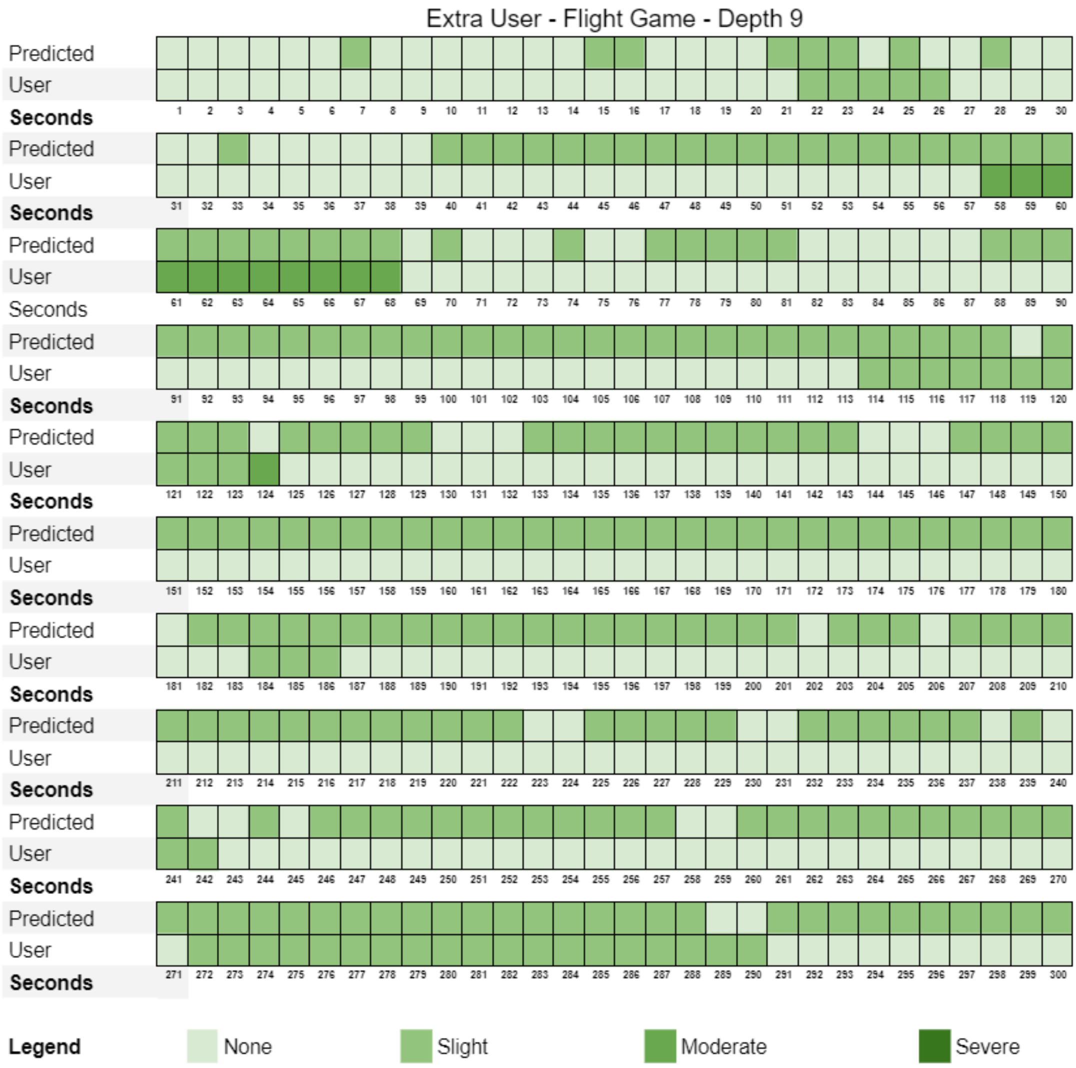

Figure E.1: CS prediction and CS-user discomfort level from 0 to 5 minutes in the flight game.

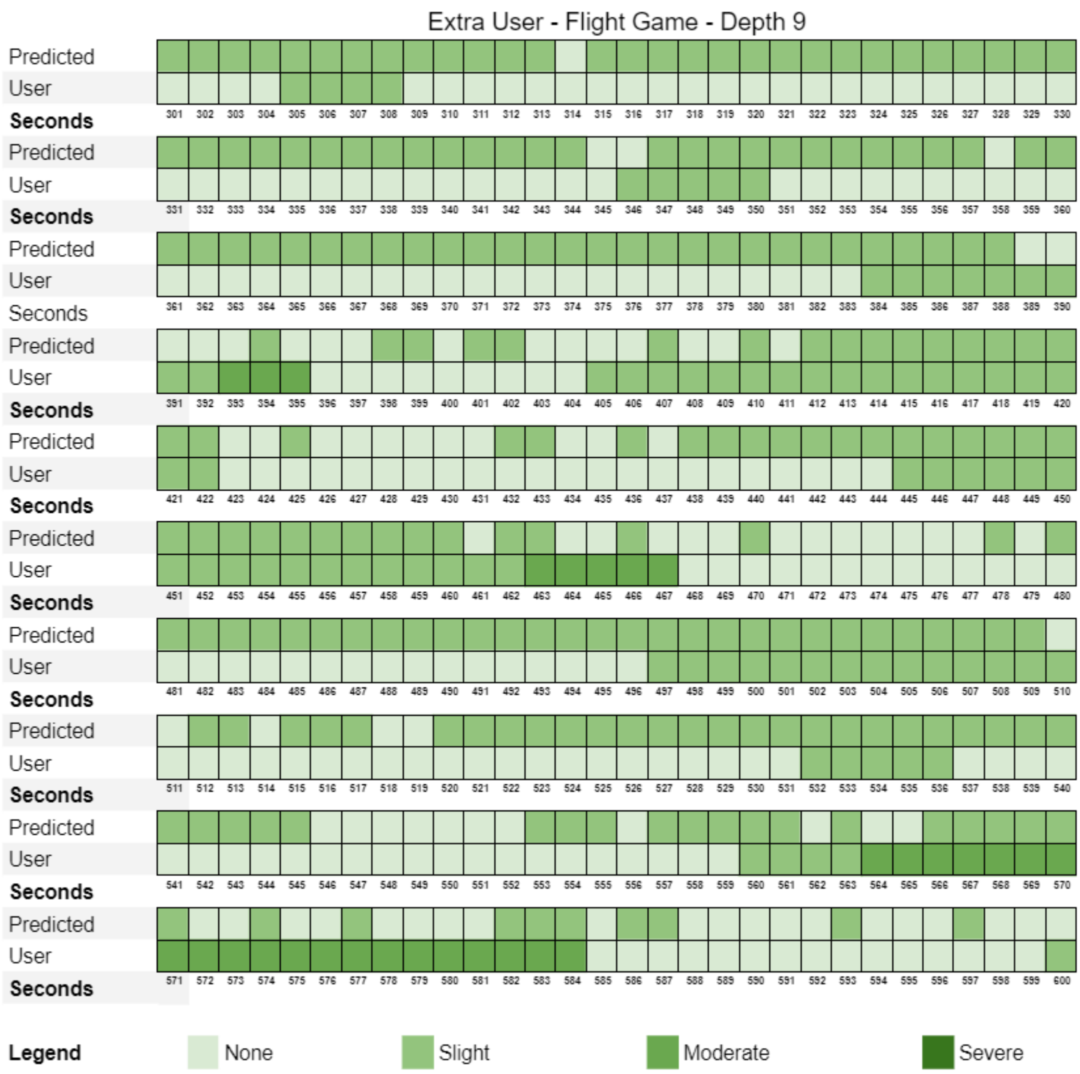

Figure E.2: CS prediction and CS-user discomfort level from 5 to 10 minutes in the flight game.

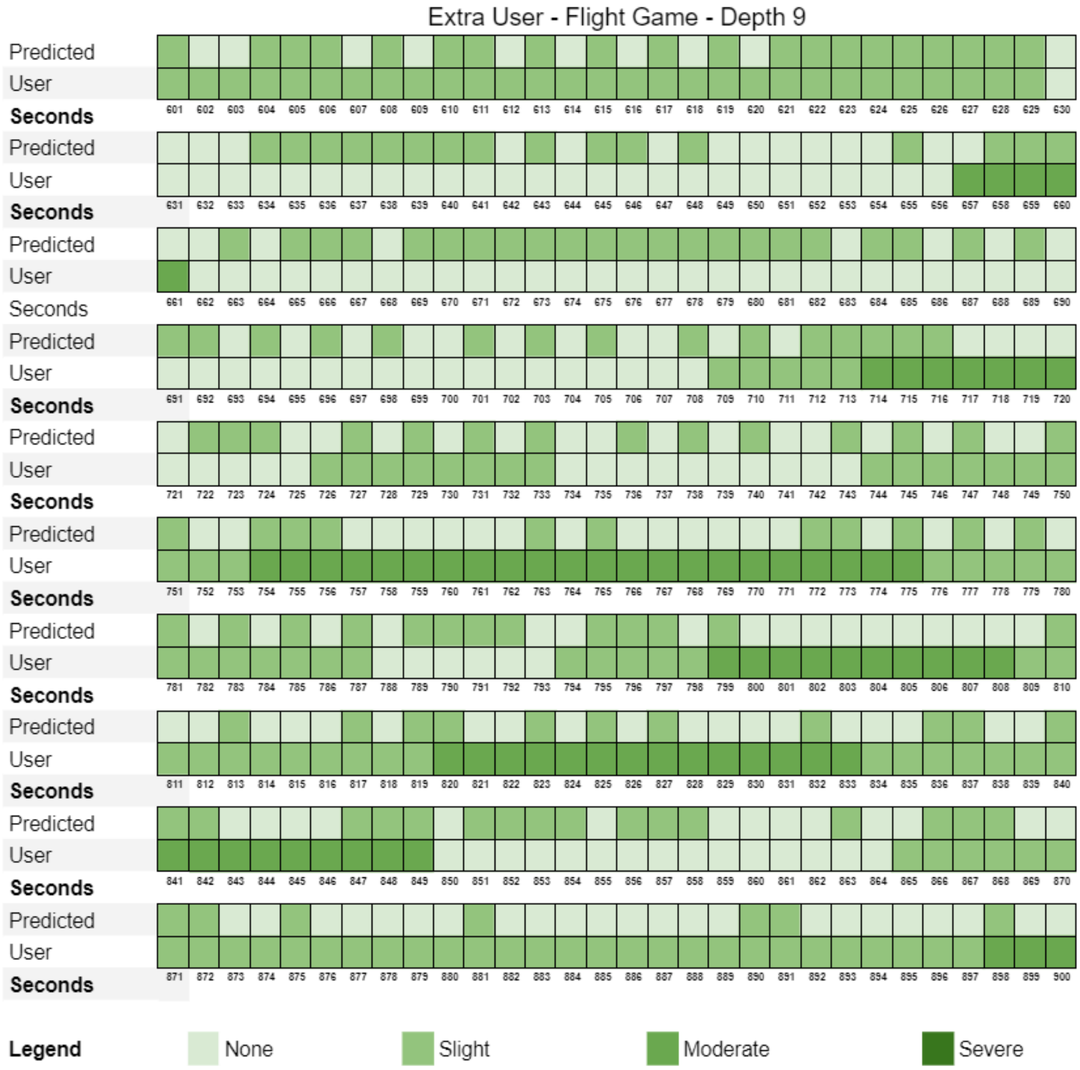

Figure E.3: CS prediction and CS-user discomfort level from 10 to 15 minutes in the flight game.

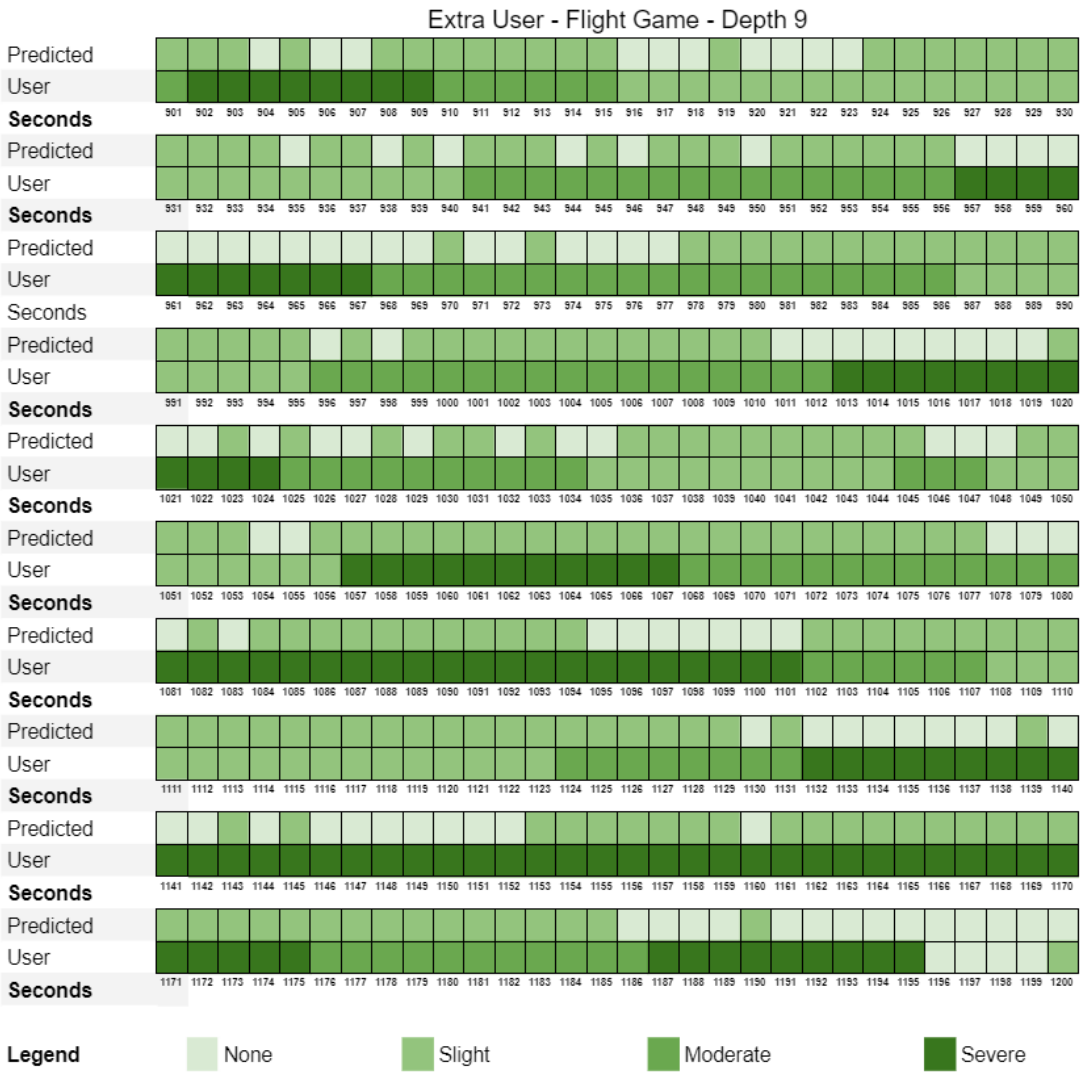

Figure E.4: CS prediction and CS-user discomfort level from 15 to 20 minutes in the flight game.